IMPACT OF LAND USE AND CLIMATE CHANGE ON WATER BALANCE - A CASE STUDY OF ROKEL-SELI RIVER BASIN IN SIERRA LEONE

A Dissertation

Submitted in partial fulfilment of the requirements for the Award of degree

Of

MASTER OF TECHNOLOGY

In

WATER RESOURCES DEVELOEMENT AND MANAGEMENT

By:

SARAMADIE THORLU-BANGURA

DEPARTMENT OF WATER RESOURCES DEVELOPMENT AND MANAGEMENT

INDIAN INSTITUTE OF TECHNOLOGY

ROORKEE-247667(INDIA)

MAY, 2018

CANDIDATE'S DECLARATION

I hereby certify that the work which is being presented in this Dissertation entitled, "**IMPACT OF LAND USE AND CLIMATE CHANGE ON WATER BALANCE - A CASE STUDY OF ROKEL-SELI RIVER BASIN IN SIERRA LEONE",** in partial fulfillment of the requirement for the award of the Degree of Master of Technology in Water Resources Development and Management and submitted in the Department of Water Resources Development and Management of the Indian Institute of Technology Roorkee, is an authentic record of my own work carried out during the period from July 2016 to May 2018 under the supervision of Dr. M. L. Kansal**,** Water Resources Development and Management Department, Indian Institute of Technology Roorkee, Roorkee (India) and Dr. S.K. Chandniha, Surface Water Hydrology Division, National Institute of Hydrology, Roorkee (India).

The matter presented in the Dissertation has not been submitted by me for the award of any other degree of this or any other institute.

Date …… **Saramadie Thorlu-Bangura**

Place: **IIT Roorkee** **Enrollment No. 16548036**

This is to certify that the above statement made by the candidate is correct to the best of our knowledge.

Dr. S.K. Chandniha
Co-Supervisor
Surface Water Hydrology Division
National Institute of Hydrology
Roorkee-247677(Uttarakhand).

Prof. M.L. Kansal
Supervisor
Water Resources Development and
Management Department,
Indian Institute of Technology, Roorkee
Roorkee-247677(Uttarakhand).

ACKNOWLEDGEMENT

I wish to express my sincere thanks to Dr M.L Kansal, Professor, Department Of Water Resources Development Management**,** Indian Institute of Technology Roorkee, for his support and providing all the guidelines, which have made it possible for me to complete this Mid-Term Assessment report.

Gratitude goes to Dr. Surendra Kumar Chandniha, Post-Doctoral Fellow, National Institute of Hydrology, Roorkee for his kind co-operation and encouragement and serving as co-guide which helped me in completing this Dissertation. I am also grateful to all faculty members and staff of Department Of Water Resources Development Management, Indian Institute of Technology, Roorkee. I extend my thanks to all of my classmates and seniors who helped in diverse ways towards the completion of this Dissertation.

Saramadie Thorlu-Bangura

May 2018

ABSTRACT

Sierra Leone, a country in West Africa, has experienced substantial economic growth in recent years. It has a special significance in the West African history, though the ruinous effects of the civil war continue to be felt. The Rokel-Seli River, which is the largest river in the country, stretches across the entire northern region before joining the estuary of the Sierra Leone River that in turn joins the Atlantic Ocean. It has a basin area of 10946km^2 which infringes four major districts (Koinadugu, Bombali, Tonkolili and PortLoko Districts) having 31% (2,159,119) of the total country population. This basin is characterized by a heterogeneous forest-savanna mosaic and experiences a humid tropical climate with annual rainfall averaging 3000mm and mean monthly temperature of 25.78oC.). There are two main seasons: Rainy/wet season (May to October) and Dry season (November to April). There are several small traditional villages in the area with rice cultivation in wet depressions and harvesting of non-timber forest products such as oil palm nuts. This river basin is of critical importance to the country's economy as it supplies water to the Bumbuna hydroelectric power scheme as well as water for the agriculture, fisheries, mining and transportation and for ecological purposes.

Keeping the long term water resources planning in mind, it is desired to study water balance of Rokel-Seli River Basin due to impact of land use and climate change. In this study, an attempt has been made to study the past variation of rainfall and to identify the trend. The long term trend has been detected using the MK and MKK test(s) for historical and projected (future) time series in terms of monthly, seasonal and annual basis. Further, shift change point has been detected for break point identification using SNHT and MWP test(s). Further, rainfall has been forecasted till 2050s under different climate scenarios with various CMIP5 emission conditions, i.e., RCP-2.6, RCP-4.5 and RCP-8.5. Climate change scenarios will help the future planning of water resources in the Rokel-Seli river basin (RSRB). The forecasted results are at 95% level of significance. Further, the runoff at the catchment outlet has been estimated and the effect of rainfall variability on the runoff estimates is highlighted.

Moreover, the study also investigate the morphometric charactieristics of the basin using geospatial techniques in order to prioritize the basin interms of soil conservation measures. Through the morphometric analysis the basin is more prone to soil loss on the mid and downstream of the basin. The landuse land cover classification of the basin has been reclassified into five classes with most part of the basin covered with pasture (41%) and

forest(40), only 15% of the basin is under agriculture and 3% residential areas with just 1% as water bodies. The water balance over the basin have been simulated using SWAT model for a period of 14 years (2000-2014). The water balance component of the RSRB was analysed that out of 2180mm precipitation 23% flows out as runoff, 30% as ground water and 47% as evapotranpiration.

The present study highlights the rainfall variability over the Rokel-Seli River Basin in Sierra Leone. The adopted analysis provides key information of basin's water availability and hence this work offers benchmark information that can be used to increase the capacity of long-range water resource planning and management, land use planning, agricultural water development and conservation, and industrial water use over the next several decades at basin level. The results of the study also helps in the assessment of the future impact of climate change over the basin which affects changes in the hydrologic cycle of the basin.

TABLE OF CONTENTS

LIST OF TABLES

LIST OF FIGURES

ABBREVIAIONS AND ANNOTATIONS

ABBREVIATION	Title
CanESM2	Canadian Centre for Climate Modeling
CMIP5	Coupled Modelled Inter-comparison Phase Five
CRU	Climatic Research Unit
DEM	Digital Elevation Model
ETM+	Enhanced Thematic Mapper Plus
GCM	Global Circulation Models
GPCC	Global Precipitation Climatology Centre
HRU	Hydrological Response Unit
LULC	Land-Use Land-Cover
LUCC	Land Use Land Cover Change
NASA	National Aeronautics and Space Administration
NCEP	National Center of Environmental Prediction
NIWR	Net Irrigation Water Requirement
NSE	Nash Sutcliff Efficiency
OLI	Optical Land Imager
PBIAS	Percent Bias Index
PMW	Pettitt's-Mann-Whitney
RCP	Representative Concentration Pathways
RSRB	Rokel-Seli River Basin
SRTM	Shuttle Radar Topographic Mission
SNHT	Standard Normal Homogeneity Test
SWAT	Soil and Water Assessment Tool

TRMM	Tropical Rainfall Measuring Mission
USGS	United States Geological Survey
UTM	Universal Transvers Mercator

CHAPTER

1

INTRODUCTION

OVERVIEW OF CHAPTER

This chapter describes the general background of the study. It explains the meaining of the study topic, the importance of the subject, how relevant it is to the case study and what impact has this study created to the society and policy makers and why the study has been carried out. It further ellaborate on the issues related to land use, as well as climate change which affect the study area. Moreover, this section gives a brief overview of the techniques (Remote Sensing and GIS) used in executing the study and explains how they are related to hydrological modelling for quantifying water components in the study area. The specific objectives of the research are also highlighted and hence outlines the questions the research seeks to answer. Finally, it gives clear outline on the organizational structure of the Dissertation.

1.1 GENERAL BACKGROUND

Growing awareness of climate change and land use land cover pattern over all basins has impact to water resources. Keeping this in mind and to establish long term water resources planning therefore, this study seeks to evaluate the water balance over the Basin.

The adopted analysis provides key information of basin's water availability, storage, surface runoff and soil moisture. Hence this work offers benchmark information that can be used to increase the capacity of long-range water resource planning and management, land use planning, agricultural water development and conservation, and industrial water use over the next several decades at basin level. Further, this study helps in the assessment of the future impact of climate change over the basin which affects changes in the hydrologic cycle of the basin. Also this study can be used as a guide to simulate rainfall variability over other basins in Sierra Leone to determine the water balance within those basins.

1.2 HYDROLOGICAL MODELLING

Hydrologic modelling is the interpretation of part or whole of the hydrological cycle which includes surface water, soil water, groundwater, wet lands and estuaries that helps in

understanding, predicting and managing water resources. The quality, quantity and flows of water are usually investigated using hydrological modelling to interpret the important components that relate hydrologic inputs to outputs. The various components in the hydrologic cycle describes the importance of the system and characterizes the relationship that exists between them. Therefore, hydrological modelling of a basin categorizes the specific important characteristics of a basin which takes account of atmospheric exchanges (precipitation and evapotranspiration), flow route (base flow, interflow, channel flow and overland flow) human applications (agricultural, municipal, hydroelectric power generation), transport processes (nutrients, sediments) and eventual scenarios (floods, droughts and mean-flow conditions).

Hence, for the purpose of this study, the concept of hydrological modelling has been employed to investigate the specific components of the hydrologic cycle to describe the water balance of Rokel-Seli River Basin. This process could be could be achieved by the application of Remote Sensing and GIS.

1.3 REMOTE SENSING AND GIS

Remote sensing applications have also been used to estimate precipitation, runoff and interception, evapotranspiration, and soil retention. Geographic Information System (GIS) is a system created to capture, store, manipulate, analyze, manage, and present spatial or geographic data and is the technique underlying geographic concepts and applications. Land use land cover interpretation could be achieved by using satellite imagery which gives the physical and real sense of the land features.

1.4 RESEARCH OBJECTIVES

The focus of this research is to explore the impact of land use land cover and climate change on water resources through, remote sensing (RS) and Geographic Information System (GIS) techniques, and hydrological modeling.

The specific objectives of this research are highlighted as follows:

- ✓ To assess the climatic variability and projections, using past and CMIP5 climatic database respectively.
- ✓ To assess the existing water resources of RSRB to know the current water availability in the basin

- ✓ To assess the existing and future water requirements and determine the deficit/surplus as on 2017 and 2050
- ✓ To assess the existing land use land cover pattern in the study area
- ✓ To assess the impact of land use and climate change on water balance in RSRB using semi distributed SWAT Model

1.5 RESEARCH QUESTIONS

The research has been undertaken in order to answer the following key questions:

- What is the average rainfall over the basin and how does it varies from upstream to downstream in order to identify specific zones on the basin for effective water use and agricultural production?
- What is the current and future conditions of water resources on the RSRB and how can it be quantified?
- Does the water resources available in the basin justifies that the basin is surplus or deficit and to what extent?
- What is the water balance of RSRB due to the effect and changes of climatic conditions and how does it affect future water resources of the basin?
- What particular location should soil erosion conservation measures be more focused or prioritized base on morphometric characteristics of the basin in terms of sub-basin wise?

1.6 OUTLINE OF DISSERTATION

This dissertation is outlined and organized into six chapters:

Chapter 1: Describes the general background of the study, the importance of the research and why the study has be done for the particular case study. It highlights the main objectives of the reseach, the questions that the research tries to answer and how the Dissertation is organised by chapters.

C**hapter 2:** Here, what other researchers have achieved in their various studies and the gaps identified during their studies are also elaborated. More specifically, their achievements, outcomes, challenges and the approaches applied in carrying out their studies which are similar to the ones incorporated in this research are discussed.

C**hapter 3:** Discusses the methodologies applied in the study. It clearly explains the dataset used, how and where were they acquired and how were they processed to make them fit and usable to produce output. It also demonstrates the kind of application software (GIS) used and the techniques (Remote Sensing) involved in order to give the expected results. It further talks on the methods used in quantifying water resources available over the basin, the techniques used to project future water resources and how it varies and distributed throughout the entire basin. Finally, it describes the SWAT model techniques which were used to quantify the water balance. Thereafter, it is followed by the next chapter which talks about the results.

C**hapter 4:** Discusses the results obtained from the specific methodologies applied in the research. It clearly demonstrates the outputs derived from climatic variability assessment and rainfall pattern and distribution. It highlights the quantities of the current water availability, the water resources projected and quantities of variation of rainfall pattern on the RSRB. It explains how the water balance is affected based on the outputs of the SWAT Model and how does the climate change and land use is reflected due to the outcomes.

C**hapter 5:** Talks the summary and conclusions of the overall methodologies applied in the research. It summarizes all the various steps used in carrying out the study and gives a conclusive remarks on the outputs derived. Hence it gives the final reason why this research was carried out using SWAT Model to investigate the impact of land use and climate change on the water balance of Rokel-Seli river basin.

Chapter 6: Highlights all the books, theses, journals and papers inquired during the study. It further enumerates the authors of the various texts mention above and the year published. Overall it gives the references of the texts consulted and those cited in this dissertation.

CHAPTER 2

LITERATURE REVIEW

OVERVIEW OF CHAPTER

This chapter gives a summary of several scholarly researches, journals and papers on the various methods applied in investigating land use and climate change impacts on water resources. It elaborates on a variety of literatures of different scholars ranging from climate change assessment, rainfall variability, rainfall projection, land use data classification and reclassification. It further gives a review on researches carried out on basin water balance, application of SWAT Model, calibration and validation criteria of SWAT Model and basin morphometric characterization.

2.1 CLIMATE CHANGE

(Shreepada Devi, 2017) Climate may change in various courses, over various time scales and at various topographical scales. The ecosystem and social orders have dependably been vulnerable against outrageous climate and intense move in the dispersion of climate designs. However, in most recent couple of decades, it has been confirmed that climate designs are defenseless against anthropogenic factors too. Universally, change in climate has found expanding consideration in the field of investigations because of its immediate and abnormal effects on every single real part, for example, hydro-meteorological, natural, organic and socio-economic divisions. Change in climate is a long haul process. It has raised as most concern subject globally. Accordingly, evaluation of climatic changes has turned out to be fundamental.

(Surendra K. C., 2015) studied watershed sustainability index framework and its estimation for a watershed in which it was emphasized that change in climate can seriously affect the earth, water resources, farming, earthbound biological systems, food security, biodiversity, and beach front zones.

(Arun M., 2012) reported that considerable number of researchers have made aware that significant changes in specific climatic variables have occurred especially over the last century. It has been shown that a reduction in extremely cold times and a rise in extremely hot times over many parts in the globe in the past century.

The climate change and its extensive variability due to anthropogenic impact have got a special attention by IPCC (2001). In another sense, climate change means the shifting of climatic or meteorological parameters viz. precipitation, maximum temperature, minimum temperature, solar radiation, relative humidity, wind speed etc. and many other factors whereas global warming or cooling which refer the changes of the surface temperature

2.1.1 Rainfall Variability

(Dinpashoh Y et al., 4014) Precipitation is crucial for human survival and at the same time its extreme events can lead to devastating impacts on the society as well as on the environment. Hence understanding historical changes of precipitation extreme events is therefore very important in better projection of future changes and to develop better climate adaptation strategies.

(IPCC 2007) Precipitation have a significance effect on our environment, as water resources are affected by both the precipitation and the air temperature in the form of evapotranspiration. Water is important for life so it is extremely important to know how climate change affects water resources, which is an important issue while planning for the future water supply.

2.1.2 Rainfall Projections

(Mou Leong Tan et al., 2016) Rainfall and other precipitation levels are important factors affecting crop selection and ecological changes in a region. Accurately predicting precipitation trends can play an important role in a country's future economic development. Rahman and Begum noted that predicting trends using precipitation time series data is more difficult than predicting temperature trends. Recently, meteorologists and other researchers worldwide have paid significant attention to analyzing precipitation time series trends.

2.1.3 Response of Streamflow to Climate Change

(McGuffie, K., et al., 2011) It is widely recognized that runoff is influenced by both climatic variations and human activities. Climatic variations, like precipitation and potential evaporation, have a significant impact on river runoff. Human activities such as land-use changes, irrigation, and dam construction also lead to significant hydrological alterations. In recent decades, considerable effort has been devoted to elucidating the impact of both climatic variations and human activities on water resources. Some studies have investigated the effects of human activities and climatic variations on the discharge of major rivers.

2.2 APPLICATION OF SWAT MODEL FOR WATER BALANCE STUDIES

(Winfred B. 2017) undertook a studied on Assessing the Hydrology of a data-source tropical watershed using SWAT. Base on this research, the monthly and daily simulations results were classified as very good according to the NSE (MORIASI et al., 2007) and PBIAS (VAN LIEW et al., 2007), except for the monthly time step during the calibration period, in which the PBIAS was greater than |10%|. The P-factor values for the monthly and daily time steps were above 0.7 during the calibration period, which indicates that the model results are adequate.

(Van Vuuren, D.P., et al. 2011) It is interesting to notice that the NSE and P-factor values of the monthly simulation were higher for the validation period than in the calibration period. Such results indicate a good model performance, demonstrated by its capacity to simulate average monthly discharge values. Moreover, the low PBIAS values observed in monthly and daily time steps of the validation period indicate that the prediction error is low. In the daily time step, the simulated data is less accurate, which is expected, given that in a larger time period analysis the hydrological processes tend to be more stable. In this sense, greater accuracy from hydrological models forecasts are expected at monthly and annual time steps.

CHAPTER 3

METHODOLOGY

OVERVIEW OF CHAPTER

This chapter discusses the dataset used, how they are acquired and the methodologies applied in the research. Hence it gives full description of the study area. It went on to talk about the different methods used to assess rainfall variability using non-parametric methods (Mann-Kendall- MK, Modified Mann-Kendall MMK Tests and Sen's slope estimator in estimation trends in rainfall time series. Further, it explains the method used in projecting rainfall onto 2020s and 2050s using CMIP5 climatic datasets with RCP-2.6, RCP-4.5 and RCP-8.5 scenarios by applying Multiple Linear Regression (MLR) base statistical downscaling method (SDSM). Also, shift change point detection methods of SNHT and MWP tests in identify homogeneity in the trends at 95% level of significance were discussed. This chapter describes morphometric analysis using geospatial techniques in prioritizing sub-basins in terms of soil erosion conservation measures. Finally, it elaborates on the techniques used in SWAT model to simulate runoff in order to determine the water balance and examines the impact of climate change to runoff.

3.1 DESCRIPTION OF STUDY AREA

3.1.1 Study Area

The Rokel-Seli River Basin is one of the thirteen (13) river basins in Sierra Leone as shown in Fig 3.1. Sierra Leone is a country in West Africa, on the Atlantic Ocean (**Fig. 3.2**) and has 7,075,641 population. It is divided into four (4) regions with fourteen (14) Administrative Boundaries commonly known as Districts. The Northern Region consists of five major Districts, Southern Region comprised of four major Districts, Eastern Region with three main Districts and Western with only two important Districts.

The Rokel-Seli River Basin has a basin area of 10946km^2 with an elevation ranging between 19m to 975m above mean sea level. The basin lies between North latitudes 8°22'35" to 10°325'18" and East longitudes 10°031'54" to 13°06'32".The Rokel-Seli River, which is one of the largest rivers in the country is 356 km (221 mi) in length and has a width varying from 6.4–16.1 km (4–10 miles). It stretches across the entire northern region before joining the estuary of the Sierra Leone River that in turn joins the Atlantic Ocean. It infringes four

major districts (Koinadugu, Bombali, Tonkoliliz and PortLoko Districts) across the entire north of Sierra Leone (Fig. 3.3), having 31% (2,159,119) of the total country population (7,075,641).This basin is characterized by a heterogeneous forest-savanna mosaic and experiences a humid tropical climate with annual rainfall averaging 2435mm and mean monthly temperature of 28.78ºC. There are two main seasons: Rainy/wet season (May to October) and Dry season (November to April). There are several small traditional villages in the area with rice cultivation in wet depressions and harvesting of non-timber forest products such as oil palm nuts.

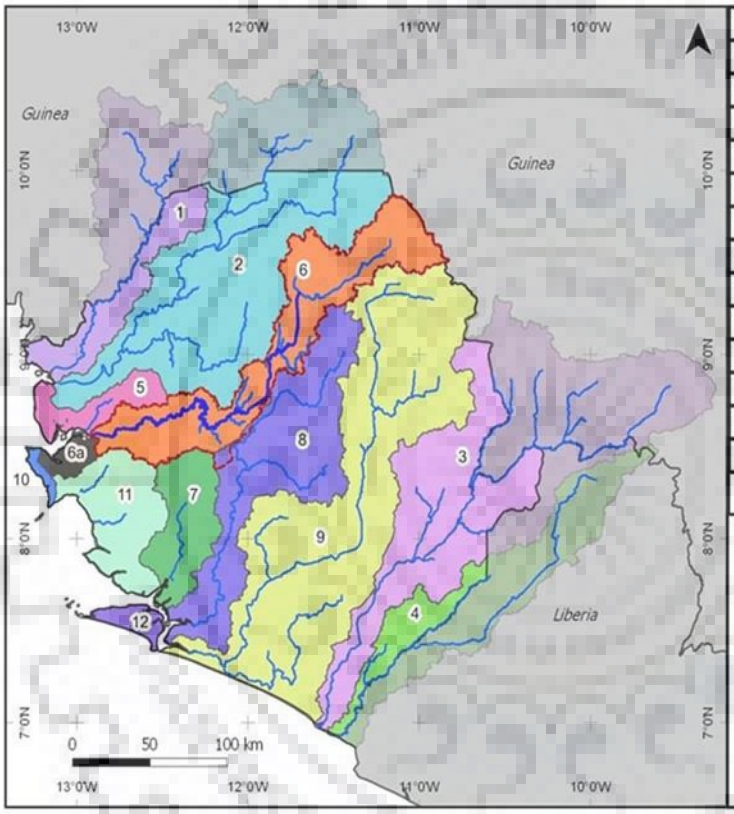

Basin	Name	Country Area	Total Area
B 1	Great Scarcies Basin	2979	8303
B 2	Little Scarcies Basin	13383	18955
B 3	Moa Basin	9583	19835
B 4	Mano Basin	1959	7776
B 5	Lokko Basin	1565	1565
B 6	Rokel Basin	8236	8236
B 6a	Rokel Estuary (South)	579	579
B 7	Gbangbaia Basin	3121	3121
B 8	Jong Basin	8288	8288
B 9	Sewa Basin	19022	19022
B 10	Western WRA	223	223
B 11	Ribbi/Thauka WRA	3670	3670
B 12	Sherbro WRA	612	612
	Totals	**73220**	**100185**

Notes:
* Source HydroSHED catchment boundaries http://hydrosheds.cr.usgs.gov/index.php
* Rokel basin area has been modified after manually digitising the Rokel boundary (Red line)
* All areas are in square kilometres
* WRA - Water Resources Area
* "Country Area" is basin area inside Sierra Leone
* "Total Area" is total basin area
* Basin 6a is part of the Rokel River management area shown in GOSL documents. It is subdivided here for clarity

Figure 3. 1: River Basins of Sierra Leone

3.1.2 Importance of the Basin

The Rokel-Seli River Basin provides water for Bumbuna Hydroelectric Project (BHP) which generates electricity for the entire country (Although the construction work is yet to be completed and currently generates 75 MW, but will generates 350MW after completion in 2020). BHP is today the country's largest infrastructure project and hence the nation's biggest hydroelectric power supply source and wholly depends on the Rokel-Seli River.

ADDAX Bio-energy abstracts water from the river for irrigation and as well for generating electricity. The occasional precipitation variation and the extensive time of dries on basin region, water system is important to meet crop water requirement, with which the demand

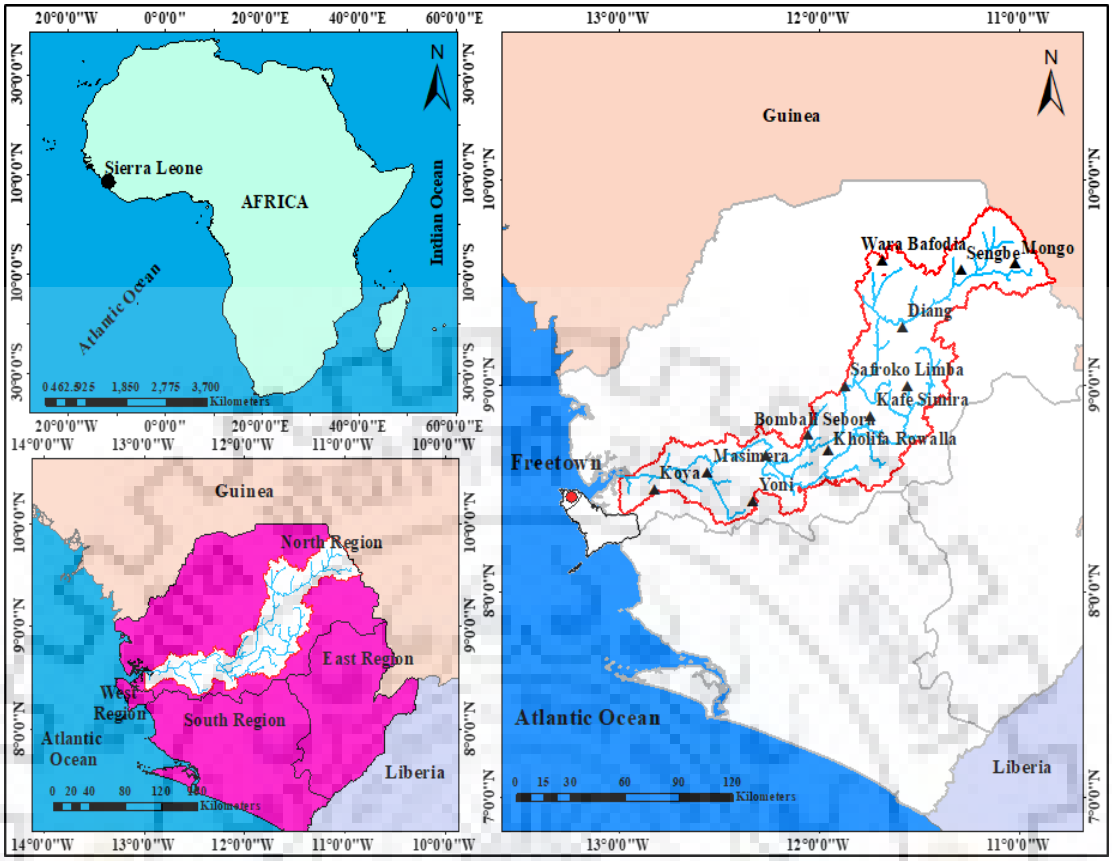

Figure 3. 2: Location Map of Study Area

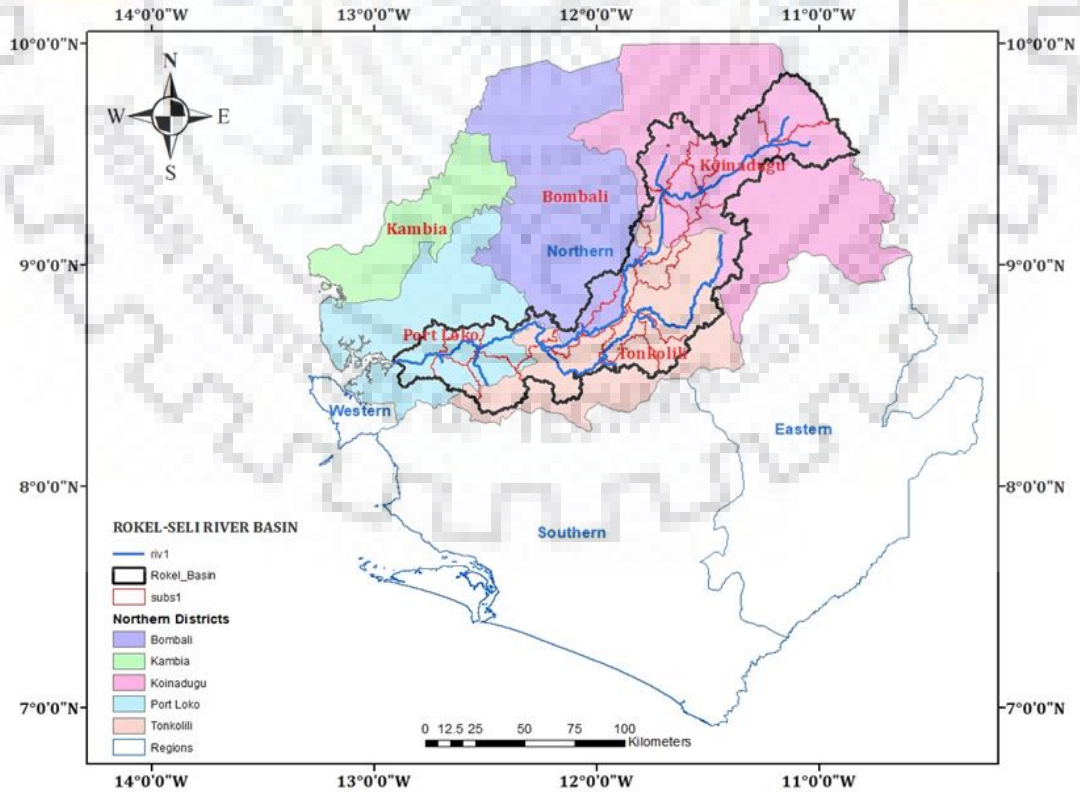

Figure 3. 3: Map of Northern Region Showing RSRB laying across five Districts

is complemented through withdrawal from river discharge during the worst periods in the dry season. This influences the Addax Bio-energy project to expand significantly in respect of water resources requirement, specifically guaranteeing conjunctive water needs at downstream of the Rokel-Seli River.

Moreover, London Mining Ltd and Africa Minerals Ltd, which were known to be the country's largest mining companies depends on the river to pre-process iron ore. Plenty of other mining companies depend on it for sand and gold.

3.2 HISTORICAL RAINFALL DATA SETS

The Ministry of water Resources (MWR), the lead government institution of Sierra Leone responsible for monitoring water resources has in collaboration with multiple and diverse organizations re-established hydrological monitoring activities. Through this, the Sierra Leone water Security website (https://www.salonewatersecurity.com/data) was created to serve as a repository for hydrological (rainfall, surface water and groundwater) data. The Sierra Leone Water Security portal has made available river-wise daily/monthly rainfall for the entire country from 1960 to date.

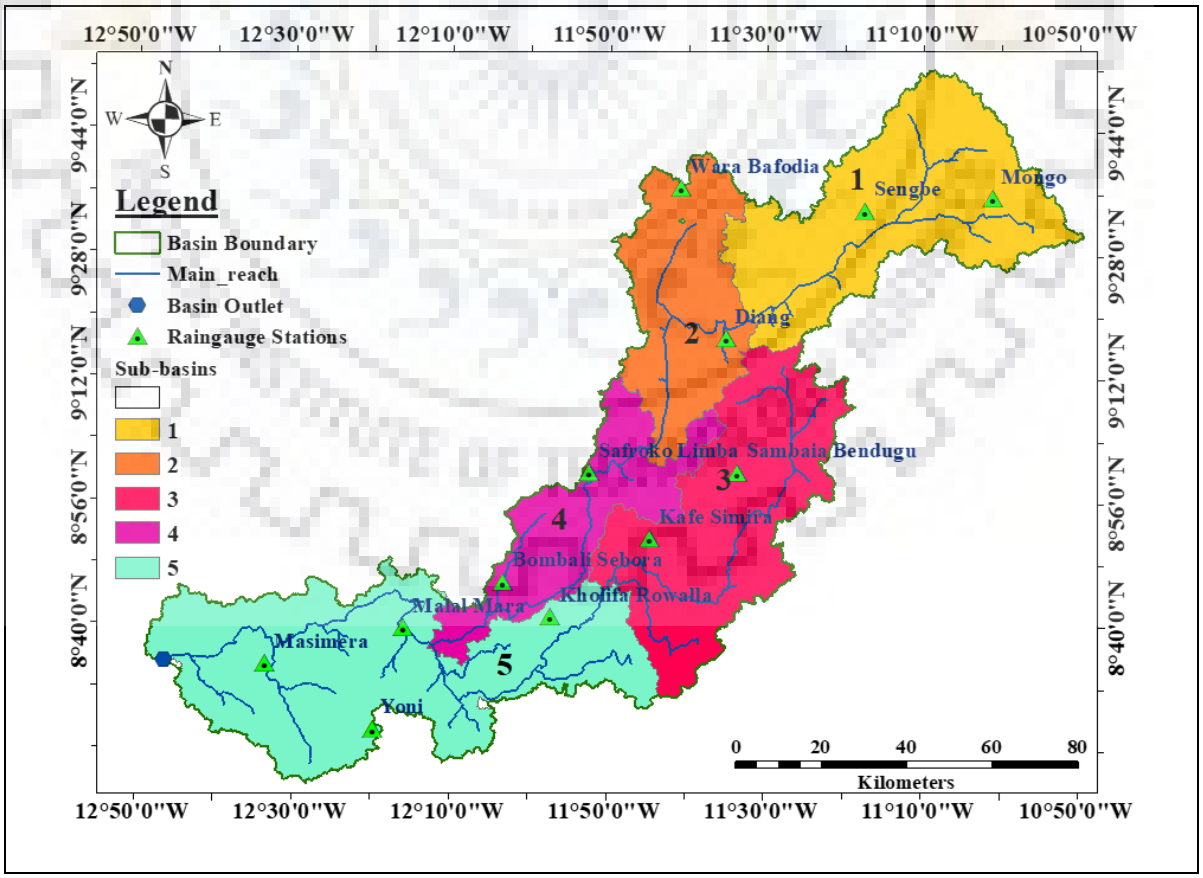

Figure 3. 4: Map of RSRB with location of Rain Gauge Stations

In this research, the rainfall data used has been provided by this portal and there are thirteen (13) rain gauge stations in the Rokel-Seli river basin from 1961 to 2005. Each of these stations is located on the basin as shown in **Fig. 3.4.** Thus, the average historical monthly, annual and seasonal rainfall of Rokel-Seli River Basin for the period of 1961 to 2005 is shown in **Table 3.1**

Table 3. 1: Historical Average monthly, annual and seasonal rainfall (mm) of Rokel-Seli River Basin for the period of 1961 to 2005

Station	J	F	M	A	M	J	J	A	S	O	N	D	Annual	Wet Season	Dry Season
Bombali	10	15	47	115	300	361	374	483	435	265	91	13	2507	2217	290
Diang	12	17	31	91	276	394	493	545	480	278	126	28	2772	2467	305
Kafe Simera	6	11	18	74	251	360	460	599	508	318	106	18	2729	2496	233
Kholifa Rowala	14	14	25	97	279	323	337	487	427	338	125	20	2486	2191	295
Koya	3	9	25	74	188	300	355	421	362	279	80	10	2106	1905	202
Malal Mara	5	7	17	72	310	361	449	550	483	268	91	14	2627	2421	206
Masimera	10	11	31	97	246	306	312	443	418	339	109	11	2333	2064	269
Mongo	9	8	21	76	203	284	312	406	363	221	62	9	1972	1787	185
Safroko Limba	9	13	25	104	307	351	426	518	455	281	104	13	2605	2338	268
Sambaia	9	11	16	66	223	365	417	508	439	269	84	17	2425	2220	204
Sengbe	7	6	20	83	241	317	341	419	348	203	61	9	2054	1868	186
Warra Bafodia	7	9	20	92	257	310	356	454	437	364	150	17	2474	2179	295
Yoni	13	10	24	120	333	399	445	519	442	235	68	11	2618	2373	245
Average Rainfall	**9**	**11**	**25**	**89**	**263**	**341**	**390**	**488**	**431**	**281**	**97**	**15**	**2435**	**2194**	**245**
Standard Deviation	**3**	**3**	**8**	**17**	**43**	**37**	**61**	**58**	**49**	**48**	**27**	**5**	**256**	**232**	**45**

3.2 RAINFALL TRENDS

Increasing dependability on water resources is on rise to fulfilling water requirement for irrigation domestic and industrial growth for growing population. Researchers have indicated that the global warming is one of the factors which highly influences the changes in rainfall pattern at regional scale as well as in all over the world.

3.3.1 Non-Parametric Trend Analysis Methods

These methods are employed when detecting monotonic trends in environmental data, climate data and hydrological data. In this study the Mann-Kendall Test (MKT), the Modified Mann-Kendall test (MMKT) and Theil Sen's Slope methods were applied for detection of trends during the period of 1961-2005 over RSRB.

3.3.1.1 Mann-Kendall (MK) Test Procedure

The Mann-Kendall test statistic *S* is calculated using the formula as follows:

$$S = \sum_{i=1}^{N=1} \cdot \sum_{j=i+1}^{N=1} \mathrm{sgn}\left(x_j - x_i\right) \tag{3.1}$$

Where and are the annual values in years j and i, j>i respectively, and N is the number of data points. The value of $\mathrm{sgn}(x_j - x_i)$ is computed as follows:

$$\mathrm{sgn}\left(x_j - x_i\right) = \begin{cases} 1 if\left(x_j - x_i > 0\right) \\ 0 if\left(x_j - x_i\right) = 0 \\ -1 if\left(x_j - x_i\right) < 0 \end{cases} \tag{3.2}$$

This statistics represents the number of positive differences minus the number of negative differences for all the differences considered. For large samples (N>10), the test is conducted using a normal approximation (Z statistics) with the mean and the variance as follows:

$$E[S] = 0 \tag{3.3}$$

$$Var(S) \frac{1}{18}\left[N(N-1)(2N+5) - \sum_{p=1}^{q} t_p\left(t_p - 1\right)\left(2t_p + 5\right)\right] \tag{3.4}$$

Here q is the number of tied (zero difference between compared values) groups, and t_p is the number of data values in the p^{th} group. The values of S and VAR(S) are used to compute the test statistic Z as:

$$Z = \begin{cases} \frac{S-1}{\sqrt{Var(S)}} if S > 0 \\ 0 if S = 0 \\ \frac{S+1}{\sqrt{Var(S)}} if S(S) < 0 \end{cases} \tag{3.5}$$

The presence of a statistically significant trend is evaluated using the Z value. A positive value of Z will indicate an upward trend and its negative value a downward trend.

3.3.1.2 Modify Mann-Kendall Test (MMKT) Technique

The Modified Mann-Kendall test has been used for trend detection of autocorrelation series. Therefore, in this analysis the autocorrelation between the ranks of the observations 'pk' has been estimated after subtracting the non-parametric Sen's median slope from the slope.

$$\frac{n}{n^*} = 1 + \frac{2}{n(n-1)(n-2)} \times \sum_p^q (n-k)(n-k-1)(n-k-2)p \quad (3.6)$$

Significant values of 'pk' have only been used for calculating the variance correction factor n/n* and it was calculated from the equation proposed by Hammed and Rao (1998).

Where:

n represents the actual number of observations,

n* is represented as effective number of observations to account for the autocorrelation in the data and pk is the autocorrelation function for the ranks of the observations.

The corrected variance is then given as (Hamed et al, 1998).

$$Var^*(S) = Var(S) \times \frac{n}{n^*} \quad (3.7)$$

Where: Var*(S) is from equation (3.4)

3.3.1.3 Theil Sen's Slope Estimator

Sen (1968) developed a non-parametric method to estimate the magnitude (slope) of the trend in a time series (Sen, 1968). This method assumes a linear trend in the time series. In this method, the slope Qi of all data value pairs are calculated according to:

$$Qi = \frac{x_j - x_k}{j - k} \quad (3.8)$$

Where: j>k. If there are n values x_j in the time series we get as many as N = n(n-1)/2 slope estimates Qi. The Sen's estimator of the slope is the median of these N values of Qi. The N values of Qi are ranked from the smallest to the largest and the Sen's estimator as follows:

$$Q = \left(Q_{\left[\frac{n+1}{2}\right]} \right), \text{ if N is odd} \quad (3.9)$$

Or

$$Q = \frac{1}{2}\left(Q_{\frac{n}{2}} + Q_{\left[\frac{n+2}{2}\right]} \right), \text{ if N is even} \quad (3.10)$$

A simple Flow Chat of the non-parametric trend analysis using the described methods can be shown in Fig. 3.5 as follows:

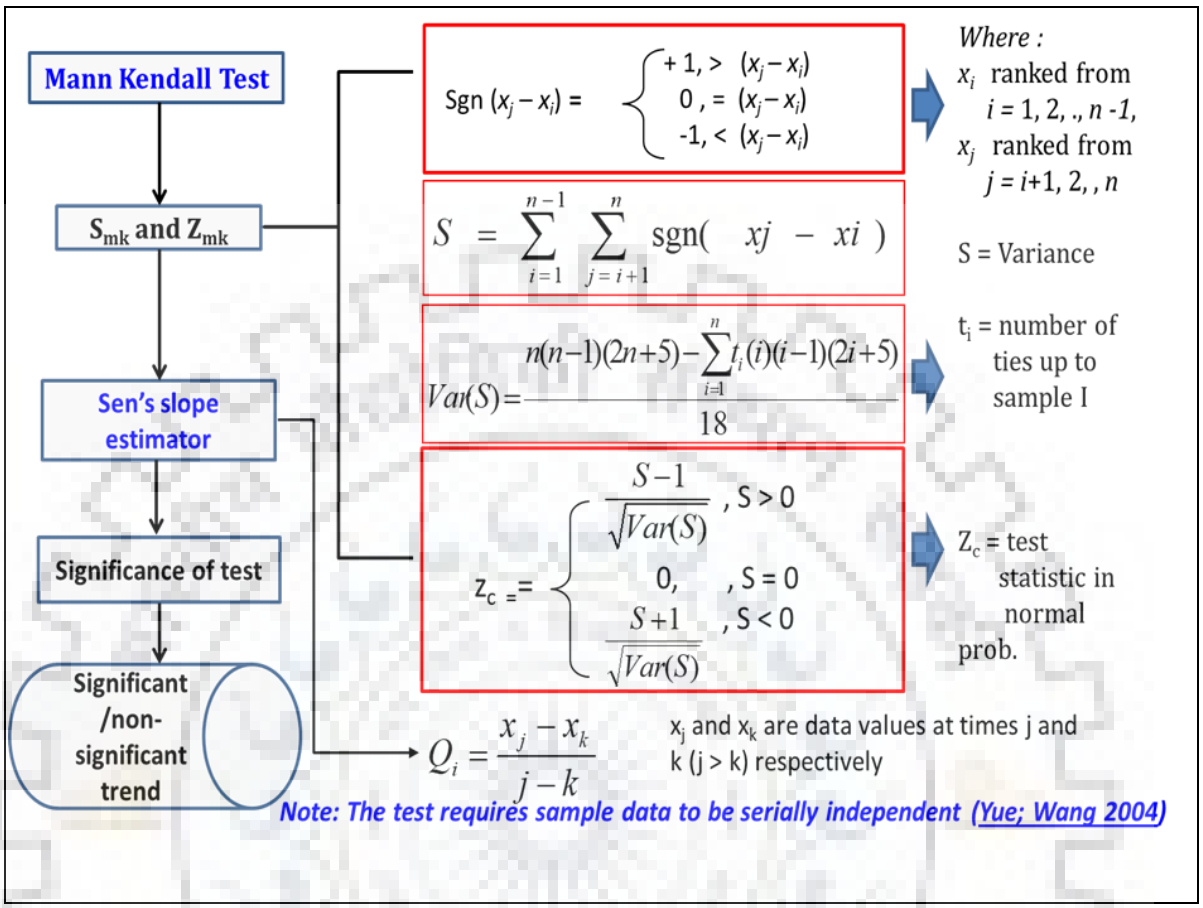

Figure 3. 5: Flow Chart of Non-Parametric Trend Analysis Methods

3.3.2 Homogeneity Shift Change Detection Method

3.3.2.1 PMWT and SNHT Pettitt's Mann-Whitney Test (PMWT) and Standard Normal Homogeneity Test (SNHT)

Application of homogenization on climatic time series preserve the climatic signal and reduce the impact of non-climatic factors in the time series. Therefore, it is important to address these factors in order to develop homogenized records for studying climate change. Change-point analysis examines climate data discontinuities and it directly addresses the question of where the change in the mean value of the observations is likely to have occurred.

45years time series (1961-2005) data were investigated for homogeneity using PMT and SNHT at 5% significance level (i.e. 95% Confidence interval) for the all stations in RSRB. This methods were executed using XLSTAT4014.5.03 software for examination of homogeneity in the time series.

3.3 FUTURE RAINFALL PROJECTIONS

With population growth, increasing human activities (e.g., land use/cover change and irrigation) as an external force exerts more and more influences on the hydrology cycle. Thus, evaluating the future variation of hydrologic cycle and water resources has special significance for regional planning and water resources management. Therefore, inquiring how climate and land use land cover change affect the seasonal and annual characteristics of hydrological variables is important in projecting the future variation of hydrology and water resources.

Climate variables including precipitation and temperature being the most important affects the environment and these parameters changes in both space and time. Climate change means the long term regular changes of geometrical properties of climatic variables. A change in climate can be identified in terms of statistical analysis of extended time series of climatic variables from its mean values.

Global Climate Models (GCMs) are the basic tools which provide future projections for climate variables in a changing ecosystem. GCMs are complex geometric models capable of replicating the performance of the mesosphere, ocean and land surface in three dimensions. Though they remain relatively coarse in resolution, and are unable to resolve significant sub-grid scale features often necessary in any hydrologic study. Therefore, studies dealing with the climate change impact assessment at catchment scale require downscaling of GCM projections to an appropriate scale to represent the catchment heterogeneity. Various statistical and dynamic downscaling methods have been adopted in the past to downscale large scale atmospheric variables from the GCMs to a regional scale or to a finer scale representative of a catchment.

Climate change projections are based on the Green House Gas (GHG) emission scenarios in different conditions of economic and technological development, also the balance between global and local growth. The World Climate Research Programme Coupled Model Intercomparison Project phase 3 (CMIP3) and CMIP5 datasets each contain output from a large number of GCMs. The amount of greenhouse gas in the atmosphere in the future is described both datasets using different scenarios. CMIP3 uses scenarios from the Intergovernmental Panel on Climate Change's (IPCC) Special Report on Emissions Scenarios (SRES) and CMIP5 uses Representative Concentration Pathways recommended in the Intergovernmental Panel for Climate Change (IPCC) Fifth Assessment Report (AR5).

In 2014, four new greenhouse gas scenarios for the fifth Assessment Report (AR5) were released by the IPCC, known as Representative Concentration Pathways (RCPs) 2.5, 4.5, 6 and 8.5. These scenarios were named according to their possible range of radiative forcing values (Wm-2) by the end of the 21st century compared to the pre-industrial values [20]. Some hydro climatic studies have been carried out using the GCMs and RCP scenarios as future climate scenarios under three RCP 2.6, 4.5 and 8.5 scenarios. Therefore for the purpose of this study, the same scenarios; RCP 2.6, 4.5 and 8.5 have been considered. Hence the current study helps to understand the sensitivity of the basin to the projected climate scenarios.

Further, the spatial and temporal uneven distribution of utilizable water resources makes the situation more complex. Growing awareness of climate change and land use/cover pattern over the basin has effects on both quantity and quality of water resources leading to increasing demand for better management planning options for the optimum utilization of available resources. Nevertheless, sustainable planning of water resources in the basin requires information on the present spatial and temporal variability of rainfall, as well as the hydrological response to development policies on climate change Impact.

3.4.1 Statistical Downscaling Method (MLR Technique)

Researches dealing with climate change impact assessment at catchment scale require downscaling of GCM projections to an appropriate scale to represent the catchment heterogeneity (Silberstein et al, 2012). Various statistical and dynamic downscaling methods have been adopted in the past to downscale large scale atmospheric variables from the GCMs to a regional scale or to a finer scale representative of a catchment (Silberstein et al, 2012 Annand et at, 2008). For the purpose of this study, statistical downscaling method (SDSM) has been applied.

MLR technique is a SDSM used in this research for downscaling monthly rainfall for the future rainfall projection for RSRB which gives reasonable results. The methodology can be shown in the form of flow chart as in **Fig. 3.6**

The critical steps of the suggested methodology can be described as follows

1. Perform consistency check of observed monthly rainfall (Predictand) using Hydrognomon (Ver.4) for the period of 1961-2005

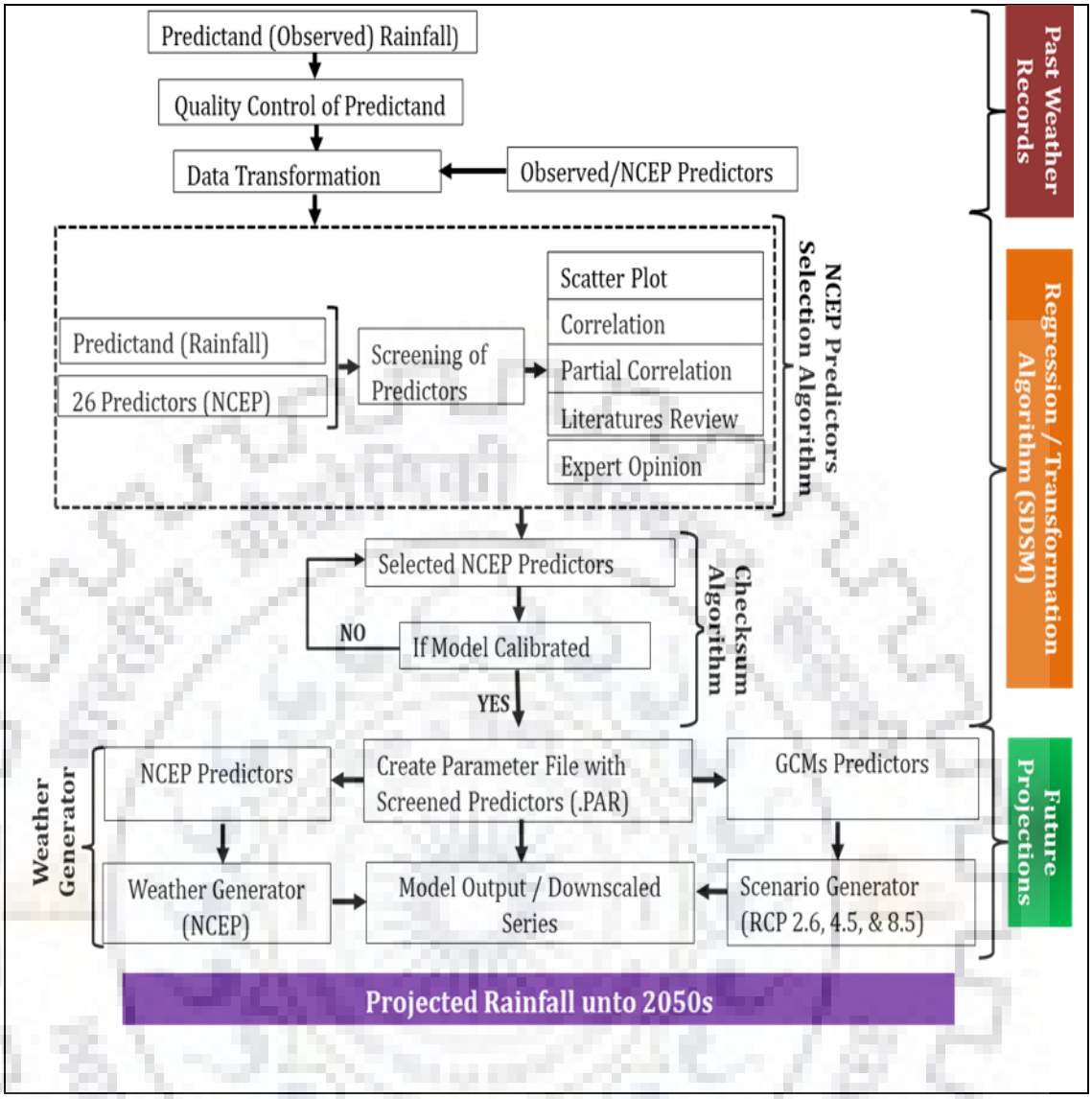

Figure 3. 6: Flow diagram of future rainfall projection Methodology

2. Transfer National Centre of Environmental Predictions (NCEP) and Global Circulation Models (GCM) predictors for the study area from Canadian Centre for Climate Modeling and Analysis (CanESM2) http://www.climate-scenarios.canada.ca corresponding to Representative Concentration Pathways (RCP2.6, RCP4.5 and RCP8.5) emission scenarios and then convert the predictors from daily to monthly basis taking average of each predictor over the month.

3. Identify calibration period (from 1961-1990) and validation period (from 1991-2005) for the calibration and validation of the model

4. Develop the empirical relationship between historical rainfall (predictand) and the 26 predictors using MLR technique on calibration period data

5. Using expert opinion based on scatter plot, partial correlation, correlation etc. the most suitable predictors were identified

6. Rainfall (Predictand) were estimated during the validation period using the selected predictors and compared with the observed values

7. The probable error in the observed and the estimated values were calculated and bias correction was applied to correct the predicated values

8. The important indicators of the goodness of regression were checked by the following parameter; Nash-Sutcliffe Error Estimate (NS-EE), Coefficient of Correlation (CC), Normalized Mean Square Error (NMSE), and the Root Mean Square Error (RMSE)

9. The suggested series of NCEP Corresponding to RCP2.6, RCP4.5 and RCP8.5 scenarios and the selected predictors were used to generate the future series of the predictand for the periods of 2020s and 2050s.

Statistical downscaling method was applied for downscaling the monthly rainfall of RSRB for future projections using traditional downscaling regression based approach; Multiple-Linear Regression (MLR). The general formular of MLR is written as:

$$Y^{MLR} = \alpha + \sum_{i=1}^{n} \beta_i X_i + \varepsilon$$

Where, Y^{MLR} is the estimated predictand (rainfall), α is the intercept; β is the regression coefficients, X_i is the predictor (26 parameters and ε is the error term. Regression coefficients at 95% confidence level were estimated with Durbin-Watson technique for residuals estimation. SPSS (Ver.24) was applied for model fit, correlation values, coefficient of determination, descriptive statistics etc.

However, the estimated rainfall series to be compared with her observe rainfall, frequency assessment is necessary. Hence performance evaluation for calibration and validation periods, Root Mean Square Error (RMSE), Normalized Mean Square error (NMSE), Nash-Sutcliffe Coefficient (NS-EE), and Correlation Coefficient (CC) are considered as given below:

1. Root Mean Square Error

$$RMSE = \sqrt{\frac{1}{N}\sum_{i=1}^{N}\left(y_i - \hat{y}_i\right)^2}$$

2. Normalized Mean Square error

$$NMSE = \frac{\frac{1}{N}\sum_{i=1}^{N}\left(y_i - \hat{y}\right)^2}{\sigma^2}$$

3. Nash-Sutcliffe error estimate (Nash and Sutcliffe, 1970)

$$NS = \frac{\frac{1}{N}\sum_{i=1}^{N}\left(y_i - \hat{y}\right)}{\frac{1}{N}\sum_{i=1}^{N}\left(y_i - \overline{y_i}\right)^2}$$

4. Correlation coefficient (CC)

$$CC = \frac{N\sum\left(y_i \times \hat{y}\right) - \left(\sum y_i\right) \times \left(\sum \hat{y}_i\right)}{\sqrt{\left[N\sum y_i^2 - \left(\hat{y}_i\right)^2\right] \times \left[N\sum y_i^2 - \left(\hat{y}\right)^2\right]}}$$

Where, y_i and $\hat{y}_i$ are the observed and simulated predictand time series. N is number of data point used in simulation, σ^2 is variance of n target values.

In applying the above methodology for the future projection of rainfall over Rokel-Seli river Basin the daily observed predictor data of atmospheric variables derived from NCEP 2.8^0 (latitude) x 2.8^0 (longitude) grid-scale for 45 years (1961-2005) were obtained from CanESM2. The data was extracted between latitude 8.92^0N to 9.3^0N and longitude -11.98^0E to -11.53^0E (BOX_125X_36Y). The Representative Concentration Pathways (RCP2.6, 4.5 8.5) emission scenarios were also downloaded from CanESM2. Full descriptions of NCEP variables (predictors) are elaborated in the **Table 3.2**

The Geostrophic air flow velocity, Vorticity, Zonal velocity component, Meridional velocity, Divergence and Wind direction are variables derived using the geostrophic approximation at different atmospheric levels.

Table 3. 2: Variables and description of NCEP and GCM predictors (26 Variables)

SNo.	Variable	Description	Unit	SNo.	Description	Unit
1	ncepmslpgl	Mean sea level pressure	Pa	**14**	Geostrophic air flow velocity	m/s
2	ncepp1_fgl	Geostrophic air flow velocity	m/s	**15**	Zonal velocity component	m/s
3	ncepp1_ugl	Zonal velocity component	m/s	**16**	Meridional velocity component	m/s
4	ncepp1_vgl	Meridional velocity component	m/s	**17**	Vorticity	/s
5	ncepp1_zgl	Vorticity	/s	**18**	Wind direction	
6	ncepp1thgl	Wind direction	m/s	**19**	Divergence	/s
7	ncepp1zhgl	Divergence	m/s	**20**	500 hPa geopotential height	m
8	ncepp5_fgl	Geostrophic air flow velocity	m/s	**21**	850 hPa geopotential height	m
9	ncepp5_ugl	Zonal velocity component	m/s	**22**	Near surface relative humidity	%
10	ncepp5_vgl	Meridional velocity component	m/s	**23**	Specific humidity at 500 hPa height	kg/kg
11	ncepp5_zgl	Vorticity	/s	**24**	Specific humidity at 850 hPa height	kg/kg
12	ncepp5thgl	Wind direction	m/s	**25**	Near surface specific humidity	kg/kg
13	ncepp5zhgl	Divergence	/s	**26**	Mean temperature at 2m	K

The vorticity measures the rotation of the air, Zonal velocity component is the velocity component along a line of latitude (i.e. east-west), Meridional velocity component is the velocity component along a line of longitude (i.e. north-south), Divergence relates to the stretching and outflow of air from the base of an anticyclone. Wind direction variable is the only variable which is not normalized. The same parameters are considered in comparing the results based on MLR method. The MLR equations derived for each rainfall station can be given as follows:

Bombali: $207.1 + 24.3X_{15} – 9.8X_{19} + 30.3X_{20} + 169.3X_{22}$

Diang: $253.6 + 45X_{7} + 68.4X_{11} + 103.3X_{22} + 39.5X_{23} + 45.4X_{24} – 45.4X_{25}$

Kafe Simera: $236.5 + 29.4X_{15} – 0.5X_{19} + 18.4X_{20} + 215.7X_{22}$

Kholifa Rowala: $226.4 + 29.4X_{7} + 41.8X_{11} + 69.1X_{22} + 41.5X_{23} + 30.2X_{25}$

Koya: $182.1 + 13.8X_{15} – 0.3X_{19} + 18.7X_{20} + 164.2X_{22}$

Malal Mara: $210.5 + 42.8X_{15} + 12.9X_{19} + 35.3X_{20} + 183.1X_{22}$

Masimera: $213.2 + 22.8X_{7} + 40X_{11} + 64.7X_{22} + 39.9X_{23} + 32.8X_{25}$

Mongo: $162.1 + 25X_{15} – 1.5X_{19} + 24.4X_{20} + 142.3X_{22}$

Safroko Limba: $244.6 + 68.8X_{11} + 56.8X_{22} + 52.3X_{23} + 25.1X_{24} + 29X_{25}$

Sambaia: $223.8 + 25.6X_{7} + 22.1X_{11} + 184.9X_{22} – 0.9X_{23} – 13.7X_{25}$

Sengbe: $162.2 + 25.1X_{15} + 2.9X_{19} + 36.8X_{20} + 137.9X_{22}$

Warra Bafodia: $227.1 + 16.5X_{7} + 25.6X_{11} + 100.6X_{22} + 26.9X_{23} + 37X_{25}$

Yoni: $199.4 + 56.4X_{15} – 13.6X_{19} + 41.8X_{20} + 158.3X_{22}$

Where, X_7 = Divergence; X_{11} = vorticity; X_{15} = Zonal velocity component; X_{19} = Divergence; X_{20} = 850 hPa geopotential height; X_{22} = near surface relative humidity; X_{23} = Specific humidity at 500 hPa height; X_{24} = specific humidity at 850 hPa height; X_{25} = near surface specific humidity.

3.4 BASIN CHARACTERISTICS AND MORPHOMETRY

3.5.1 Basin Characteristic Terminologies

In runoff phenomenon, river basin is the basic hydrologic unit. The physical characteristics of a basin, like drainage channel, shape, area, and slope pattern in a basin are some of the main characteristics that influence volume of surface runoff and shape of runoff hydrograph from a basin due to storm. Analyzing the basin characteristics forms a major component of the subject of geomorphology. Hence, quantitative morphometric analysis such as evaluation of different segments, including, gradient, watershed region, stream order, height contrast, watershed boundary, and profile of a land are relevant to the characteristic advancement of a basin. Some geometrical parameters of a basin as connected to runoff process are briefly described below:

Stream Area (A)

Area is the most utilized parameter to represent the characteristics of a basin. Area of the basin is characterized as the territory of the close curve forming the even projection of the basin limit. The typical units are hectare (ha) for little basin and square kilometer (km^2) for bigger drainage areas.

Relief (H)

Maximum basin relief is the elevation difference (in meters) between the catchment outlet and the highest point on the basin perimeter.

Relief Ratio (H_f)

This is the proportion of relief (H) to the length of basin (L_b) and it is given as

$$R_h = \frac{H}{L_b}$$

Stream Perimeter (P_r)

The overall length of outer boundary of the basin is referred to as Basin Perimeter is measured by an instrument called planimeter.

Stream Order

Stream order is a characterization mirroring the outline of branches that join to shape the trunk stream leaving the basin. The least stream from the beginning of the system is assigned as 'order 1'. Two channels of 'order 1' when joined forms a stream of 'order 2'. Two channels of 'order 2' when joined forms a stream of 'order 3' etc. Realizing that when a lower order stream (say order 2) meets a higher order stream (say order 3) the order of the subsequent stream is as yet the higher order stream entering the confluence. The storage trunk stream releasing out of the drainage basin will be the highest stream order. The drainage network of RSRB is shown in **Fig. 3.7** which gives all stream orders of the basin as related to elevation.

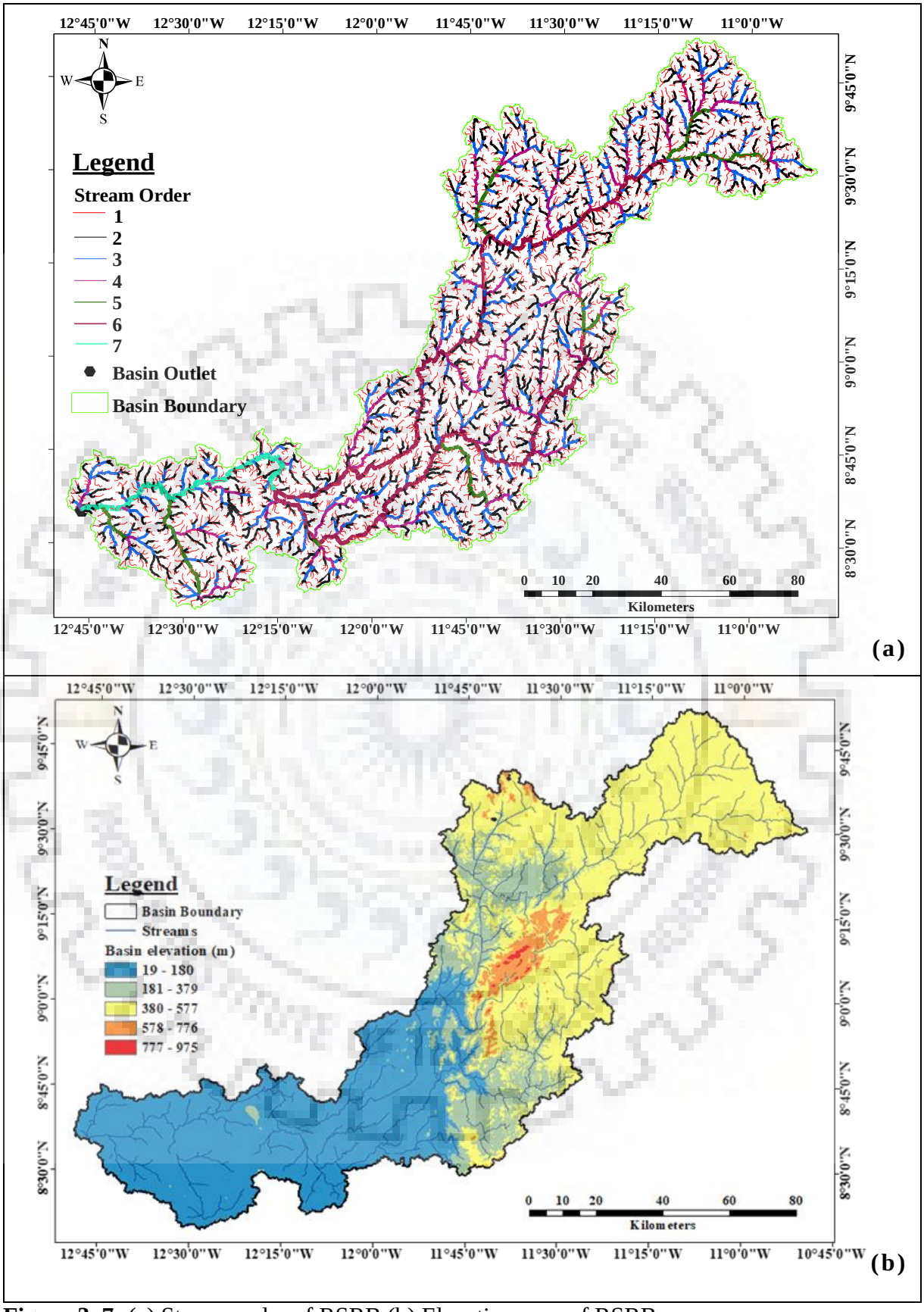

Figure 3. 7: (a) Stream order of RSRB (b) Elevation map of RSRB

Stream order is practical in assigning the idea of a drainage pattern of basin and is useful in finding watershed treatment structures like check dams and Nala bunds. Maps of stream orders and elevation for each sub-basin are shown in **Fig 3.8-3.12 (a, b)** respectively. This serves to better understand the stream network for each sub-basin.

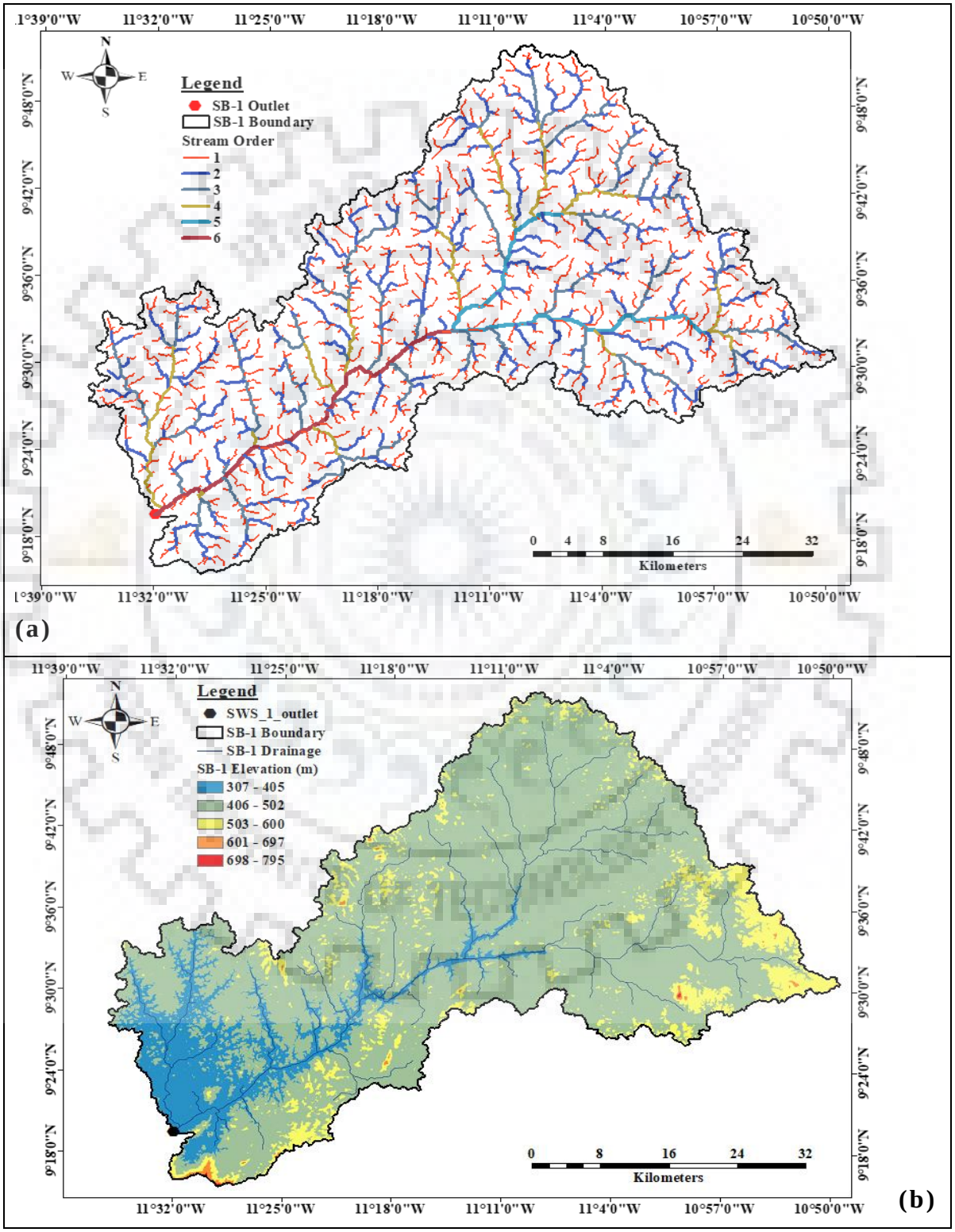

Figure 3. 8: (a) Stream order of Sub-Basin-1 (b) Elevation map of Sub-Basin-1

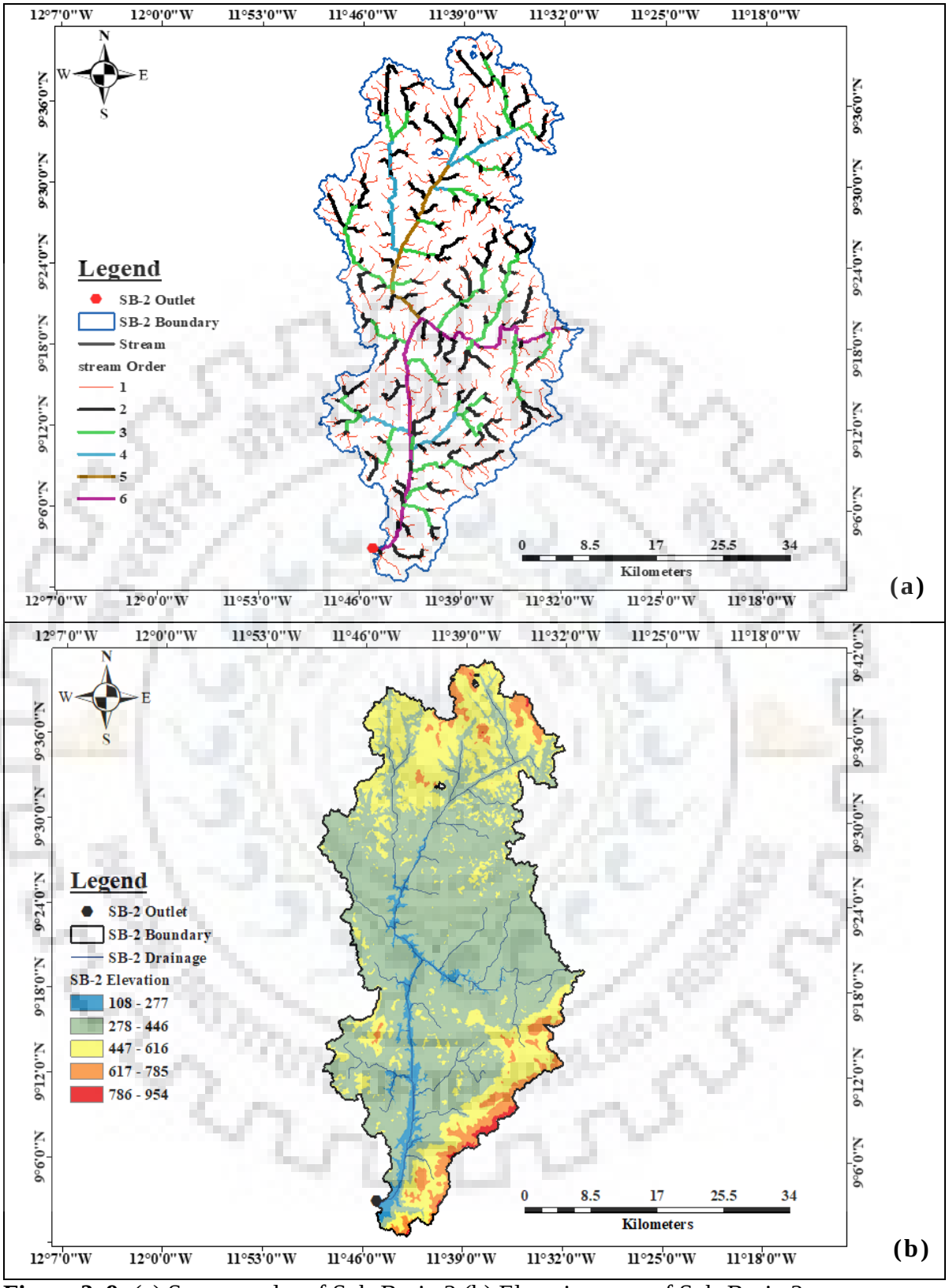

Figure 3. 9: (a) Stream order of Sub-Basin 2 (b) Elevation map of Sub-Basin 2

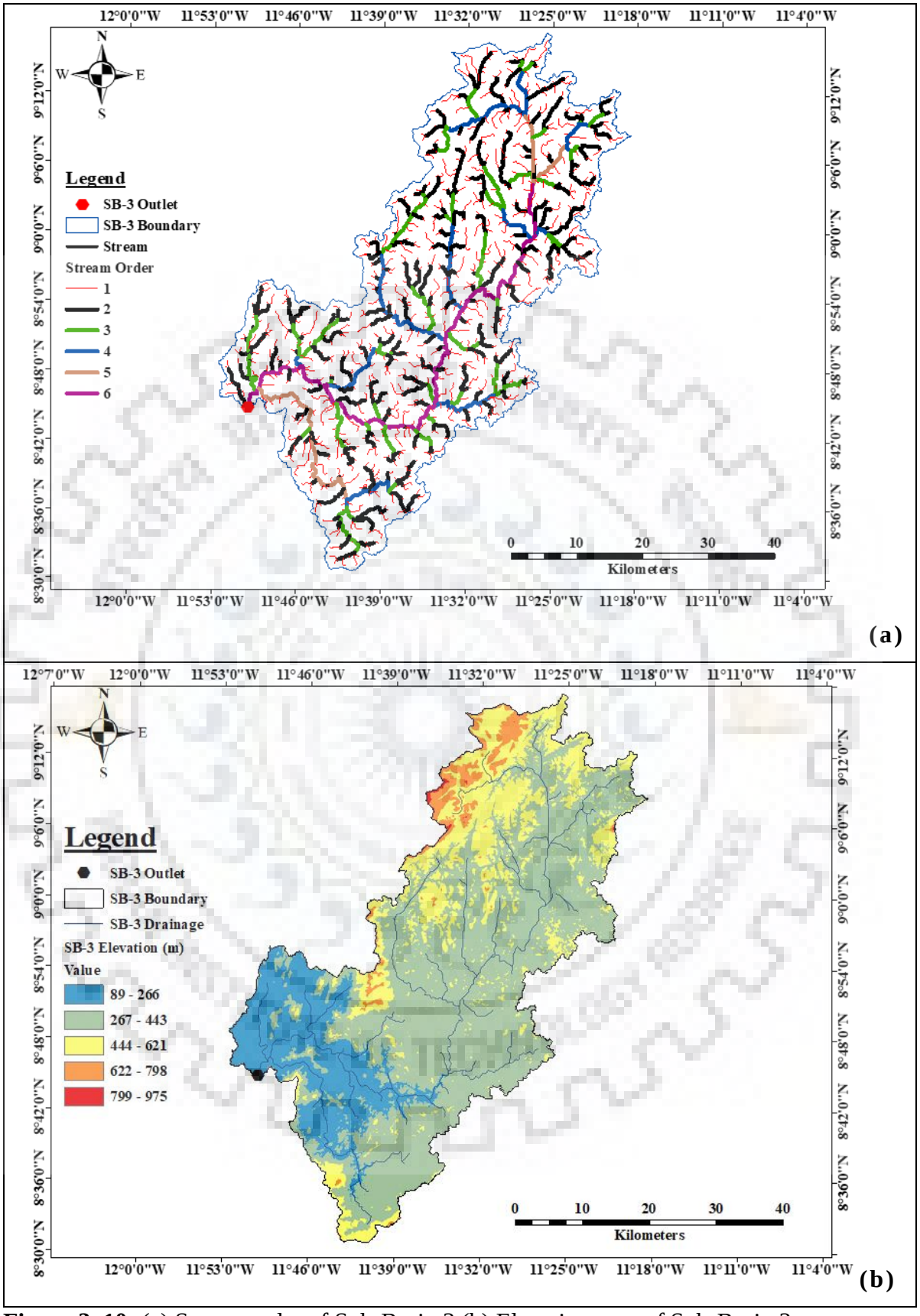

Figure 3. 10: (a) Stream order of Sub-Basin 3 (b) Elevation map of Sub-Basin 3

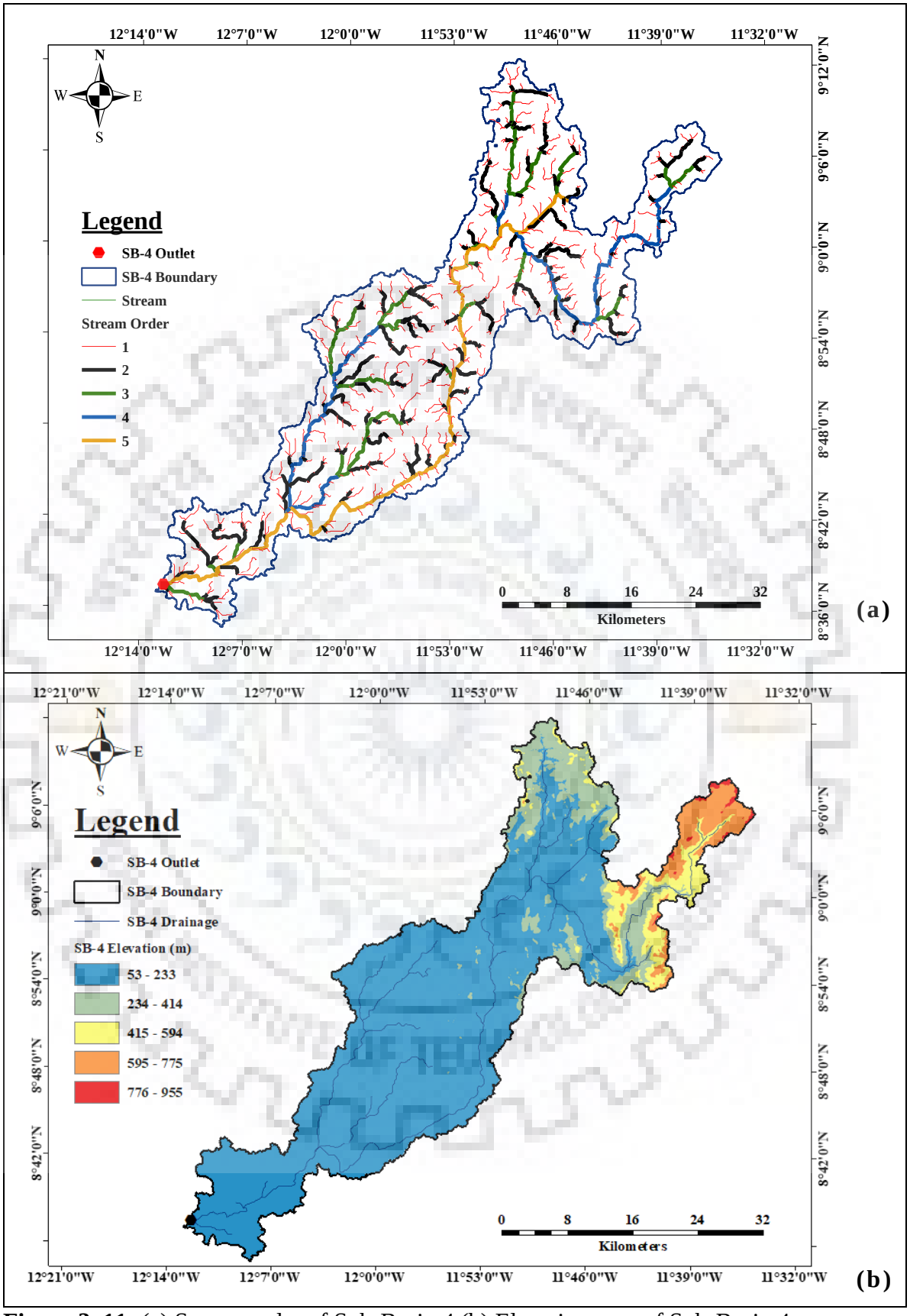

Figure 3. 11: (a) Stream order of Sub-Basin 4 (b) Elevation map of Sub-Basin 4

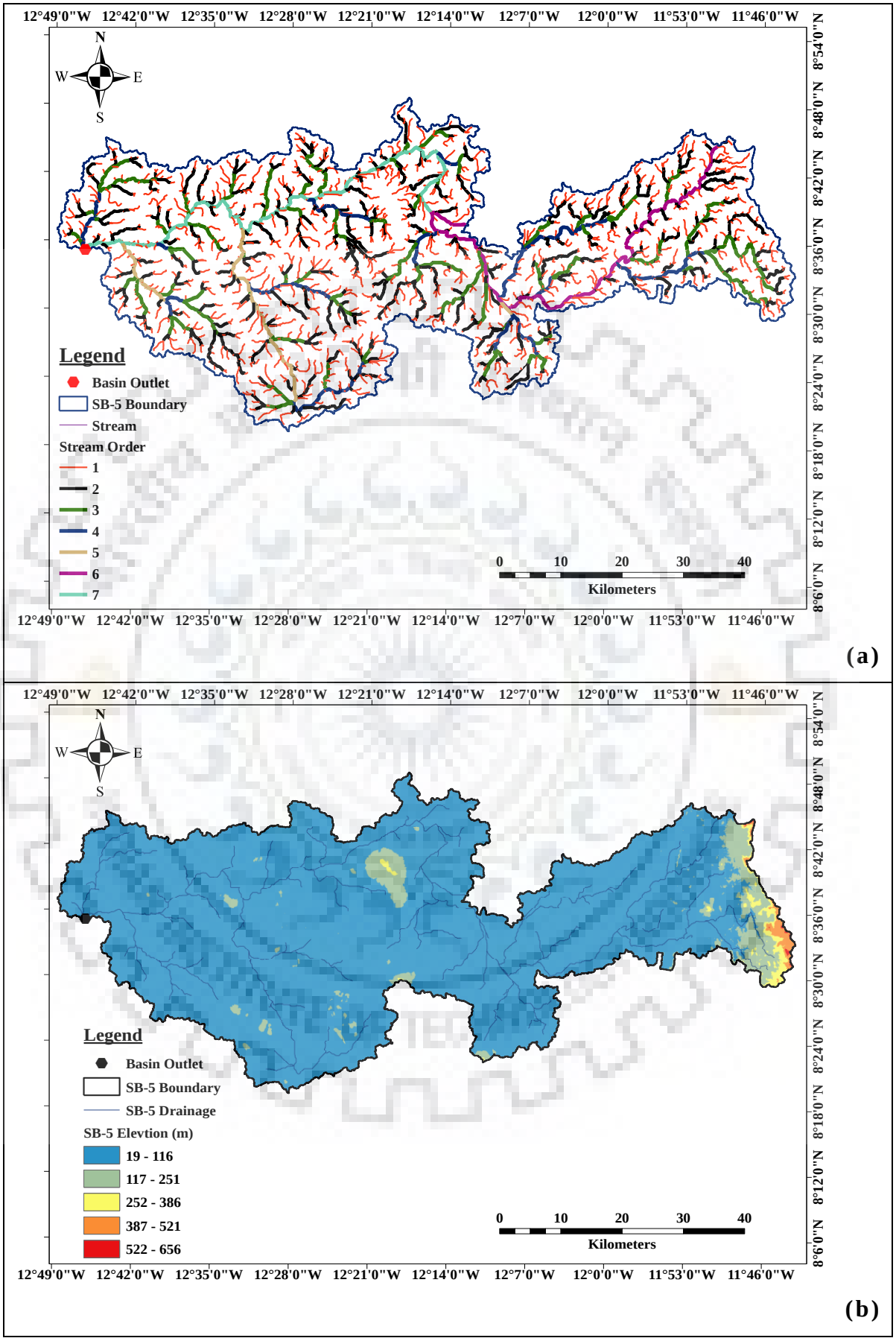

Figure 3. 12: (a) Stream order of Sub-Basin 5 (b) Elevation map of Sub-Basin 5

Compactness of Coefficient (C_c)

This is simply the shape parameter of the basin and the proportion of the basin perimeter to the circumference of equivalent circular area of the basin. It is given as:

$$C_c = \frac{P_r}{\sqrt{4\pi A}}$$

Texture ratio (T)

This is calculated as the proportion of the aggregate number of first order stream segments (N_1) with regards basin's perimeter and hence given as:

$$T = \frac{N_1}{P_r}$$

Slope

A slope profile arranged along the principal stream is utilized to describe the slope of the basin. For a given extent of the stream, the proportion of level expanse between the two end parts of the expanse to the difference in rise between this two points give the slope of the basin. When in doubt, the catchment incline is the most elevated toward the start of the stream and progressively diminishes as one moves along the stream to the bowl outlet. Slope is a vital parameter in numerous watershed recreation models and henceforth it diminishes with its expansion in stream other.

Total Stream Length (L_u)

The total length of all the ordered streams flowing in a continuous path starting from the origin of the least order to the outlet of the largest order within the watershed is known as the total stream length and is given by L_u.

Length of Basin (L_b)

The length of the basin is defined as the length of the main stream measured form its outlet to the remotest point on the basin boundary**.**

Drainage Density (D_d)

The drainage density is a measure of how well the drainage basin is drained by the stream network and hence it is the ratio of the total length of streams of all orders within a basin to its area. It is given as:

$$D_d = \frac{L_b}{A} = \frac{L_u}{A}$$

Stream Number (N_u)

Stream Number is defined as the total count of stream segments of different orders and is given by N_u.

Drainage Frequency (F_s)

This is given as

$$F_s = \frac{N_u}{A}$$

Where, N_u = number of streams, and A = basin area

Form Factor (R_F)

This is given as:

$$R_f = \frac{A}{L_b^2}$$

Where, L_b^2 = basin's maximum length, and A = basin area

Stream Density (S_d)

The proportion of the streams number (N_u) of all orders to the area of the basin (A) of the basin is known as stream density (S_d). It characterizes the quantity of streams per unit area and is symbolic of the drainage channel in the basin. This is given by;

$$S_d = \frac{N_u}{A}$$

Bifurcation Ratio (R_b)

The bifurcation ratio is defined as the ratio of the number of streams in lower order (N_u) to the next order (N_{u+1}). It is noted that the bifurcation ratio is higher in hilly areas than in alluvial areas and this is given by;

$$R_b = \frac{(N_u)}{(N_{u+1})}$$

Circulatory Ratio (R_c)

This is given by;

$$R_c = \frac{12.57A}{P_r^2}$$

Where, P_r^2 = basin's maximum Perimeter, and A = basin area

Elongation Ratio (R_c)

It is estimated as:

$$R_c = \frac{2}{L_b}\sqrt{\frac{A}{\pi}}$$

Where, L_b = basin's maximum Perimeter, and A = basin area

3.5.2 Basin Morphometry Methodology

Morphometric analysis starts by getting digital elevation model (DEM) of the particular study area. In this analysis, DEM of the investigation zone was downloaded. The Shuttle Radar Topography Mission (SRTM) DEM was used for this application. Before utilizing the downloaded DEM, it was required to apply the geometric amendment. Consequently, the SRTM GDEM was re-project to Universal Transverse Mercator (UTM) co-ordinate system at the standard Datum of WGS 1984 (Zone-29N) with a corresponding spatial resolution of 30m. This DEM was then opened in Arc-GIS 10.3 programming application for morphometric investigations. The Arc-GIS 10.3 programming application has Spatial Analyst Tools with a sub-module for Hydrology. This hydrology module was used for getting distinctive layers of data, for example, Fill, Flow Direction, Flow Accumulation, stream

length, Stream Network, Stream Order, and border limits of different basins and sub-basins as per stream system. Morphometric investigation was sub-partitioned into three characteristics i.e., linear, elevation and aerial Characteristics. However, bifurcation ratio, stream length ratio, stream length and stream order, were considered to conform with linear characteristics, relief ratio and basin relief were taken to conform with relief characteristics and circulatory ratio, elongation ratio, drainage density, stream frequency, form factor, length of overland flow were regarded to conform with aerial characteristics, which were considered to be accounted for the characterization of the basin.

Erosion of soil in the basin could either be proportional or inversely proportional to the basin characteristics. For instance, soil erosion is proportional to the bifurcation ratio, relief ratio, texture ratio, drainage density, stream frequency, and length of overland flow. On the other hand, it is inversely proportional to circulatory ratio, elongation ratio, form factor, and compactness coefficient. Sub-bans were given score for each of the parameters accordingly. The sub-basins which are more vulnerable to soil erosion will have higher value of the directly proportional characteristics which denotes a lower ranking (say 1) the reverse is same. All the basin characteristics were regarded to be equally important. Further, the average value of the rank score for each of the sub-basin were estimated. In respect of this phenomenon, the sub-basins with lower rank were categorized as the most vulnerable to soil erosion. Hence, the sub-basin with lower rank score were then considered to be prioritized for soil conservation measures. Summary of the morphometric analysis as elaborated above can be shown in **Fig 3.13.**

3.5 LAND-USE LAND-COVER APPLICATIONS

3.6.1 Land-Use Land-Cover Dataset

Land-use data was obtained from the USGS Global Visualization Viewer (GloVis) website (http://glovis.usgs.gov/) which is freely available. Landsat-8 at 30m resolution multispectral image data was downloaded and for the period of February, 2010. The select month was appropriate since cloud free and hence it is the driest period of the year. These images were then processed into Band 4, 3, 2 (false color) composites that highlight vegetation and water while enhancing interpretation as the images produced are visually similar to those from color infrared aerial photography. Various studies have used these bands to study land use change and monitor drainage patterns. The benefits of using remotely sensed data to better manage

water resources, particularly in irrigated agriculture to determine land use and irrigated crop acres.

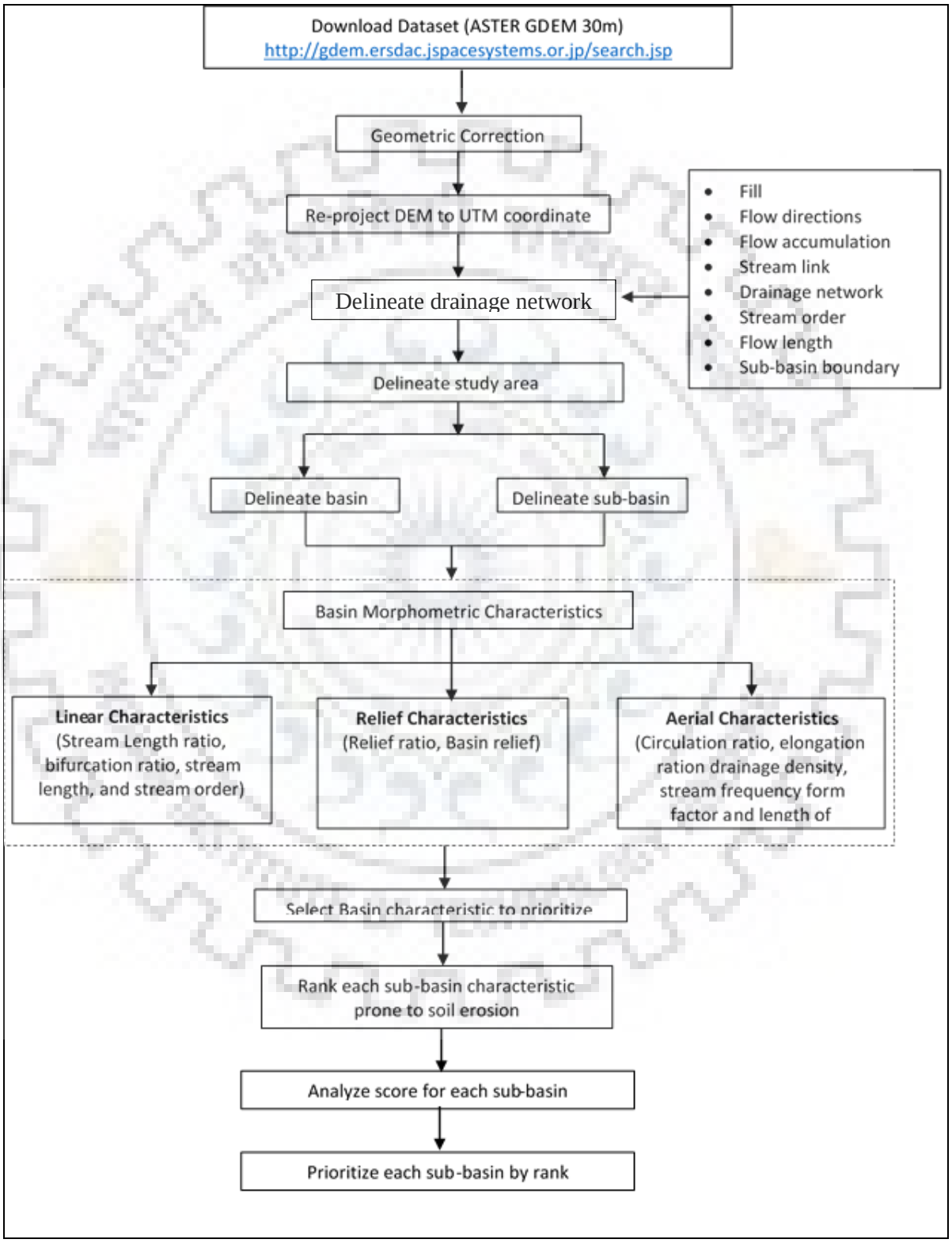

Figure 3. 13: Summary of morphometric methodology

3.6 LULC CLASSIFICATION APPROACH

In carrying out the basic land use land cover (LULC) classification approach in this study, the study area was extracted according to boundary of the basin and recognized the possible features of land-use/land-cover with defined classes. The supervised training samples were then selected from the supervised classification and create the signature file (.sig). The final result of (LULC) relies on the nature of signature file and user accuracy.

Further, major confusion matrix and accuracy analysis was done. Maximum likelihood image classification method was used for this Analysis. Lastly, different class validation methods can be selected i.e., references (statistical data, thematic maps Topographic maps, , etc.) google and by earth visual interpretations. These two approaches have been applied. If the accuracy of the LULC is satisfactory, then the processed land-use is also satisfactory. These processes described above for the LULC change detection are better explained in the flow chart in **Fig. 3.14**

3.7 LULC AND CLIMATE CHANGE IMPACT WITH SWAT MODEL APPLICATION

3.8.1 Overview of SWAT Model

Soil and Water Assessment Tool (SWAT) (Arnold et al., 1993), among other semi-distributed watershed models such as European hydrological system MIKE SHE (Laflen et al., 1991), Hydrological Simulation Program-Fortran (HSPF), Areal Non-point Source Watershed Environment Response Simulation (ANSWERS) (Beasley et al., 1977),

Agricultural Non-Point Source Pollution (AGNPS) (Young et al., 1989), has been observed to be broadly acknowledged which is a continuation of almost 40 years of prototypical works led by USDA Agricultural Research Service (ARS) (Tripathi, et al., 2005 and 2006). SWAT has increased global acknowledgment as a strong interdisciplinary watershed demonstrating device. A few alignment systems have been created for SWAT. As of late, SWAT-Calibration and Uncertainty Program (SWAT-CUP) has been created that gives a basic leadership structure which incorporates the semi-computerized approach (SUFI2) utilizing both manual and computerized graduation and integrating sensitivity and uncertainty investigation.

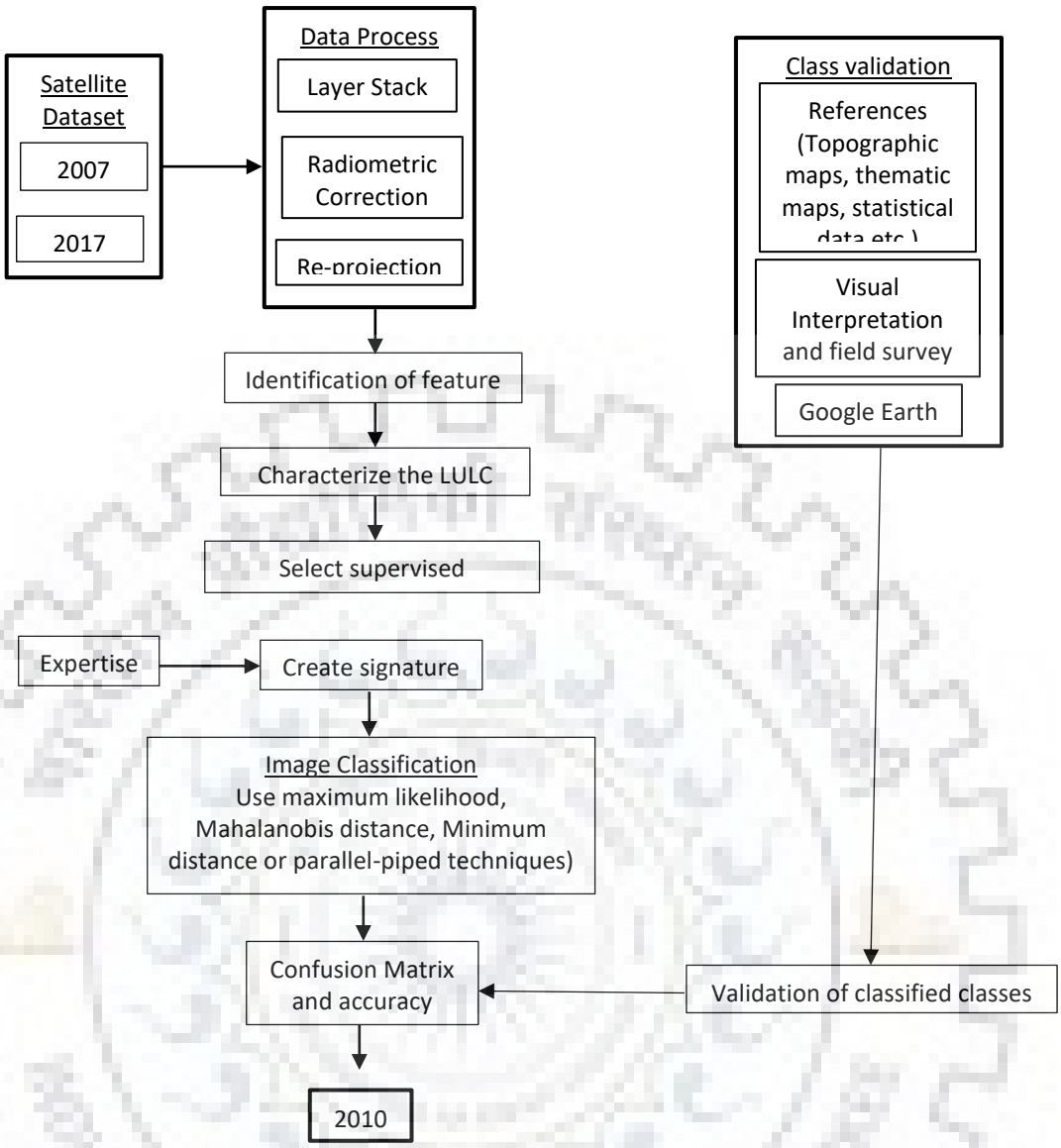

Figure 3. 14 Methodology used in land-use/ land-cover change

SWAT allow a number of different physical processes to be simulated in a basin. In this study, ArcSWAT 2013, sideways with ArcGIS 10.3 has been used for the hydrological simulation of Rokel-Seli River Basin. This programme can do examination on every day, month to month, or yearly time step premise and hence, the outcomes are presented on month to month premise. The hydrological input information from 2000 to 2009 was considered for calibration and information from 2010 to 2013 was considered during validation. The model has been assessed for hydrology based on Coefficient of Determination (R^2), Nash-Sutcliffe coefficient of Efficiency (NSE), Percent Bias (PBias), Root Mean Square Error (RMSE) and Standard deviation Ratio (RSR). The water resources of the basin was assessed based on observed climatic data from 1984 to 2010 along with 2017 land use.

3.8.2 Description of SWAT Model

Though number of rainfall-runoff models are available in the market, selection of suitable model for a given watershed is very difficult for efficient planning and management of watershed. Numerous models as mentioned earlier have been developed by various researchers for rainfall- runoff modelling. However, SWAT model results have been found to be more acceptable and widely used than any other hydrologic models. Water balance equation used by SWAT model is as follows:

$$SW_t = SW_0 + \sum_{t-1}^{t} (R_{day} - Q_{surf} - ET_a - W_{seep} - Q_{gw})$$

Where:

SWt = Final soil water content (mm); SW0 = Initial water content (mm); T = Time (day), Rday = Amount of precipitation (mm); Qsurf = Amount of surface runoff (mm); ETa = Amount of Evapotranspiration (mm); Wseep = Amount of water entering the vadose zone from the soil profile (mm); Qgw = Amount of return flow (mm)

SWAT is a semi-distributed, continuous-time step model that operates on a daily time step and is designed to predict the impact of management on water, sediment, and agricultural chemical yields in watersheds. The model is physically based, computationally efficient, and capable of continuous simulation over long time periods. Major components in SWAT model includes weather, hydrology, soil properties, plant-growth, nutrients, pesticides, bacteria and pathogens, and land management practices. In SWAT model, a watershed is divided into multiple sub- watersheds, which are further subdivided into different hydrologic response units (HRUs) that consist of homogeneous land use, slope, and soil characteristics. The general objective of SWAT model is to estimate the impact of agriculture or land management on water and sediment, and agricultural chemical yields in a basin. It has option of high level of spatial and point source data as input, and simulation may be run on daily, monthly, or yearly time steps. However, the model components includes weather condition, soil properties, hydrology, erosion, plant growth, land management, nutrients, pesticides, and stream routing etc. In this study, SWAT is used for hydrological analysis of the watershed.

3.8.2.1 Modules of SWAT Model

The major units involved in the process of running SWAT are as follows:

a) Watershed delineation module; this module, the morphometry of the watershed, i.e. stream delineation stream definition, flow direction and accumulation inlet and outlet definition is obtain from DEM.

b) Hydrological Response Unit (HRU); this module analysis provides information related to LULC (satellite imagery), soil map and slope definition in different layers

c) Hydro Meteorological data: In this module, precipitation, minimum/maximum temperature, relative humidity, solar radiation, wind speed, dew point and its location and elevation etc. are provided

d) Defined Weather Station; this module provides weather stations location with elevation details and other geographical as well as other statistical details of various parameters highlighted in step (c)

e) Edit Database (Optional); in this module other point source information such as point source discharge, inlet discharge, reservoir, sub-basin or watershed discharge can be edited.

f) Run SWAT Model, after inputting all required data as mentioned in steps (a) to (b), the model is then applied or run. An outlined methodology of running SWAT is shown in the **Fig. 3.15**

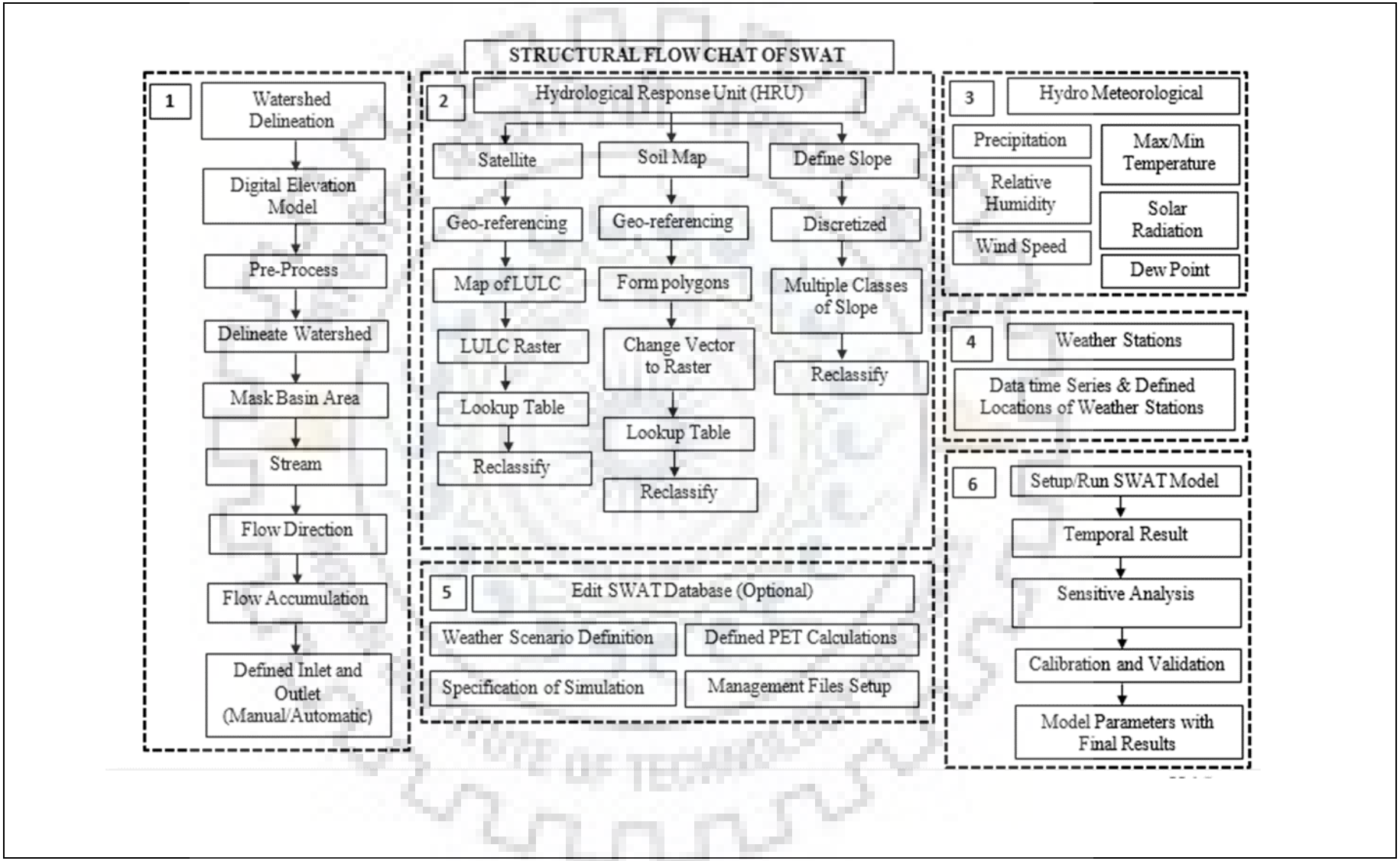

Figure 3. 15: Processes Flow Chart of SWAT Application

3.8.2.2 SWAT Model Setup for Rokel-Seli River Basin

The SWAT Model setup procedure applied for the RSRB can be outlined as follows:

1) Upload DEM in Arc-SWAT ver. 10.3 interface after re-projecting in UTM coordinate system (WGS 84, Zone-44 datum system)..
2) The drainage network is produced using a threshold basin area. In this research, threshold catchment area of 750 ha was applied. Least of the threshold value, the more dense the drainage network. The stream network has been shown earlier in **Fig. 3.7** for the whole basin and from **Fig. 3.8 – 3.12** sub-basin wise respectively.
3) Sub-basin outlets with the location of gauging site are then uploaded to ensure the calibration procedures are done at the specified locations. The sub-basin is then defined base on the outlets identified and respective parameters then calculated.
4) Other parameters like soil, slope and LULC maps are now uploaded in the HRU unit of the SWAT Toolbar
5) In the HRU analysis menu on the SWAT Toolbar, the, characterization maps are taken as input. The Lookup tables of all the LULC maps are prepared and taken as input. Digitized soil map **Fig.3.16** and its look up attributes for the study area is prepared and provided as input. Physical and chemical properties of the soil series in this basin are shown in **Table 3.3.** The corresponding variable description of physical and chemical soil properties is tabulated in **Table 3.4.** The slope definition information is taken from the DEM and is shown in **Fig. 3.17.** Then 3 categories of the slopes i.e., <2%, 2-5%, 5-10% and >10% are taken. Thereafter, all the three layers are overlaid and the HRUs are created by applying multiple HRU options.
6) In the hydro-meteorological data section, the rainfall, min/max temperature, relative humidity, solar radiation, wind speed, and dew point are provided at each of the station in the watershed. 5 hydrological stations are considered as the input sites for the RSRB as shown in **Fig.3.18**

Table 3.5 gives a summary of data sources of the various input datasets assimilated in to ArcGIS – Ver. 10.3, ArcSWAT– Ver. 2013 and ERDAS IMAGINE – Ver. 2015 for the successive hydrological modelling of the basin.

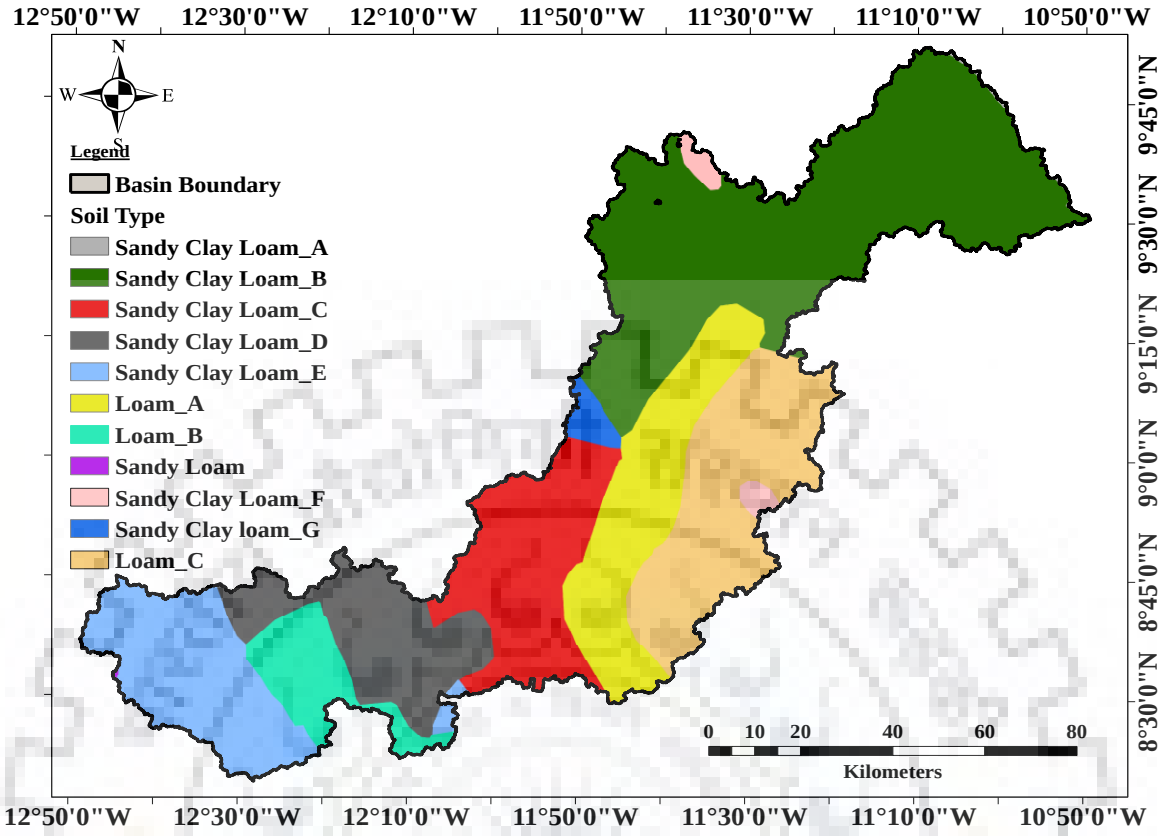

Figure 3. 16: Soil Map of RSRB

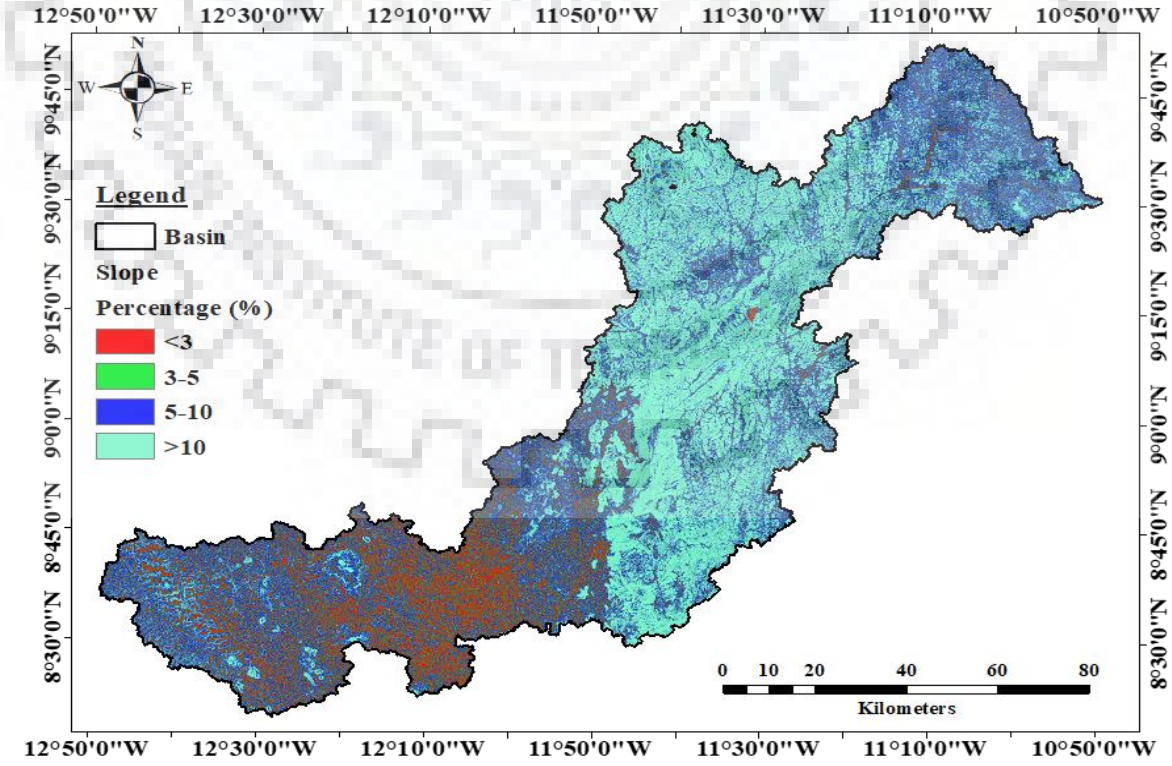

Figure 3. 17: Slope Map of RSRB

Table 3. 3: Physical and Chemical Properties of Soil in RSRB

Soil Parameter	Sandy Clay Loam_A		Sandy Clay Loam_B		Sandy Clay Loam_C		Sandy Clay Loam_D		Sandy Clay Loam_E		Sandy Clay Loam_F		Sandy Clay Loam_G		Sandy Loam		Loam_A		Loam_B		Loam_B	
Soil Component Parameters																						
NLAYERS	2		2		2		2		2		2		2		2		2		2		2	
HYDGRP	D		C		C		C		C		C		C		C		D		D		D	
SOL_ZMX (mm)	910		910		820		1000		1000		550		690		1000		510		1000		550	
ANION_EXCL	0.5		0.5		0.5		0.5		0.5		0.5		0.5		0.5		0.5		0.5		0.5	
SOL_CRK (cm3/cm3)	0.5		0.5		0.5		0.5		0.5		0.5		0.5		0.5		0.5		0.5		0.5	
Soil Layer Parameters																						
	Layer 1	Layer 2	Layer 1	Layer 2	Layer 1	Layer 2	Layer 1	Layer 2	Layer 1	Layer 2	Layer 1	Layer 2	Layer 1	Layer 2	Layer 1	Layer 2	Layer 1	Layer 2	Layer 1	Layer 2	Layer 1	Layer 2
SOL_Z (mm)	300	1000	300	1000	300	1000	300	1000	300	1000	300	1000	300	1000	300	1000	300	1000	300	1000	300	1000
SOL_BD (g/cm3)	1.40	1.40	1.30	1.20	1.20	1.30	1.30	1.30	1.20	1.20	1.20	1.40	1.30	1.40	1.40	1.50	1.40	1.30	1.40	1.30	1.40	1.40
SOL_AWC (mm/mm)	0.15	0.15	0.10	0.10	0.09	0.09	0.11	0.11	0.18	0.18	0.10	0.10	0.11	0.11	0.13	0.13	0.09	0.09	0.08	0.08	0.10	0.10
SOL_CBN (%wt)	1.00	0.40	1.30	0.30	1.60	0.40	1.60	0.50	1.70	0.40	1.30	0.30	1.10	0.30	2.70	0.90	0.90	0.30	2.90	1.10	1.00	0.0.4
SOL_K (mm/hr)	5.96	4.92	16.27	16.61	27.16	13.17	13.29	9.63	22.47	16.09	19.69	6.22	22.31	9.30	18.80	8.76	6.78	7.47	6.28	7.18	5.89	4.18
CLAY (%)	27.00	39.00	23.00	32.00	24.00	33.00	23.00	31.00	21.00	29.00	25.00	34.00	21.00	31.00	16.00	26.00	17.00	25.00	18.00	27.00	30.00	20.00
SILT (%)	27.00	26.00	21.00	20.00	17.00	16.00	24.00	23.00	24.00	23.00	23.00	21.00	17.00	16.00	20.00	14.00	41.00	37.00	41.00	34.00	36.00	40.00
SAND (%)	46.00	35.00	56.00	48.00	59.00	52.00	52.00	46.00	54.00	49.00	53.00	45.00	62.00	53.00	24.00	61.00	41.00	37.00	40.00	38.00	34.00	41.00
SOL_ALB (fraction)	0.07	0.23	0.04	0.27	0.02	0.23	0.02	0.19	0.02	0.23	0.04	0.27	0.06	0.27	0.00	0.09	0.09	0.27	0.00	0.06	0.07	0.23
USLE_K	0.24	0.24	0.20	0.20	0.21	0.21	0.21	0.21	0.21	0.21	0.22	0.22	0.21	0.21	0.21	0.21	0.21	0.21	0.20	0.20	0.21	0.21

Table 3. 4: Variable description of Physical and Chemical Soil Properties

Variable	Description
NLAYERS	Number of Layers
HYDGRP	Hydrological Soil Group
SOL_ZMX (mm)	Maximum rooting depth
ANION_EXCL (fraction)	Fraction of porosity (void space) from which annions are excluded
SOL_CRK (cm3/cm3)	Potential or maximum crack volume of the soil profile expressed as a fraction of the total soil volume
SOL_Z (mm)	Depth from soil surface to bottom of layer
SOL_BD (g/cm3)	Moist bulk density
SOL_AWC (mm/mm)	Available water capacity of the soil layer (mm H2O/mm soil)
SOL_CBN (%wt)	Organic carbon content
SOL_K (mm/hr)	Saturated hydraulic conductivity
CLAY (%)	Hydrological Soil Group
SILT (%)	Hydrological Soil Group
SAND (%)	Hydrological Soil Group
SOL_ALB (fraction)	Moist soil Albedo
USLE_K	USLE equation soil erodibility (K) factor

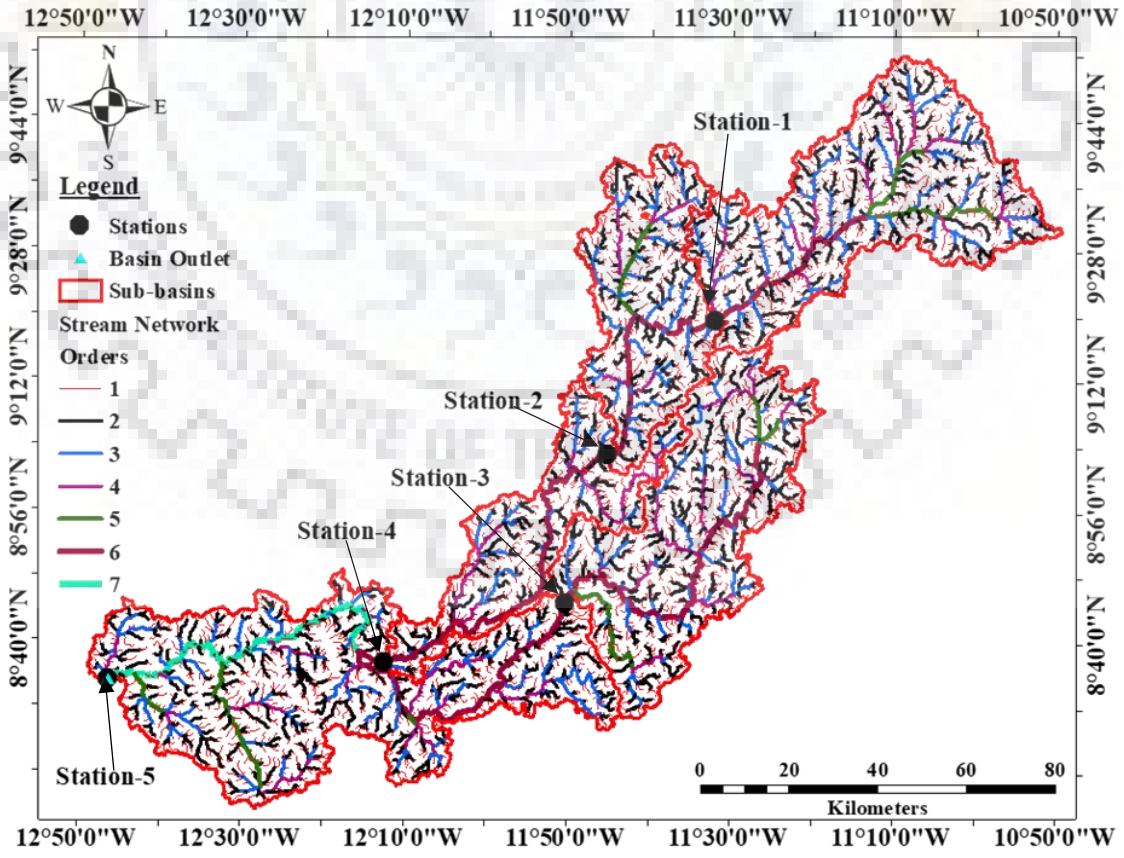

Figure 3. 18: Stream Network, outlets and weather Stations (sub-basin wise) of RSRB

Table 3. 5: Summarized Details of Data source

SI No.	Data	Source
1	DEM	Shuttle Rada Topography Mission (SRTM-DEM) at 30m Resolution sources: https://earthexplorer.usgs.gov/
2	Imagery	Landsat-8 at 30m Resolution sources: https://earthexplorer.usgs.gov/
3	Rainfall	Government of Sierra Leone, Ministry of water Resources and Sierra Leone Water Security sources: https://www.salonewatersecurity.com/ https://www.mwr.gov.sl
4	Discharge Data	
5	Temperature	Source: http://power.larc.nasa.gov/cgi-bin/cgiwrap/solar/agro.cgi?email=agroclim@larc.nasa.gov NASA Prediction of world wide Enerengy Resource (POWER)
6	Solar Radiation	
7	Relative Humidity	
8	Wind Speed	

3.8.2.3 Fundamental Equations Applied in SWAT Model

For SWAT model estimation of runoff, the SCS-CN (USDA, 1972; Bhadra et al., 2010): is most appropriate and applied in this research which is as follows:

$$Q = \frac{(R - 0.2s)}{R + 0.8s}, \qquad R \geq 0.2s$$

$$Q = 0, \qquad R \leq 0.2s$$

Where, Q is the daily runoff; R is daily rainfall, and s is a retention parameter. The parameter s is related to curve number (CN) by the SCS equation (USDA, 1972).

$$s = 254\left(\frac{100}{CN} - 1\right)$$

The constant, 254 in the above equation gives s in mm. Thus, R and Q are also expressed in mm. CN is the curve number for antecedent moisture content (AMC-II). The value of curve number for different landuse conditions and hydrological soil group are applied to AMC-II only i.e., for average condition. The equation gives the value of runoff (Q) depth. In this study, runoff curve number (AMC-II) values for general conditions are adopted.

Potential evapotranspiration (PET)

Three methods are normally used to determine PET i.e., Penman- Monteith method (Monteith 1965), the Priestley- Taylor method (Priestley and Taylor 1972), and the Hargreaves method (Hargreaves and Samani 1985) depending on data availability. For the purpose of this study Penman-Monteith method is used to determine PET.

Penman-Monteith equation is as follows:

$$\lambda E = \frac{\Delta.(H_{net} - G) + \rho_{air.} c_p \cdot \left[e_z^o - e_z\right] / r_a}{\Delta + \gamma.\left(1 + r_c / r_a\right)}$$

where, λE is the latent heat flux density (MJ m^{-2} d^{-1}), E is the depth rate evaporation (mm d^{-1}), Δ is the slope of the saturation vapour pressure-temperature curve, de/dT (kPa $^oC^{-1}$), H_{net} is the net radiation (MJ m^{-2} d^{-1}), ρ_{air} is the air density (kg m^{-3}), c_p is the specific heat at constant pressure (MJ kg^{-1} $^oC^{-1}$), e_z^0 is the saturation vapor pressure of air at height z (kPa), γ is the psychometric constant (kPa $^oC^{-1}$), r_c is the plant canopy resistance (s m^{-1}), and r_a is the diffusion resistance of the air layer (aerodynamic resistance) (s m^{-1})

For well-watered plants under neutral atmospheric stability and assuming logarithmic wind profiles, the Penman-Monteith equation may be written (Jensen et al., 1990):

$$\lambda E_t = \frac{\Delta \cdot \left(H_{net} - G\right) + \gamma \cdot K_1 \cdot \left(0.622 \cdot \lambda \cdot \rho_{air} / P\right) \cdot \left(e_z^o - e_z\right) / r_a}{\Delta + \gamma \cdot \left(1 + r_c / r_a\right)}$$

(3.6)

Where, λ is the latent heat of vaporization (MJ kg-1), Et is the maximum transpiration rate (mm d- 1), K1 is the dimension coefficient needed to ensure the two terms in the numerator have the same unit (for uz in m s-1, K1=8.64 x 104), and P is atmospheric pressure (kPa). The calculation of net radiation, Hnet, is discussed in previously. The remaining undefined term are the soil heat flux, G, the combined term K10.622λρ/P, the aerodynamic resistance, r_a, and the canopy resistance, r_c.

Lateral sub-surface flow

According to (Sloan et al., 1984) it is given as:

$$q_{lat} = 0.024 \frac{\left(2sSC\sin(\alpha)\right)}{\theta_d L}$$

Where, qlat is lateral flow (mm/d), S is drainable volume of soil water (mh-1), α is slope (m/m), θd is drainable porosity (mm-1 and L is flow length (m).

Percolation

The percolation relation given SWAT is:

$$TT_i = \frac{(SW_i - FC_i)}{H_i} \quad (3.10)$$

$$H_i = SC\left(\frac{SW}{UL_i}\right)^{\beta} \quad (3.11)$$

Where SCi is the saturated conductivity for layer i in mm/h, UL_i is soil water content at saturation in mm/mm.

The constant (-2.655) in equation (5.11) was set to assure Hi = 0.002SCi at field capacity. Upward flow may occur when a lower layer exceeds field capacity. The soil water to field capacity ratios of the two layers regulates movement from a lower layer to an adjoining upper50 layer. Percolation is also affected by the soil temperature. If the temperature in a particular layer is at 0°C or below, no percolation is allowed from that layer.

3.8.3 SWAT Basic Input and Output Files

File crop.dat – Land cover/plant growth database (watershed level file)

This required (watershed level file) file contains plant growth parameters for all land covers simulated in the watershed. Information required to simulate plant growth is stored by the plant species in the plant growth database file. It contains the plant specific parameters. When the crop to be planted is specified in the management (.MGT) file, the parameters for that crop are taken from CROP.DAT file

3.8.3.1 SWAT Model Input Files

1. **File till.dat – Tillage database (watershed level file)**

This required file contains (watershed level file) information on the amount and depth of mixing caused by tillage operations simulated in the watershed. The model uses five databases

(tillage, fertilizer, pesticide properties, and land characteristics) to store information required for plant growth

2. **File pest.dat Pesticide database (watershed level file)**

This required file contains (watershed level file) information on mobility and degradation for all pesticides simulated in the watershed.

3. **File fert.dat – Fertilizer database file. (Watershed level file)**
4. **File urban.dat – Urban database (Watershed level file)**

This required file contains information on the build-up/wash-off of solids in urban areas simulated in the watershed.

5. **File .sub – Sub-basin file. (Sub-basin level file)**

This required file for each

6. **File .wgn – Weather generator (Sub-basin level file)**

The weather generator input file contains the statistical weather parameters needed to generate representative daily climatic data for the sub basins.

7. **File .pnd – Pond/Wetland (Sub-basin level file)**

3.8.3.2 SWAT Model Output Files

The SWAT model outputs include four main summary table of information for the sub-basins HRUs, reaches and reservoirs (out.sub, out.hru, out.rch and out.res) respectively.

1. **File .hru – HRU Output File**

The HRU output file contains summary information for each of the hydrologic response units in the watershed. HRU output file reports output for over 60 variables regarding crops, water, meteorological details, soil etc.

2. **File .rsv – Reservoir Output file**

This is an optional output which contains summary information for reservoirs in the basin. In this study reservoir simulation is not considered.

When using SWAT, these tables can be loaded into a Microsoft Access database for analysis purposes. This provides information in two .dbf files. The first .dbf is the result database (including that of input) and the second part is the comment sheet.

3.8.4 SWAT Model Basin Attributes

The attributes of sub-watersheds, tributary channels and main channels are determined in the Arc-SWAT interface as follows (Neitsch et al., 2005).

1. **Sub-basin**

The first level of subdivision is the sub-basin. Sub-basins possess a geographic position in the watershed and are spatially related to one another.

2. **Reach/Main Channel**

Reach or Main channel is associated with each sub-basin in a watershed. Loadings from the sub-basin enter the channel network of the watershed in the associated reach segment. Outflow from the upstream reach segment(s) will also enter the reach segment.

3. **Tributary Channels**

The term tributary channel is used to differentiate inputs for channelized flow of surface runoff generated in a sub-basin. Tributary channel inputs are used to calculate the time of concentration for channelized flow of runoff generated within the sub-basin and transmission losses from runoff as it flows to the main channel.

4. **HRU**

3.8.5 SWAT Model Evaluation Criteria

Evaluations always involve a comparison of the model's output to corresponding measured variable. When presenting model results, the model developers typically do not provide consistent or standard statistical evaluation criteria to assist the readers or users in determining how well their model reproduces the estimated data and how well their model compares to Other models. Haan et al. (1982) suggested that the graphical representation of the results could easily be interpreted if the calibration is done for only one watershed at one stream gauge location. In the present study continuous time series of the observed and estimated data and prepared a scatter gram of the same. Although scatter gram method does not preserve the flow sequence contained in the time series plots, difference between a linear regression line through the plotted points and equality line of scattergram help to identify errors that cannot be detected as easily from the time series plot. Several types of statistics provide useful numerical measures of the degree of agreement between model outputs (estimated results) and recorded (observed

data) quantities. Selection requires choice on how to aggregate groups of measured differences in a single statistics. The numerical and graphical performances criteria described below are used in the study.

3.8.5.1 Coefficient of Determination (R^2)

It describes the proportion of the total variance in the observed data that can be explained by the model. It ranges from 0.0 to 1.0, with higher values indicating better agreement, and is given by

$$R^2 = \left(\frac{\sum_{i=0}^{n} \left(Y_i^{obs} - Y_{mean}^{obs}\right)\left(Y_i^{sim} - Y_{mean}^{sim}\right)}{\sqrt{\sum_{i=1}^{n} \left(Y_i^{obs} - Y_{mean}^{obs}\right)^2} \sqrt{\sum_{i-1}^{n} \left(Y_i^{sim} - Y_{mean}^{sim}\right)^2}} \right)^2$$

(3.16)

Where, Yi^obs is the ith observed data, obs Y_{mean} is mean of observe data, sim Y_i is the ith simulated value, sim Ymean is the mean of model simulated value, and N is the total number of events. The correlation or correlation based measurements R^2 have been widely used to evaluate the goodness of fit in the hydrological models. These measures are over sensitive to extreme values and are insensitive to additive and proportional difference between the estimated and observed values (Willmott, 1981, and Leagates and McCabe, 1999).

3.8.5.2 RMSE – Observations Standard Deviation Ratio RSR)

RSR is calculated as the ratio of the RMSE and standard deviation of measured data, as shown in the following equation.

$$RSR = \frac{RMSE}{STDEV_{obs}} = \frac{\left(\sqrt{\sum_{i=1}^{n} \left(Y_i^{obs} - Y_i^{sim}\right)^2} \right)}{\left(\sqrt{\sum_{i=1}^{n} \left(Y_i^{obs} - Y^{mean}\right)^2} \right)}$$

(3.17)

Where, Y mean is the mean of observed data for the constituent being evaluated and n is the total number of observations. RSR varies from the optimal value of 0, which indicates zero

RMSE or residual variation and therefore perfect model simulation, to a large positive value. Lower is the RSR, lower will be the RMSE, and better will be the model performance (Moriasi et al., 2007). In the present study, criterion suggested by Moriasi et al. (2007) and shown in Table 5.1 are adopted for evaluating the performance of the model.

3.8.5.3 Nash-Sutcliffe Efficiency (NSE)

The Nash-Sutcliffe efficiency (NSE) is a normalized statistic that determines the relative magnitude of the residual variance ("noise") compared to the measured data variance ("information") (Nash and Sutcliffe, 1970). NSE indicates how well the plot of observed versus simulated data fits the 1:1 line. NSE is computed from the following equation:

$$NSE = 1 - \left[\frac{\sum_{i=1}^{n} \left(Y_i^{obs} - Y_i^{sim} \right)^2}{\sum_{i=1}^{n} \left(Y_i^{obs} - Y_{mean}^{obs} \right)^2} \right] \quad (3.18)$$

Where, Yiobs is the ith observation for constituent being evaluated, Yisim is the ith simulated value for the constituent being evaluated, obs Ymean is the mean of observed data for the constituent being evaluated, and n is the total number of observation

The NSE values vary from 0 to 1, where 1 indicates a perfect fit. If the daily measured flows approach the average value, the denominator of the equation (5.16) goes to zero and NSE approach minus infinity with only minor model miss predictions. This statistics works best when the coefficient of variation for the observed data set is large. The NSE represents an improvement over r2 for model evaluation as it is sensitive to the differences in the observed and model simulated means and variances. The NSE has been widely used to evaluate the performance of hydrologic models (Wilcox et al., 1990)

3.8.5.4 Percent bias (PBias)

Percent bias (PBias) measures the average tendency of the simulated data to be larger or smaller than their observed counterparts (Gupta et al., 1999). The optimal value of P-Bias is zero, with low-magnitude value indicating accurate model simulation. Positive values indicate model underestimation bias, and negative value indicates model overestimation bias (Gupta et al., 1999). PBias is calculated by using following equation:

$$PBias = \left[\frac{\sum_{i=1}^{n} Y_i^{obs} - Y_i^{sim}}{\sum_{i=1}^{n} Y_i^{obs}} \times 100 \right]$$

Where PBias is the deviation of data being evaluated, expressed as a percentage

The table below gives the performance ranking statistics for monthly time steps as necessary for SWAT performance evaluation

Table 3. 6: General performance ranking statistics for a monthly time step as recommended

Performance rating	*RSR*	*NSE*	*PBIAS (%)*
Very Good	*0.00 < RSR < 0.50*	*0.75 < NSE < 1.00*	*PBIAS <±10*
Good	*0.50 < RSR <0.60*	*0.65 < NSE <0.75*	*± 10 < PBIAS < ± 15*
Satisfactory	*0.60 < RSR <0.70*	*0.50 < NSE < 0.65*	*± 15 < PBIAS < ± 25*
Unsatisfactory	*RSR >0.70*	*NSE < 0.50*	*PBIAS > ± 25*

Source: Moriasi et al., (2007)

CHAPTER

4

RESULTS AND DISCUSSION

OVERVIEW OF CHAPTER

This chapter discuss on the results or output of the various methodologies applied in the previous chapters. Rainfall variability has been assessed, trends analyzed with the nonparametric test so that the result are outline in this chapter. Further, the projected rain fall could be understood from this chapter and hence elaborate on the magnitudes on the past and future rainfall of the basin. Clear understanding of morphometry parameters of the basin are outlined here, land use land cover classification of the basin is elucidated. Results of the application of SWAT model are also mention here which gives the various components of the hydrologic cycle of the bason. Over all, the main objectives of the study are clarified and answers to the key questions which call for the study are outlined in this chapter.

4.1 CLIMATE VARIABILITY AND TREND ANALYSIS

Climate variability will probably affect surface and groundwater resources because of the normal changes in precipitation, evapotranspiration and the spatiotemporal dissemination of the basic water balance segments. Expanded amount of precipitation will prompt higher rates of surface runoff, a rise in flood and diminished rates of groundwater restoration. An increase in temperature causes higher evapotranspiration, and, thus, additionally facilitates the requirement of water for irrigation, and by a wide margin considered the greatest water user under current conditions. Keeping in mind the end goal to empower water resources management to adapt to future encounters, the effect of climate change on the water balance should be quantified from provincial (regional) to basin scales. Research exercises amid the most recent decades progressively address this issue.

4.1.1 Current Water Availability

Climate changes impacts the rainfall distribution all around the world. The variation in rainfall distribution would alter the storage, recharge surface runoff and soil moisture. Moreover, the rainfall variation can increase or decrease the discharge and water availability to a river basin. Increased variation in the intensity and frequency of precipitation and higher temperatures are some of the major impacts of climate change.

The extracted monthly, annual and seasonal rainfall data for the entire basin (station-wise) can be shown in **Table 4.1.**

The average annual rainfall for the entire basin was estimated as the area weighted rainfall. The area covered by each rain gauge station in the basin with their corresponding annual and seasonal rainfall values were computed to give the mean annual rainfall of RSRB. This is shown in Table 4.2 on the page that follows:

Table 4. 1: Historical Average Monthly, Annual and Seasonal rainfall (mm) of RSRB for the period of 1961-2005

Station	Jan	Feb	Mar	Apr	May	Jun	Jul	Aug	Sep	Oct	Nov	Dec	Annual	Wet Season	Dry Season
Bombali	10	15	47	115	300	361	374	483	435	265	91	13	2507	2217	290
Diang	12	17	31	91	276	394	493	545	480	278	126	28	2772	2467	305
Kafe Simera	6	11	18	74	251	360	460	599	508	318	106	18	2729	2496	233
Kholifa Rowala	14	14	25	97	279	323	337	487	427	338	125	20	2486	2191	295
Koya	3	9	25	74	188	300	355	421	362	279	80	10	2106	1905	202
Malal Mara	5	7	17	72	310	361	449	550	483	268	91	14	2627	2421	206
Masimera	10	11	31	97	246	306	312	443	418	339	109	11	2333	2064	269
Mongo	9	8	21	76	203	284	312	406	363	221	62	9	1972	1787	185
Safroko Limba	9	13	25	104	307	351	426	518	455	281	104	13	2605	2338	268
Sambaia	9	11	16	66	223	365	417	508	439	269	84	17	2425	2220	204
Sengbe	7	6	20	83	241	317	341	419	348	203	61	9	2054	1868	186
Warra Bafodia	7	9	20	92	257	310	356	454	437	364	150	17	2474	2179	295
Yoni	13	10	24	120	333	399	445	519	442	235	68	11	2618	2373	245
Average Rainfall	**9**	**11**	**25**	**89**	**263**	**341**	**390**	**488**	**431**	**281**	**97**	**15**	**2435**	**2194**	**245**
Standard Deviation	**3**	**3**	**8**	**17**	**43**	**37**	**61**	**58**	**49**	**48**	**27**	**5**	**256**	**232**	**45**

The mean annual and seasonal depth of rainfall on the Rokel-Seli river basin was estimated to be 2435mm, 2190mm in the wet season and 245mm in the dry Season respectively as illustrated graphically in **Fig. 4.1**

This means that 90% of the average annual rainfall occurs in the wet season with only 10% contribution of rainfall in the dry season on the basin. Despite the abundance of annual rainfall there is an uneven distribution of rainfall within the Rokel-Seli River Basin due to human induce activities and other environmental factors. Rainfall variability analysis is quite

necessary in determining water availability and requirement for a catchment which can influence water use and allocation.

Precipitation is a principal influence regulating water availability, which is very important for water supply, agricultural production and many other purposes. Rainfall variability can impact to some degree in determining crop growth in diverse zones throughout the world. A sound understanding of rainfall variability is key to augment agricultural production in a sustainable way.

Table 4. 2: Mean Annual and Seasonal weighted station rainfall (mm) of RSRB for the period of 1961-2005

Rain gauge Station	Station Area (km^2)	Weightage factor	Station Reading of Average Rainfall			Weighted Station Rainfall		
			Annual	Wet Season	Dry Season	Annual	Wet Season	Dry Season
Bombali	499	0.043	2507	2217	290	109	96	13
Diang	1449	0.126	2772	2467	305	350	311	38
Kafe Simera	923	0.080	2729	2496	233	219	201	19
Kholifa Rowala	1427	0.124	2486	2191	295	309	272	37
Koya	843	0.073	2106	1905	202	155	140	15
Malal Mara	606	0.053	2627	2421	206	139	128	11
Masimera	763	0.066	2333	2064	269	155	137	18
Mongo	1141	0.099	1972	1787	185	196	178	18
Safroko Limba	201	0.018	2605	2338	268	46	41	5
Sambaia	1494	0.130	2425	2220	204	315	289	27
Sengbe	710	0.062	2054	1868	186	127	115	12
Warra Bafodia	764	0.067	2474	2179	295	165	145	20
Yoni	661	0.058	2618	2373	245	151	137	14
Total	**11481**	**1.000**				**2435**	**2190**	**245**

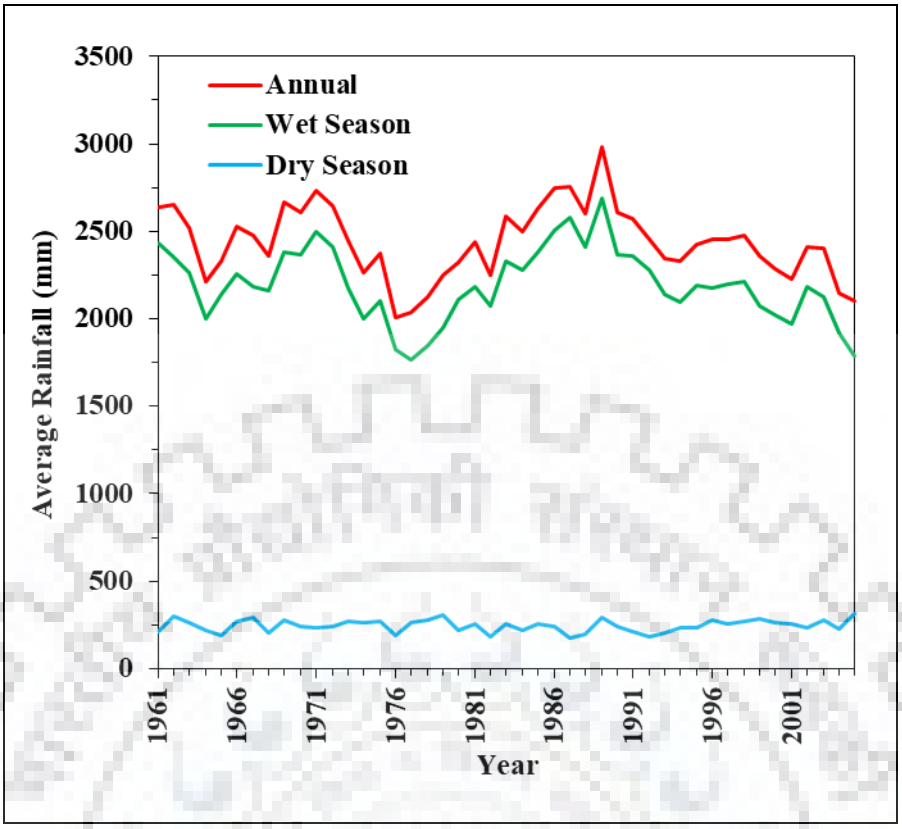

Figure 4. 1: Average Annual and Seasonal rainfall distribution over RSRB during 1961 to 2005.

Precipitation is a principal influence regulating water availability, which is very important for water supply, agricultural production and many other purposes. Rainfall variability can impact to some degree in determining crop growth in diverse zones throughout the world. A sound understanding of rainfall variability is key to augment agricultural production in a sustainable way.

4.1.2 Rainfall Variability Assessment

The assessment of rainfall variability is of crucial importance for stakeholders and policy makers to provide information for an improved water management. **Table 4.3** gives the statistics relating to the variability of the annual and seasonal rainfall of Rokel-Seli river basin.

Table 4. 3: Average annual and seasonal rainfall Statistics of RSRB for the period of 1961-2005

Station	Annual					Wet Season					Dry Season				
	Min	Max	Mean	SD	%CV	Min	Max	Mean	SD	%CV	Min	Max	Mean	SD	%CV
Bombali Sebora	887	3855	2507	468	19	857	3245	2217	402	18	30	3245	290	142	49
Diang	1099	4082	2772	560	20	1075	3747	2467	557	23	24	512	305	94	31
Kafe Simira	849	3498	2729	444	16	835	3397	2496	448	18	14	564	233	104	45
Kholifa Rowalla	892	3274	2486	439	18	883	3042	2191	450	21	9	548	295	121	41
Koya	799	3447	2106	468	22	799	3369	1905	463	24	0	521	202	96	48
Malal Mara	940	3299	2627	365	14	927	3009	2421	332	14	13	509	206	91	44
Masimera	976	3354	2333	350	15	976	3076	2064	372	18	0	562	269	124	46
Mongo	745	3261	1972	431	22	741	3193	1787	424	24	4	450	185	95	52
Safroko Limba	992	3426	2605	391	15	975	3090	2338	351	15	18	531	268	105	39
Sambaia	936	3514	2425	504	21	918	3163	2220	489	22	18	419	204	75	37
Sengbe	638	3579	2054	552	27	636	3422	1868	544	29	2	379	186	88	47
Warra Bafodia	940	3496	2474	464	19	928	3248	2179	434	20	12	568	295	118	40
Yoni	941	4569	2618	758	29	939	4369	2373	741	31	3	493	245	111	45
Rokel-Seli River Basin	**895**	**3589**	**2435**	**256**	**11**	**884**	**3336**	**2190**	**232**	**11**	**11**	**715**	**245**	**45**	**18**

Considerable aerial variation exists in the annual rainfall on the basin with highest rainfall of magnitude 3589mm annually and, 3336mm and 715mm in the wet and dry season respectively. The coefficient of variation of the annual and seasonal rainfall varies between 14 and 52 with an average value of about 25. The coefficient of variation is least at stations of high rainfall and largest in regions of scanty rainfall as indicated in **Fig. 4.2 (a, b and c)** at station Sengbe (upstream) and station Yoni (downstream) for both annually and seasonally.

This analysis can be useful to detect the changes in the precipitation-streamflow relationship and quantifies the impact of precipitation to runoff (i.e. response of streamflow to climate change) in the basin.

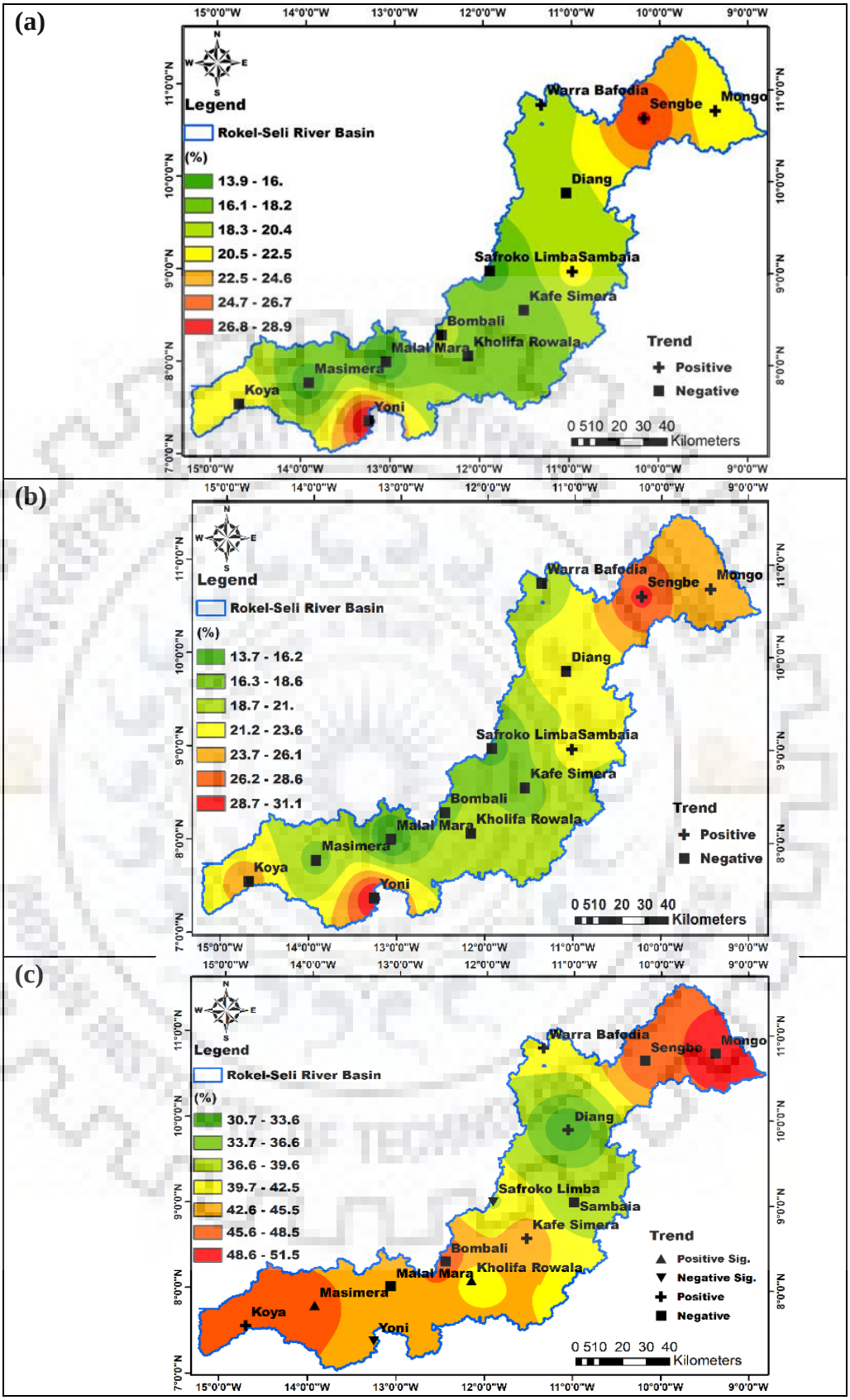

Figure 4. 2: Inter-Annual Variability of Rainfall (%CV) for (a) annual, (b) wet and (c) dry season over RSRB during the period of 1961-2005

4.1.3 Trend Analysis of Rainfall

In this study, the long term trend has been detected using Non-parametric methods and shift change point detection (Homogeneity) approach, i.e. the Mann-Kendall (MK) test, Modified Mann-Kendall Test and Theil Sen's Slope for the historical time series in terms of monthly, seasonally and annually.

4.1.3.1 MKT, MMKT and Magnitude of Rainfall Trend (Theil Sen's Slope)

The two-sided test is carried out at 100 (1 – a) % of the confidence interval to obtain the true slope for the non-parametric test in the series. The positive or negative slope Q_i is obtained as upward (increasing) or downward (decreasing) trend. In the present study, the test was carried out at 5% significance level, therefore when Z value exceeds ± 1.96 null hypotheses is rejected and show the existence of trend in the series as in **Table 4.4**

Table 4. 4: The Sen Slope and Z-statistic values of Annual and Seasonal rainfall using MK and MMK for RSRB during 1961-2005

Station	MK			MMK			Sen Slope		
	Annual	Wet Season	Dry Season	Annual	Wet Season	Dry Season	Annual	Wet Season	Dry Season
Bombali	-0.323	-0.245	-0.440	-0.254	-0.245	-0.532	-2.034	-1.203	-0.530
Diang	-0.479	-0.773	0.851	-0.479	-0.773	0.851	-2.890	-4.057	0.736
Kafe Simera	-1.947	-2.299	0.382	-1.947	-2.299	0.448	-9.758	-11.090	0.457
Kholifa Rowala	-1.105	-1.575	2.827	-1.105	-1.873	2.827	-5.961	-9.484	4.009
Koya	-0.088	-0.303	1.458	-0.068	-0.269	1.458	-0.430	-1.367	1.550
Malal Mara	-0.303	-0.284	-0.225	-0.339	-0.284	-0.225	-0.990	-1.247	-0.272
Masimera	-0.538	-1.712	3.238	-0.628	-1.622	3.533	-2.032	-6.709	4.789
Mongo	0.264	0.812	-0.147	0.208	0.631	-0.180	1.666	3.715	-0.132
Safroko Limba	-1.438	-1.145	-2.358	-1.252	-0.915	-2.358	-7.537	-4.661	-2.979
Sambaia	0.665	1.017	-1.800	0.842	1.336	-1.800	4.920	7.126	-1.647
Sengbe	1.301	1.301	-0.695	1.371	1.347	-0.779	6.591	6.928	-0.844
Warra Bafodia	0.127	-0.470	1.272	0.164	-0.372	1.272	0.267	-1.836	1.267
Yoni	-1.849	-1.477	-3.042	-1.399	-0.939	-3.042	-17.354	-12.920	-3.917

Green Box: Indicates the significant increasing trend during 1961-2005

Red Box: Indicates the significant decreasing trend during 1961-2005

The Z-statistics value was analyzed (Thorsten, 2017) as follows:

$-1.96 < Z < 1.96$ = No Trend (Not significant)

$Z > 1.96$ = Increase in trend (i.e. positively significant)

Z < -1.96 = Decrease in trend (i.e. negatively significant)

The values of +Z and –Z indicates upward and downward trend respectively. The Z values of Mann-Kendall test accept the null hypotheses of no trend when;

$$\pm Z \leq Z_1 - x/2$$

Where; x is the level of significance at two tailed trend test.

The Theil Sen's slope estimator is a robust method of robustly fitting a line of sample points in the plane by choosing the medians of the slope of all line through pairs of the points. It has been viewed as the most popular nonparametric analysis for determining a linear trend and therefore this can be illustrated by box plot in **Fig.4.3**

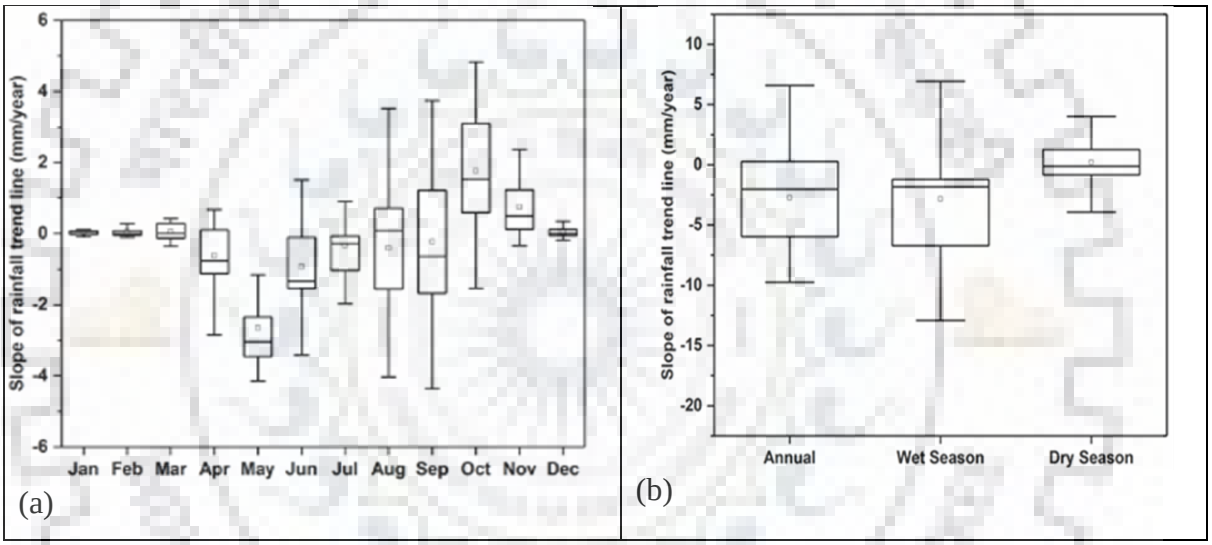

Figure 4. 3: a) Box plot of the Theil-Sen slopes for annual and seasonal rainfall time series of RSRB. (b) Box plot of the Theil-Sen slopes for monthly rainfall time series

4.1.3.2 Homogeneity Analysis in the Time Series (1961-2005)

Homogeneity in trends was tested using the Standard Normal Homogeneity Test (SNHT) to obtain the homogeneous and heterogeneous trend in the data time series with significance level of 5%. Change point (P values) has been computed using 10000 Monte Carlo simulations base on Mann-Whitney-Pettit (MWP) Test and SNHT (Alexanderson, 1986;) Alexandersson et al, 1997). The test interpretation, $H_{0:}$ stands for the homogeneous series and *Ha:* there is a date at which there is change in the data as shown in **Table 4.5.** As the computed p-value is greater than the significance level alpha = 0.05, one cannot reject the null hypothesis $H_{0.}$

Table 4. 5: The MWP test and SNHT test for RSRB (1961–2005).

Station	Pettitt's Test			SNHT Test		
	P-value	Year	Trend	P-value	Year	Trend
Bombali	0.594	1972	Ho	0.736	1972	Ho
Diang	0.875	1998	Ho	0.740	2003	Ho
Kafe Simera	0.118	1973	Ho	0.232	2002	Ho
Kholifa Rowala	0.448	1993	Ho	0.589	1998	Ho
Koya	0.342	1973	Ho	0.159	1972	Ho
Malal Mara	0.667	1980	Ho	0.913	1980	Ho
Masimera	0.178	1991	Ho	0.644	1991	Ho
Mongo	0.267	1972	Ho	0.157	1972	Ho
Safroko Limba	0.136	1967	Ho	0.044	1998	Ho
Sambaia	0.189	1967	Ho	0.060	1967	Ho
Sengbe	0.059	1982	Ho	0.253	1973	Ho
Warra Bafodia	0.546	1973	Ho	0.599	1973	Ho
Yoni	0.063	1992	Ho	0.098	1992	Ho

4.2 ANALYSIS OF FUTURE RAINFALL PROJECTIONS

Rainfall projections are necessary in determining the water balance and future water allocation in the basin. Thus, evaluating the future variation of hydrologic cycle and water resources has special significance for regional planning and water resources management. It helps in the assessment of the future impact of climate change over the basin which affects changes in the hydrologic cycle of the basin.

4.2.1 Calibration and Validation

The daily observed predictor data obtained from NCEP reanalysis, normalized over the period of 1961-1990 and hence this period was selected for calibration, while the validation period was selected from 1991-2005 to normalize the calibration and validation model. **Fig. 4.4** graphically represent the comparison between the simulated and observed rainfall values along with scatter plot in **Fig. 4.5 (a. and b.)** during calibration and validation. The important parameters or indicators of the goodness of the regression for each of the stations during the calibration and validation periods are also shown in **Table 4.6.**

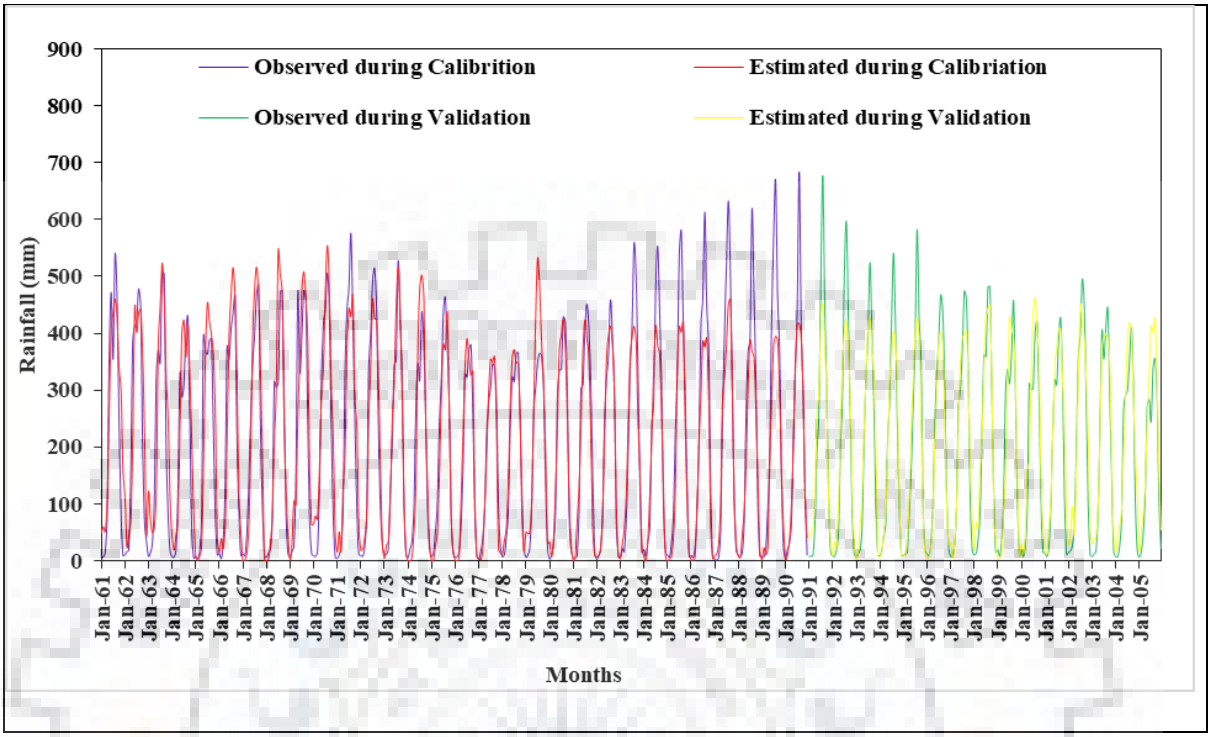

Figure 4. 4: Observed and estimated monthly rainfall during calibration and validation periods.

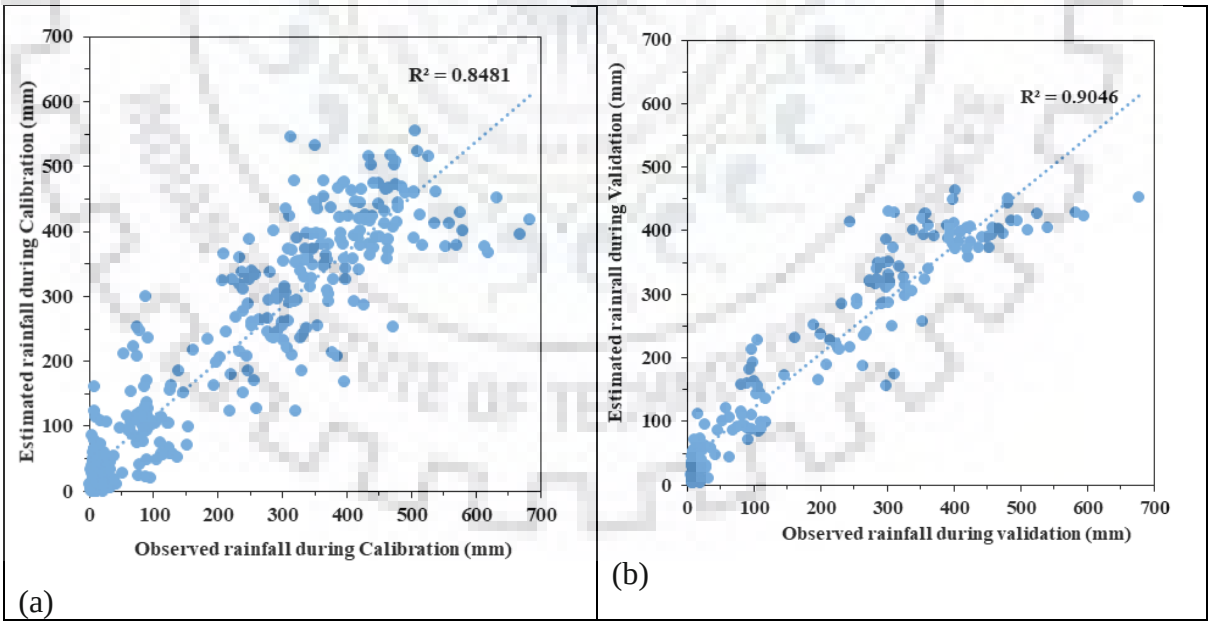

Figure 4. 5: Scattered plot between observed and estimated rainfall during (a) calibration and (b) validation

Table 4. 6: Important indicators of accuracy of results during calibration and validation for rainfall time series at the various stations of Rokel-Seli River Basin

Station	NCEP	Calibration/ Validation	RMSE (mm)	NMSE	NASH	CC
Bombali	1961-1990	Calibration	115.43	0.16	0.65	0.81
	1991-2005	Validation	104.45	0.24	0.72	0.86
Diang	1961-1990	Calibration	136.27	0.13	0.71	0.81
	1991-2005	Validation	129.56	0.30	0.70	0.84
Kafe Simera	1961-1990	Calibration	130.53	0.19	0.67	0.84
	1991-2005	Validation	126.55	0.32	0.71	0.85
Kholifa Rowalla	1961-1990	Calibration	114.72	0.15	0.69	0.82
	1991-2005	Validation	88.25	0.20	0.74	0.86
Koya	1961-1990	Calibration	103.99	0.10	0.75	0.82
	1991-2005	Validation	91.14	0.27	0.71	0.85
Malal Mara	1961-1990	Calibration	120.20	0.16	0.70	0.84
	1991-2005	Validation	127.17	0.33	0.70	0.85
Masimera	1961-1990	Calibration	104.99	0.14	0.70	0.83
	1991-2005	Validation	76.45	0.17	0.77	0.88
Mongo	1961-1990	Calibration	96.72	0.10	0.76	0.82
	1991-2005	Validation	93.99	0.31	0.70	0.84
Safroko Limba	1961-1990	Calibration	114.40	0.11	0.76	0.83
	1991-2005	Validation	89.71	0.19	0.79	0.90
Sambaia	1961-1990	Calibration	112.68	0.11	0.79	0.84
	1991-2005	Validation	98.33	0.25	0.76	0.87
Sengbe	1961-1990	Calibration	120.60	0.35	0.58	0.77
	1991-2005	Validation	93.93	0.30	0.65	0.82
Wara Bafodia	1961-1990	Calibration	114.83	0.18	0.60	0.81
	1991-2005	Validation	87.93	0.18	0.79	0.89
Yoni	1961-1990	Calibration	159.08	0.32	0.58	0.78
	1991-2005	Validation	114.49	0.31	0.60	0.82

During the calibration and validation periods the average monthly values were calculated for both observed and the estimated rainfall as in **Table 4.7.**

Table 4. 7: Calibration and validation values of monthly average rainfall of Rokel-Seli River Basin

		Monthly													Annual			
Rainfall (mm) (OBS/NCEP)		**J**	**F**	**M**	**A**	**M**	**J**	**J**	**A**	**S**	**O**	**N**	**D**	**R^2**	**Min**	**Max**	**Average**	**SD**
Calibration	Observed	8	11	24	93	277	354	401	496	431	275	93	15	0.848	1962	2820	2477	271
	Estimated	20	21	34	87	210	352	428	433	414	296	143	36		1966	2926	2474	289
Validation	Observed	11	12	26	81	233	315	370	473	430	293	104	15	0.905	1893	2798	2363	267
	Estimated	17	28	48	104	211	325	404	420	395	304	145	42		2048	2852	2444	255

The equations derived after SDSM base on MLR approach during calibration and validation periods are applied for future projections under Couple Model Intercomparison phase-5 (CMIP5) emission scenarios; RCP 2.6 RCP 4.5 and RCP 8.5 which are used in this study. For the purpose of this work, the projected rainfall has been categorized in various time step as; past (1961-2005), 2020s (2011-2040) and 2050s (2041-2070) scenarios as tabulated in **Table 4.8.** Further, climate change scenarios also helps the future planning of various activities which are associated with water and dependent with rainfall over the catchment. The forecasted rainfall is expected to help the policy makers and the stakeholders for making effective water resources planning.

Table 4. 8: Past and future rainfall statistics under RCP2.6, RCP4.5 and RCP8.5 of RSRB

Projection Scenarios		Past and Predicted Monthly Average Rainfall (mm)												Annual Rainfall (mm)			
		J	F	M	A	M	J	J	A	S	O	N	D	Min	Max	Average	SD
RCP-2.6	Past	9	11	25	89	263	341	390	488	431	281	97	15	1972	2772	2435	182
	2020s	23	16	36	143	284	373	433	458	435	233	131	20	1967	3250	2744	173
	2050s	15	18	30	144	288	385	451	460	339	251	143	20	1928	3270	2545	172
RCP-4.5	Past	9	11	25	89	263	341	390	488	431	281	97	15	1972	2772	2435	182
	2020s	16	19	37	122	269	362	420	454	389	279	115	26	2725	3907	2508	171
	2050s	29	23	45	145	292	379	443	434	410	309	118	17	2602	4568	2645	174
RCP-8.5	Past	9	11	25	89	263	341	390	488	431	281	97	15	1972	2772	2435	182
	2020s	30	25	31	145	287	372	439	461	408	306	108	18	2450	5946	2630	177
	2050s	29	26	30	135	292	379	443	434	410	309	114	21	2524	5175	2623	175

Further, climate change scenarios also helps the future planning of various activities which are associated with water and dependent with rainfall over the catchment. The forecasted rainfall is expected to help the policy makers and the stakeholders for making effective water resources planning.

4.3 DEPENDABLE ANNUAL RAINFALL OFF ROKEL-SELI RIVER BASIN

It is very important to know the annual rainfall dependability in planning water resources over the basin in order to obtain the relationship between the magnitude of the event and its probability of exceedance. Hence the 75 or 95% dependable annual rainfall are of utmost concern to identify the minimum water availability.

Therefore in this study, the dependable annual rainfall has been estimated for the past (1961-2005) and future time series of 2020s (2011-2041) and 2050s (2041-2070) as shown graphically in **Fig. 4.6.**

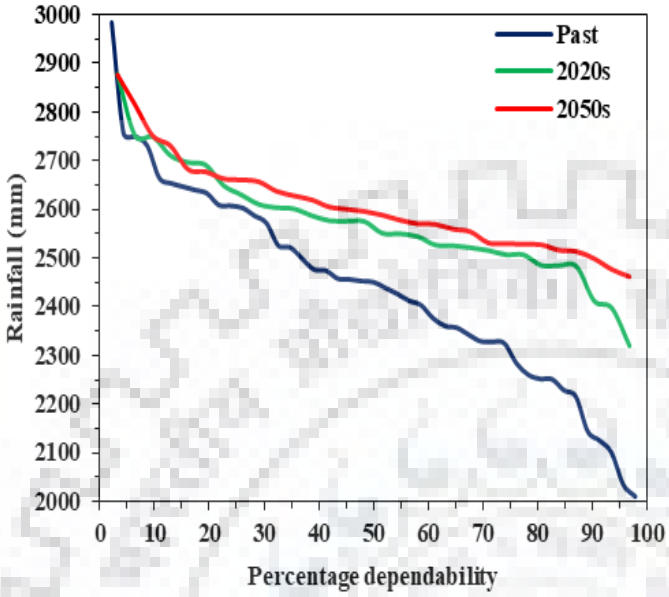

Percentage Dependability	Dependable Rainfall (mm)		
	Past	2020s	2050s
5%	2749	2751	2815
50%	2451	2551	2588
75%	2284	2507	2529
90%	2125	2412	2499
95%	2034	2320	2462

Figure 4. 6: Rainfall dependable curves for past (1961-2005), 2020s (2011-2040) and 2050s (2041-2070).

Based on the analysis carried out on the historical rainfall, it has been detected that the average annual rainfall over the basin was 2439mm, varying from minimum rainfall of 895mm to 3589 maximum rainfall. Most of the rainfall occurs during the wet season, contributing 80% of the annual rainfall over the basin ranging from minimum rainfall of 844mm to 3336mm maximum rainfall which occurs during the months of June to October. The dry season which occurs between the periods of November to December and January to April has only a maximum rainfall of 715mm contribute only 10% of rainfall in the basin with a minimum of 11mm.

It was observed that two stations; one at the extreme upstream and the other at downstream gives high value of coefficient of variation **(Fig. 2.2)** which means less rainfall occurs at those points in the basin during the period of 1961 to 2005. There is less variation in most part of the basin considering the middle part noting that much of the rainfall is received at this points. The standard deviation varies between from 105 to 477 annually and the 96% dependable rainfall in the basin is 2034mm.

Trend analysis was done applying MK and MMK tests and Sen's slope on monthly, annual and seasonal rainfall data for all stations in the basin. The MK and MMK statists at 5% significance level are shown in **Table 2.4**. Among all the 13 stations in the basin, 3 stations shows a negatively significant trend in wet and dry season and just 2 stations shows positively significant trend in the dry season. From the Z-statistics value, there is not any significant annual trend in all stations, although 9 stations shows negative trend and 4 shows positive trend annually during the period of 1961-2005.

Monthly and trends are shown in Figure 2.4 using the box plot of Theil-Sen's slope method for the Rokel-Seli River basin. The box central line represents median, upper and lower lines represent the 75^{th} and 25^{th} percentile, respectively. Also the upper and lower lines represent the maximum and minimum values of rainfall slopes. Based on the analysis, the dry season shows a positive slope and similar all the months found in the dry season (November to April) also shows positive slope in the monthly box plot. This denotes that, during periods of high rainfall the Theil-Sen's slope will show negative trend and vis-à-vis during low rainfall. Using MWP and SNHT tests to identify homogeneity in the data, results in Table 2.5 shows that there is no change shift point detected in the data series for the period of 1961 and 2005. Hence all P-values shows Ho trend (i.e. all data in the series are homogenous during the time series).

It can also be observed that, the MLR model fits between the observed and estimated monthly average rainfall during the calibration and validation periods with a coefficient of determination of 0.848 and 0.905 respectively as indicated in Table 2.8. Applying the recommended MLR model, average annual rainfall estimated for the period of 1961 to 1990 is 2474mm as compared to the observed rainfall of 2477mm. Similarly, the estimated average rainfall during1990 to 2005 is 2444mm compared to 2363mm as observed rainfall. The projected mean annual rainfall for the periods of 2020s and 2050s according to CMIP5 emission scenarios are; RCP 2.6: 2744mm and 2545mm, RCP 4.5: 2508mm and 2645mm and RCP8.5: 2630mm and 2623mm as against observed rainfall of 2439mm. The overall forecasted rainfall (taking the average of all 3 scenarios) for 2020s is 2627mm and for 2050s is 2604mm as compared to the observed value of 2439mm.

As projected for the average rainfall over Rokel-Seli River Basin, the expected rainfall to occur in 2020s and 2050s is about 7-8% higher than the observed rainfall for the periods of 1961 to

2005. The 95% dependable rainfall for the periods of 2020s is estimated as 2320mm which is probable to occur in 2031 and for 2050s as 2462mm to befall in the year 2041.

4.4 ASSESSMENT OF BASIN MORPHOMETRY

4.4.1 Analysis of Sub-basin Characteristics

Morphometric analysis of RSRB was carried out as discussed in chapter three. The results of analysis are shown in **Table 4.10 to Table 4.18.** Morphometric characteristics are needed to know hydraulic parameters of drainage basin, i.e., patterns, shape, stage of stream, permeability of bed rock, health of streams, as well as help to correlate with lithological characteristics. Hence this study has numerically identify basin morphometric characteristics of which are; stream order, stream length, bifurcation ratio, drainage density, stream frequency, circulatory ratio, form factor, elongation ratio, texture ratio, compactness coefficient, length of over land flow and area, perimeter, elevation difference, basin length, total relief, number of stream and total stream length as described above.

The soil loss in the basin could either be proportionate or inversely proportionate to the parameter calculated. In the case of bifurcation ratio, drainage density, stream frequency, texture ratio, relief ratio, and length of overland flow are directly proportional to the soil loss in the basin. On the other hand, inversely proportional to circulatory ratio, form factor, elongation ratio, and compactness coefficient.

Scores are assign to each of the sub-basins base on the parameter estimated. Sub-basins found to be more vulnerable to soil loss are sub-watersheds which are more vulnerable to soil loss carries higher score of the directly proportionate factor and hence will be assign with least rank (say rank 1, denoting first) and hence the opposite applies. Noting that the parameter are correspondingly relevant, therefore the average of all scores of each basin according to the parameters are estimated. Hence the sub-basin with lower ranking can then be identified to be more susceptible to soil loss and there is considered the first to prioritize for soil loss conservation measures. These procedures have been diagrammatically illustrated in the forgone chapter at **Fig 3.13.**

Consequently, in applying this phenomenon, the RSRB can be investigated by sub-basin wise to identify which sub-basin could be more vulnerable to soil erosion. For the purpose of this research, five sub-basins have been delineated as shown in **Fig 3.4** and the morphometric parameters are shown in Tables 4.10 – 4.16. From tables 4.10, the total number of streams and stream length of all orders are 9200 and 3588.72 km respectively.

Bifurcation ratio varies between 1.32 to 4.41 in table 4.15, noting that Lower value of buforcation ratio denotes the partially affected sub-basin without any interfering in drainage arrangement (Nag, 1998) and it ratio influence the geological as well as tectonic characteristics of the watershed. High value of R_b means the severe over land flow and low recharge for the sub-basin.

Drainage density is 0.74 to 0.82 which varies base on climate as well as physical characteristics of the drainage basins. The meaning of drainage density is a factor which indicates the time of travel by water within the basin and varies between 0.55 to 2.09km/km^2 for humid region (Langbein, 1947). Ranks for prioritization are shown in table 4.16, high runoff corresponds to high stream frequency which can be seen that sub-basin-2 has more runoff which ranges between 0.79-1.59 (i.e. SB-3 to SB-2) as shown in Table 4.17. Circulatory ratio varies from 0.07 (SB-4) to 0.12 (SB-1), this is usually affected by climatic variability, LULC, relief and slope, length and frequency of the stream and geological structures. In this study, it is found that the value of form factor varies 0.17 to 0.44 this commonly denotes that the lower form factor corresponds to more elongation of basin.

Texture ratio varies 2.12 (SB-4) to 4.03 (SB-1) noting that lower the values of texture ratio means the basin is plain with lower degree of slopes because this factor is influenced by the properties of lithology and infiltration of the soil of the basin. The compactness coefficient varies between 2.91(SB-2) to 3.87 (SB-4) and this depends on the slope. Other factors are given in table 4.9.

Table 4. 9: Sub-basin Physical Characteristics

S No.	Sub-basin Name	Area - A (km^2)	Perimeter - P_r (km)	Basin Length - L_b (km)	Total. Stream Length - L_u (km)	Total. Stream No. N_u	Elevation (m)		Relief - H (m)
							Max	Min	
1	SB-1	2512.31	521.22	75.99	1860.1	2098	795	307	488
2	SB-2	1481.16	397.08	75.31	1129.57	1560	954	108	846
3	SB-3	2304.67	514.44	75.46	1857.8	1812	975	89	886
4	SB-4	1290.64	493.14	86.62	999.35	1046	955	53	902
5	SB-5	3355.16	758.82	114.71	2741.9	2684	656	19	637
Total		10943.94			8588.72	9200			

Table 4. 10: Sub-basin-wise Total Stream Number as per Order

S No.	Sub-basin Name	Order of Streams						
		I	**II**	**III**	**IV**	**V**	**VI**	**VII**
		Total No. of Streams according to Order - N						
1	SB-1	1052	492	301	134	66	53	-
2	SB-2	580	265	572	54	27	62	-
3	SB-3	909	448	177	126	51	101	-
4	SB-4	524	231	101	90	100	-	-
5	SB-5	1347	651	304	147	55	80	100
	Total	4412	2087	1455	551	299	296	100

Table 4. 11: Sub-basin-wise Total Stream Lengths as per Order

S No.	Sub-basin Name	Order of Streams						
		I	II	III	IV	V	VI	VII
		Total Length of Streams according to Order - L (km)						
1	SB-1	895.2	545.1	292.3	127.5	57.4	47.6	-
2	SB-2	580.6	310.6	185.2	53.2	25.8	62.4	-
3	SB-3	998.0	537.6	202.1	120.1	53.0	98.0	-
4	SB-4	535.5	265.6	109.0	89.3	98.4	-	-
5	SB-5	1486.1	756.3	350.3	149.2	52.4	90.6	92.4
	Total	4495.4	2415.1	1138.9	539.3	287.0	298.6	92.4

Table 4. 12: Sub-basin-wise Total Mean Stream Lengths as per Order

SI no.	Sub-basin Name	Order of Streams						
		I	II	III	IV	V	VI	VII
		Mean Stream Length according to Order - $L_{\hat{u}}$ (km)						
1	SB-1	0.85	1.11	0.97	0.95	0.87	0.90	0.00
2	SB-2	1.00	1.17	0.32	0.99	0.96	1.01	0.00
3	SB-3	1.10	1.20	1.14	0.95	1.04	0.97	0.00
4	SB-4	1.02	1.15	1.08	0.99	0.98	0.00	0.00
5	SB-5	1.10	1.16	1.15	1.01	0.95	1.13	0.92

Table 4. 13: Sub-basin-wise Stream Lengths Ratio as per Order

SI no.	Sub-basin Name	Order of Streams						
		I	II	III	IV	V	VI	VII
		Stream Length Ratio - RL						
1	SB-1	0.61	0.54	0.44	0.45	0.83	0.00	0.00
2	SB-2	0.53	0.60	0.29	0.48	2.42	0.00	0.00
3	SB-3	0.54	0.38	0.59	0.44	1.85	0.00	0.00
4	SB-4	0.50	0.41	0.82	1.10	0.00	0.00	0.00
5	SB-5	0.51	0.46	0.43	0.35	1.73	1.02	0.00

Table 4. 14: Sub-basin-wise Mean Bifurcation Ratio as per Order

Sl no.	Sub-basin Name	Order of Streams							Mean Bifurcation Ratio
		I	II	III	IV	V	VI	VII	
		Bifurcation Ratio - R_b							
1	SB-1	2.14	1.63	2.25	2.03	1.25	0.00	0.00	2.01
2	SB-2	2.19	0.46	10.59	2.00	0.44	0.00	0.00	4.41
3	SB-3	2.03	2.53	1.40	2.47	0.50	0.00	0.00	1.99
4	SB-4	2.27	2.29	1.12	0.90	0.00	0.00	0.00	1.32
5	SB-5	2.07	2.14	2.07	2.67	0.69	0.80	0.00	2.11

Table 4. 15: Sub-basin-wise Morphometric Parameters used to Prioritize Sub-basins

Sub Basin Name	Bifurcation Ratio	Drainage Density	Stream Frequency	Texture Ratio	Relief Ratio	Length of overland Flow	Circulatory Ratio	Form Factor	Elongation Ratio	Compactness Coefficient
SB-1	2.01	0.74	0.84	4.03	6.42	0.37	0.12	0.44	0.74	2.93
SB-2	4.41	0.76	1.05	3.93	11.23	0.38	0.12	0.26	0.58	2.91
SB-3	1.99	0.81	0.79	3.52	11.74	0.40	0.11	0.40	0.72	3.02
SB-4	1.32	0.77	0.81	2.12	10.41	0.39	0.07	0.17	0.47	3.87
SB-5	2.11	0.82	0.80	3.54	5.55	0.41	0.07	0.25	0.57	3.70

Table 4. 16: Prioritized ranking of Sub-basins based on Morphometric Parameters

Sub Basin Name	Bifurcation Ratio	Drainage Density	Drainage Frequency	Texture Ratio	Relief Ratio	Length of overland Flow	Circulatory Ratio	Form Factor	Elongation Ratio	Compactness Coefficient
SB-1	3	5	2	1	4	5	4	5	5	2
SB-2	1	4	1	2	2	4	5	3	3	1
SB-3	4	2	5	4	1	2	3	4	4	3
SB-4	5	3	3	5	3	3	1	1	1	5
SB-5	2	1	4	3	5	1	2	2	2	4

Table 4. 17: Table 4.3.9: Rank Designation based on Morphometric Parameters as per Sub-basins

SI No.	Sub Basin Name	Compound Parameter	Final Parameter	Rank Designation
1	SB-1	3.6	V	Best
2	SB-2	2.6	II	Bad
3	SB-3	3.2	IV	Better
4	SB-4	3	III	Good
5	SB-5	2.6	I	Worst

4.4.2 Prioritization of sub-watersheds

The drainage system of a basin influences runoff as well as soil erosion or soil loss. Sub-basins can be prioritize by rank upon their morphometric characteristics which can be useful to apply soil conservation measures in a basin. The composite ranking is done as shown in Table 4.18

As indicated from the table maximum score is 3.6 (SB-1) and the least score is 2.6 (SB-2 and SB-5) this means that SB-2 and SB-5 should be given more priority in terms in terms soil conservation measures base on the phenomenon as explained earlier. Hence (SB-1) is considered as best in terms of ranking or requires little or no attention for soil erosion measures. **Fig 4.7** shows the map so sub-basins in terms of prioritization for soil conservation measures. I – indicates the most prioritized sub-basin, followed by II and so on.

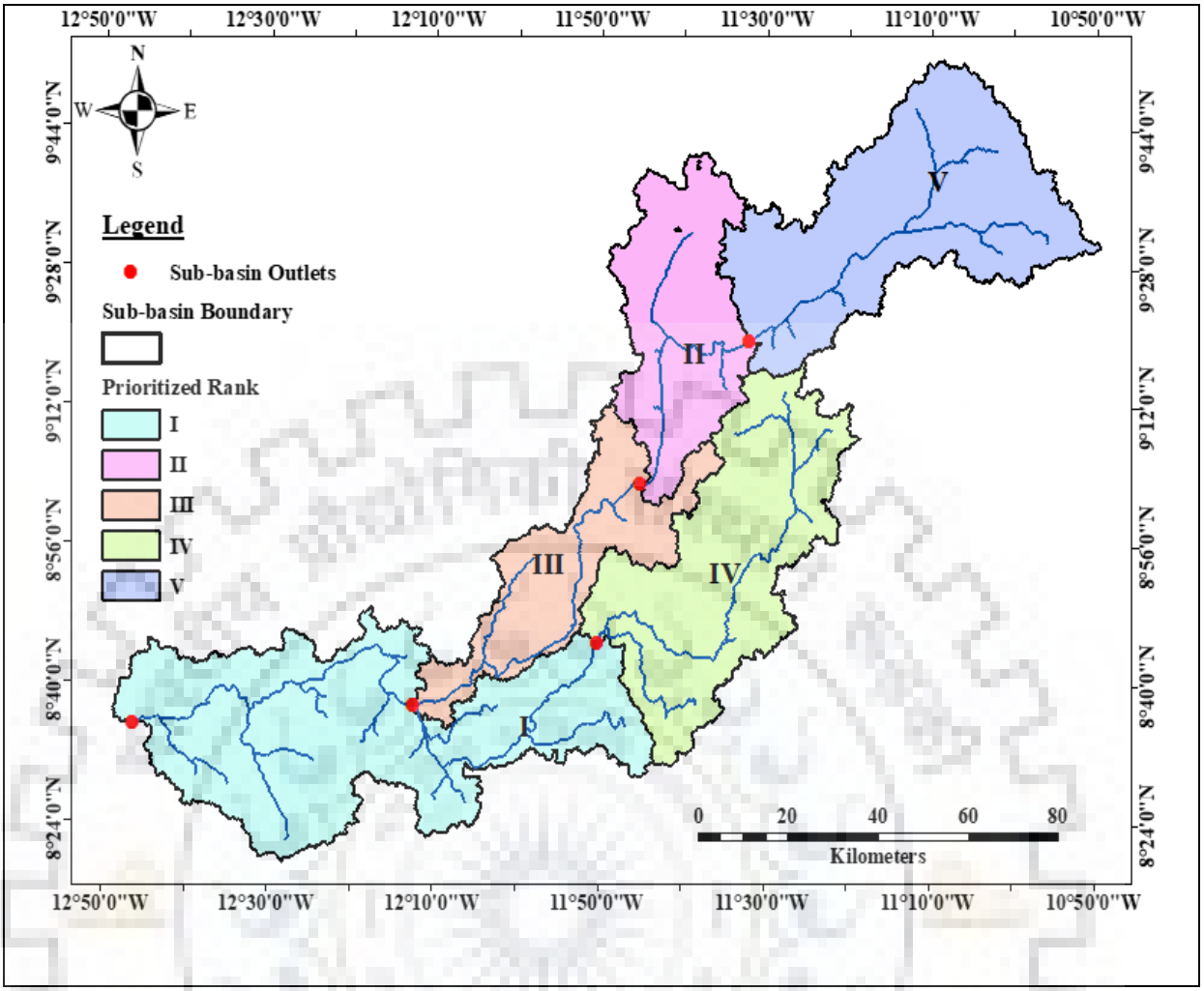

Figure 4. 7: Final Order of Priority of Sub-basins for Soil Erosion Conservation measures based on Morphometric Characteristics

4.5 LAND-USE LAND-COVER CLASSIFICATION

Analysis of land use/land cover in RSRB river basin using remote sensing data was carried out in order to study the existing land use and land cover pattern in RSRB for the year 2010. The study area is mostly occupied by Pasture land, forest land, agricultural land, settlement and then water bodies respectively in order of most covered land.

In carrying out land classification and reclassification, the satellite image was first visually interpreted, after the ground truth verification carried out and the land use and land cover was finalized, based on which the thematic maps of RSRB were prepared. The figure (Fig.4.10), and Table 4.18 and Table 4.19 below gives a detailed account of these land use/land cover classes of the study area which are described by area of land cover and percentage distribution as well as sub-basin wise. Base on the pattern of change in landuse/landcover and the factors underlying it during the study period. The land use/land cover of the area has been classified into five major classes.

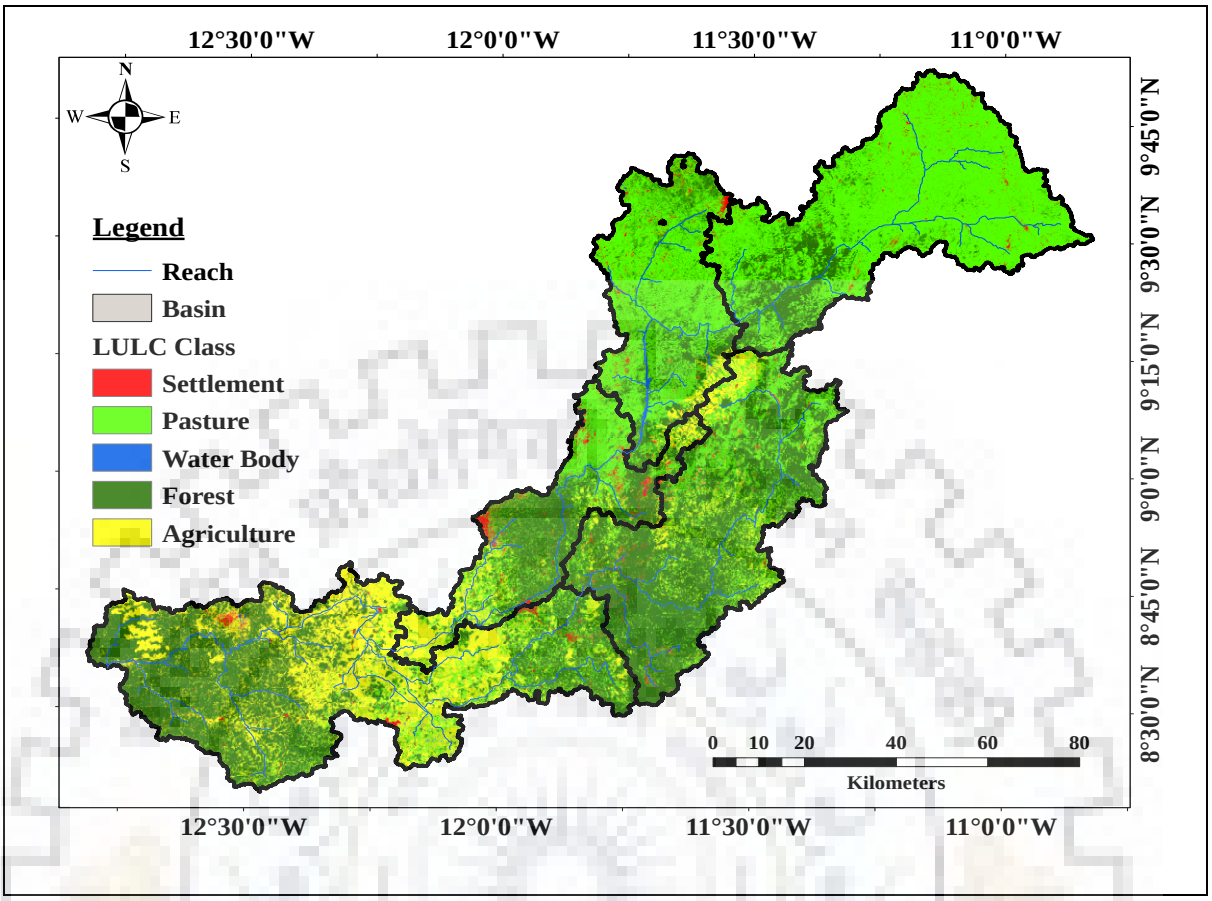

Figure 4. 8: Land Use Land Cover Map of RSRB

Table 4. 18: Area Distribution of LULC Classification in RSRB

	Area in km^2					
LULC Class	RSRB	SB-1	SB-2	SB-3	SB-4	SB-5
Settlement	276.18	46.2847	52.8445	48.9384	77.2146	50.9101
Pasture	4520.74	2052.57	1008.76	621.955	450.966	387.412
Water Body	60.80	0.6571	17.3033	3.144	11.7193	27.8748
Forest	4412.05	410.241	355.103	1435.38	522.779	1684.51
Agriculture	1676.57	2.56	47.1517	195.254	227.96	1204.45
Total	**10946.35**	**2512.31**	**1481.16**	**2304.67**	**1290.64**	**3355.16**

Considering the importance of prioritizing the sub-basins for soil erosion conservation measures, it necessary to have a good knowledge of the specific LULC class in each sub-basin. Therefore the following **Fig 4.9 – 4.10** describes the LULC classification for each sub-basin of the RSRB.

Table 4. 19: Percentage Area Distribution of LULC Classification in RSRB

	% of Total Area					
LULC Class	RSRB	SB-1	SB-2	SB-3	SB-4	SB-5
Settlement	2.52	0.42	0.48	0.45	0.71	0.47
Pasture	41.30	18.75	9.22	5.68	4.12	3.54
Water Body	0.56	0.01	0.16	0.03	0.11	0.25
Forest	40.31	3.75	3.24	13.11	4.78	15.39
Agriculture	15.32	0.02	0.43	1.78	2.08	11.00
Total	**100.00**	**22.95**	**13.53**	**21.05**	**11.79**	**30.65**

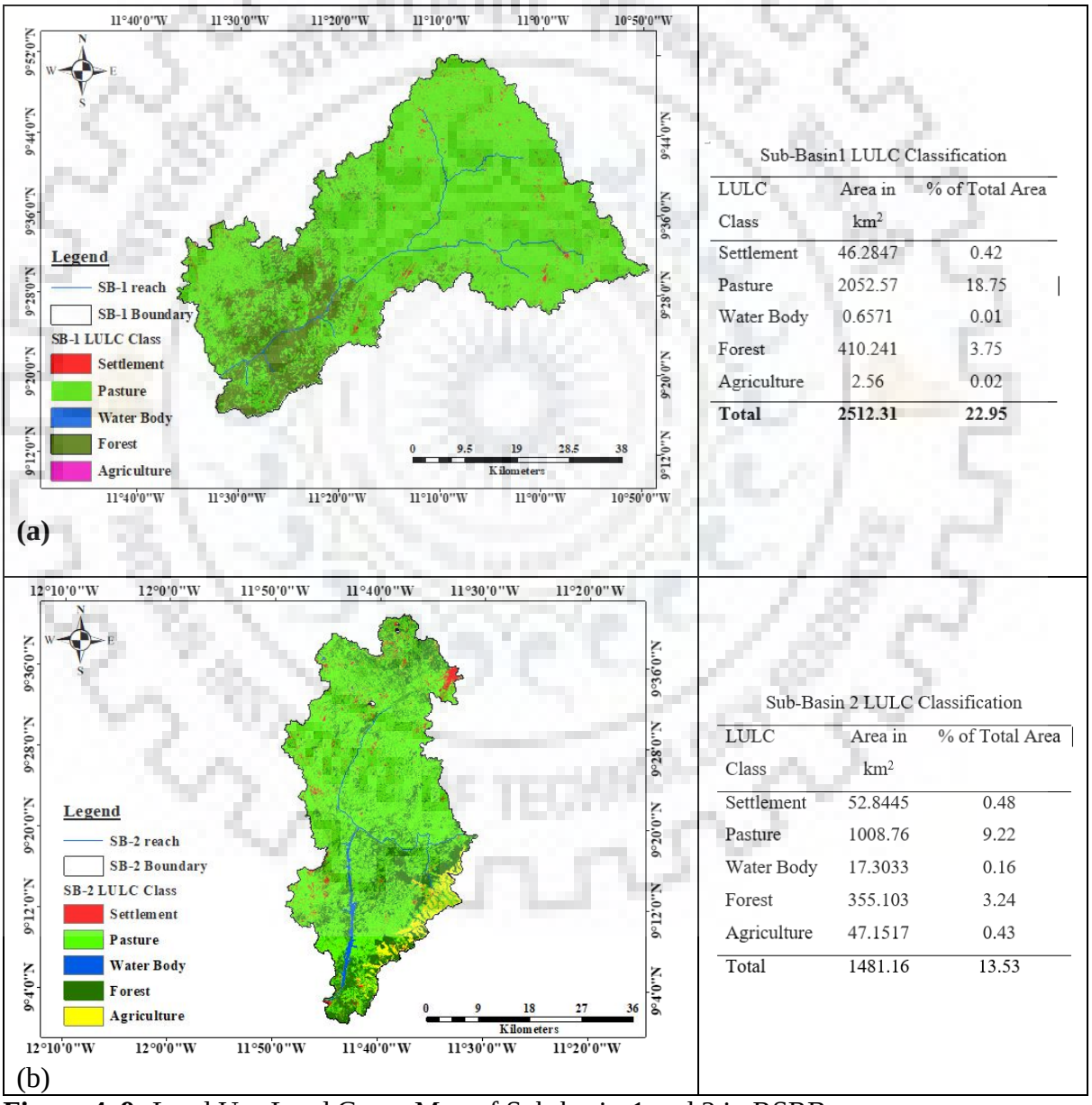

Sub-Basin1 LULC Classification

LULC Class	Area in km²	% of Total Area
Settlement	46.2847	0.42
Pasture	2052.57	18.75
Water Body	0.6571	0.01
Forest	410.241	3.75
Agriculture	2.56	0.02
Total	**2512.31**	**22.95**

Sub-Basin 2 LULC Classification

LULC Class	Area in km²	% of Total Area
Settlement	52.8445	0.48
Pasture	1008.76	9.22
Water Body	17.3033	0.16
Forest	355.103	3.24
Agriculture	47.1517	0.43
Total	1481.16	13.53

Figure 4. 9: Land Use Land Cover Map of Sub-basin-1 and 2 in RSRB

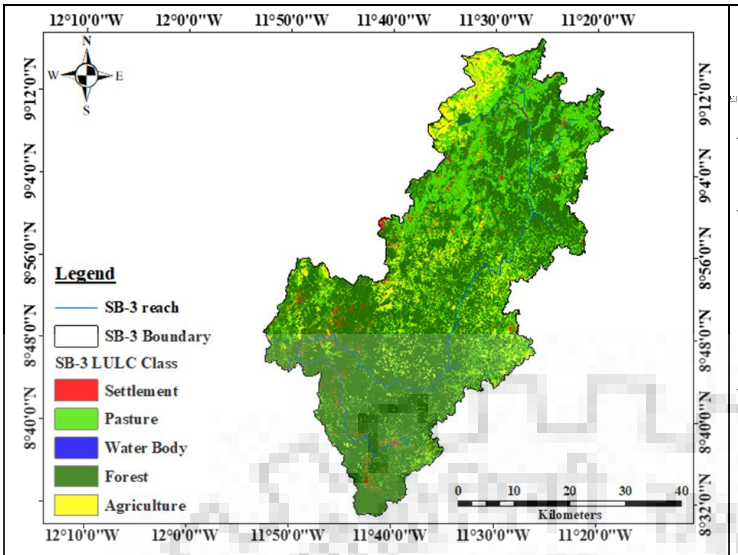

(a)

Sub-Basin 3 LULC Classification

LULC Class	Area in km²	% of Total Area
Settlement	48.9384	0.45
Pasture	621.955	5.68
Water Body	3.144	0.03
Forest	1435.38	13.11
Agriculture	195.254	1.78
Total	**2304.67**	**21.05**

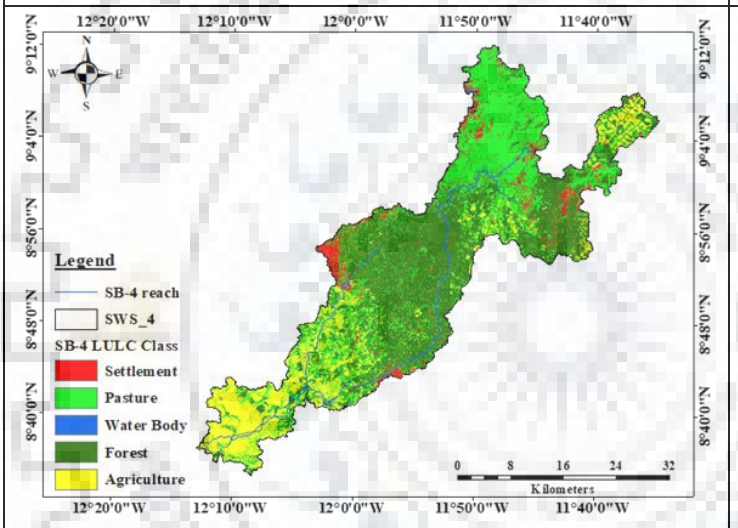

(b)

Sub-Basin 4 LULC Classification

LULC Class	Area in km²	% of Total Area
Settlement	77.2146	0.71
Pasture	450.966	4.12
Water Body	11.7193	0.11
Forest	522.779	4.78
Agriculture	227.96	2.08
Total	**1290.64**	**11.79**

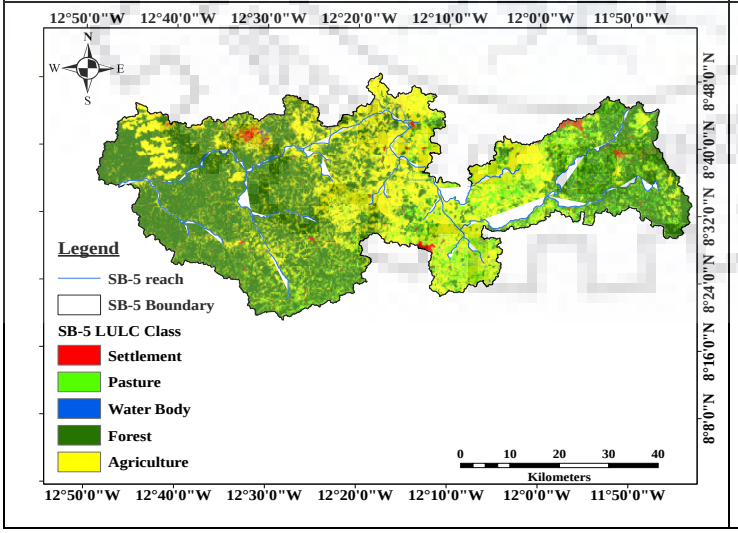

Sub-Basin 5 LULC Classification

LULC Class	Area in km²	% of Total Area
Settlement	50.9101	0.47
Pasture	387.412	3.54
Water Body	27.8748	0.25
Forest	1684.51	15.39
Agriculture	1204.45	11.00
Total	**3355.16**	**30.65**

Figure 4. 10: Land Use Land Cover Map of Sub-basin-3, 4 and 5 in RSRB

4.6 SWAT ANALYSIS ON BASIN WATER BALANCE

4.6.1 Sensitivity Analysis on SWAT Model Parameters

To replicate the behavior of a system, it is necessary to developing a model. The model is accepted if the output matches the observed values and on the other hand if it does not then is adjust to match the observed values. This process is known as the calibration. As this is done, it is then validated with another set of observed data. In completing this process, then the model is ready to be used for future simulations.

In this study manual calibration process is adopted because it is more preferable by many researchers and is being widely used. In calibration process, visual examine of simulated and observed hydrographs are necessary for the improvement of results. Therefore, in running SWAT model, specific parameters are considered for calibration especially runoff estimation. These parameters incudes such as ground water delay, soil evaporation compensation factor, soil available water content, soil bulk density, curve number, groundwater "revap" coefficient, effective hydraulic conductivity, base-flow alpha factor, threshold depth of water in shallow aquifer, average slope length, average slope steepness, manning's "n", plant uptake compensation factor etc. These parameters can varies from its lower to upper limits.

4.6.2 Evaluation of SWAT Model for RSRB

After sensitivity analysis of the model calibration is followed and for the purpose of this study, the calibration process was done using the observed discharge at the outlet of sub-basin 2 (SB-2) on monthly basis with their simulated values. The first one year (1999-2000) of the modelling period was reserved for "model warm-up" in order to set-up the states of its internal hydrological components i.e. soil moisture content, groundwater store etc. The following nine years (2000-2009) data is taken for calibration and remaining four years (2010-2013) data was used for validation purpose.

Parameter values are calibrated (in terms of multiplication/addition/ subtraction) on the basis of its impact on the result. However, a parameter is never allowed to go beyond the predefined parameter range during the calibration.

For calibrating the model, observed discharge at outlet of sub-basin SB-2 were considered. After running the model with initial model parameters values (default), the monthly discharge

was estimated. The observed and estimated (pre-calibrated) monthly discharge values during the calibration period (2000-2009) was plotted as shown in **Fig. 11**. It has been noticed that the pre-calibrated discharge values continuously over-estimate the discharge throughout the years. Therefore, the parameters of the model were revised so as to improve the performance of the model. The parameters were updated on the basis of its impact and its ranking in its role on output. The observed and estimated discharge values before and after calibration are shown in **Fig. 11(a, b)**

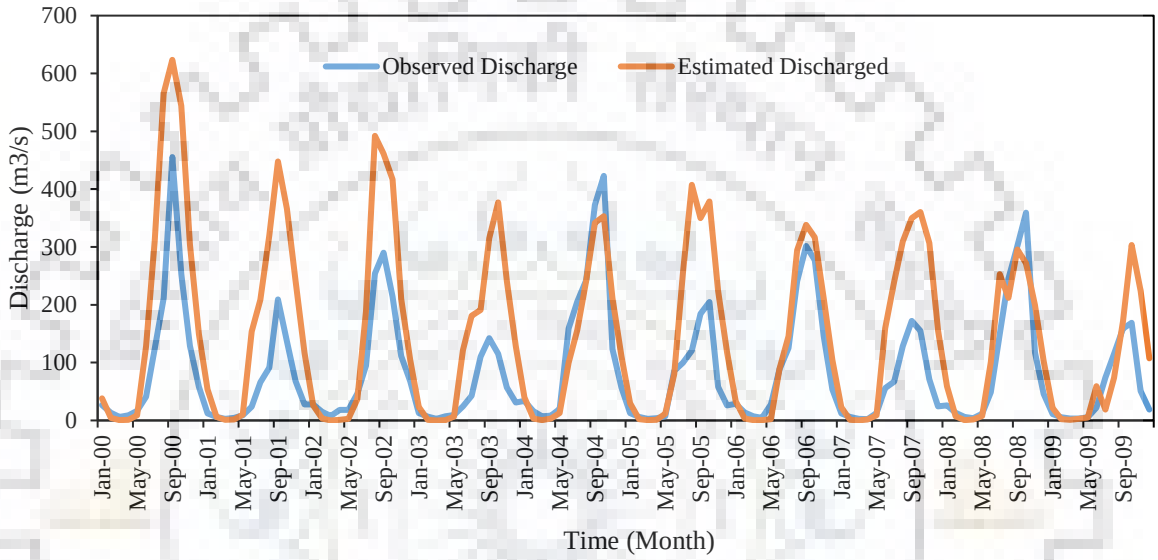

Figure 4. 11: a) Observed and Estimated discharge before calibration for the periods of 2000-2009

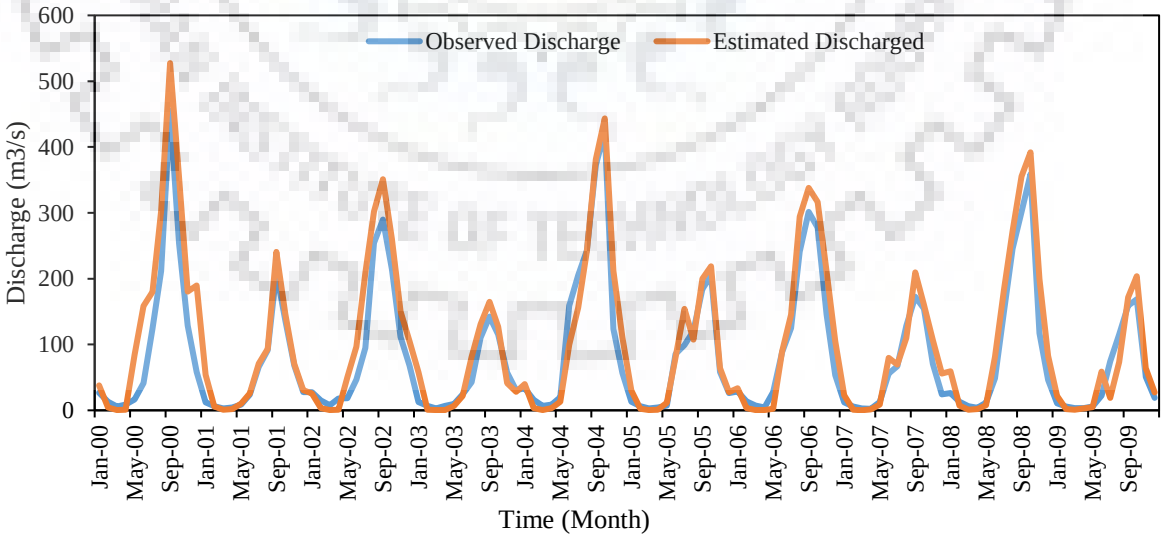

Figure 4.11 b) Observed and Estimated discharge after calibration for the periods of 2000-2009

Comparing the rising and recession curves, it is important to examine the variation of estimated discharge from the observed values. Hence a graph of scatter plot is plotted between the observed and estimated flow values as shown in **Fig. 12 (a, b)** for un-calibrated and calibrated conditions. A 45^{o} line is marked which represents the perfect estimation. From **Fig. 11(b)**, it may be observed that even the calibrated model is over estimating the monthly discharge. This is perhaps because of the reasons that the AMC conditions are not incorporated correctly or the temporary small storages in the fields are not depicted correctly in the model. For accurate depiction of the area, extensive survey is needed which could not be accomplished in this study

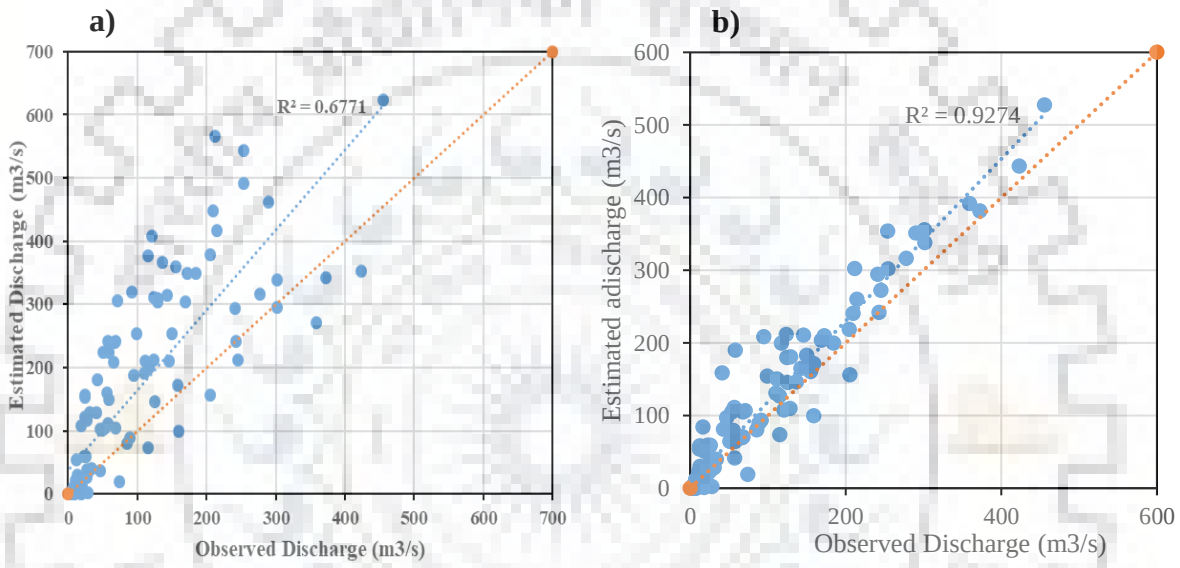

Figure 4. 12 (a, b) scatter plot of observed and estimated discharge before and after calibration at outlet of SB-2 for the periods 2000-2009

Hence various measures of performance has been estimated and tabulated in Table 5.x below:

Table 4. 20: Model Performance statistics before and after calibration for the periods of 2000-2009

Parameters	Discharge during calibration Period (2000-2009)		
	Observed	Pre-calibrated	Calibrated
Mean	84.97	146.06	115.37
Standard Deviation	99.59	153.41	139.13
Maximum	455.43	623.50	526.90
Count	120.00	120.00	47.00
Coefficient of determination	-	0.68 (Good)	0.93 (Very Good)
Nash-Sutcliffe efficiency	-	0.62 (satisfactory)	0.74 (Good)
Percent Bias	-	18 (Satisfactory)	25 (Unsatisfactory)
RSR	-	0.71 (Unsatisfactory)	0.58 (Good)

It is evident from Table 5.6 that though the coefficient of determination (R2) during the calibration period without any revision of the parameters is very good (0.89), but the other performance measures such as Nash-Sutcliffe efficiency (NSE) and Percent Bias (PBias) are highly unsatisfactory. RMSE-observations Standard deviation Ratio (RSR) is also just satisfactory (0.62). However, after revising the parameters of the model during the same period, most of the performance parameters are very good except the Percent Bias. This is again due to the reason as mentioned above that the field conditions are not perfectly depicted in the model. Overall, it may be concluded that the monthly predictions are generally satisfactory during the simulation period, except for the few months with extreme storm and hydrologic conditions. Similar conclusions have been reported by (Rosenthal et al., 1995; Borah and Bera, 2003: Gassman et al., 2007). However, one can improve the efficiency provided the ground data is available which can be incorporated in the model for its improved efficiency.

The parameters of the model are tested by running the model during the validation period of (2010-2013). It was observed that during the validation period also, the discharge values are little over-estimated throughout the time steps as shown in **Fig. 4.13** before and after validation.

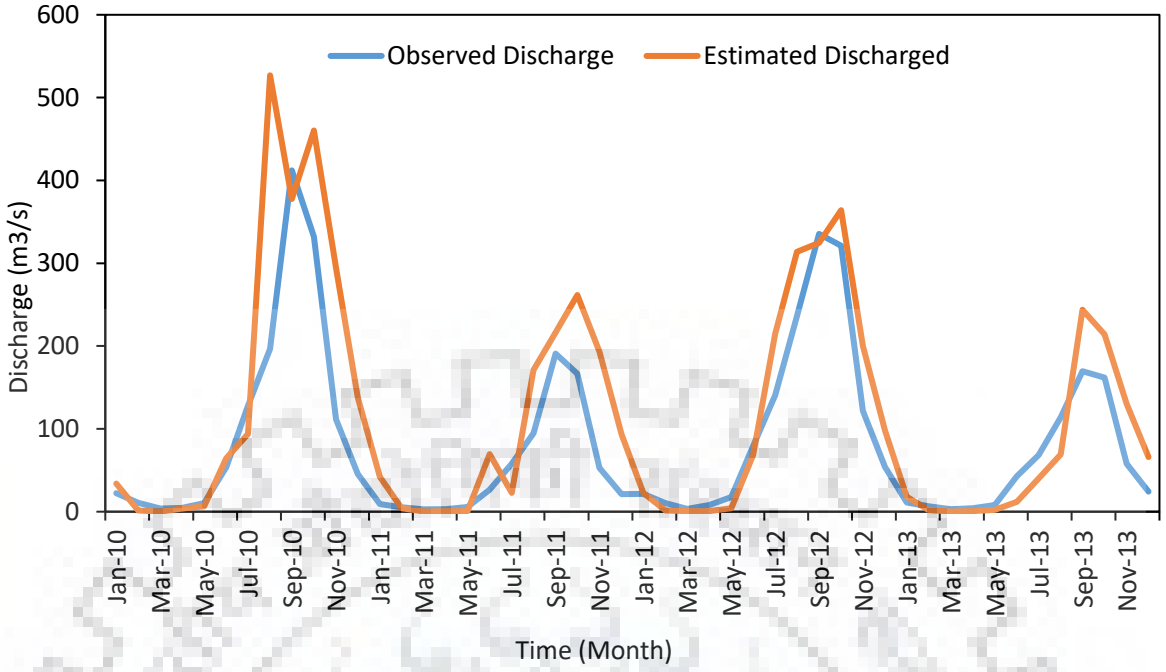

Figure 4. 13 a) Observed and Estimated discharge before validation for the periods of 2010-2013

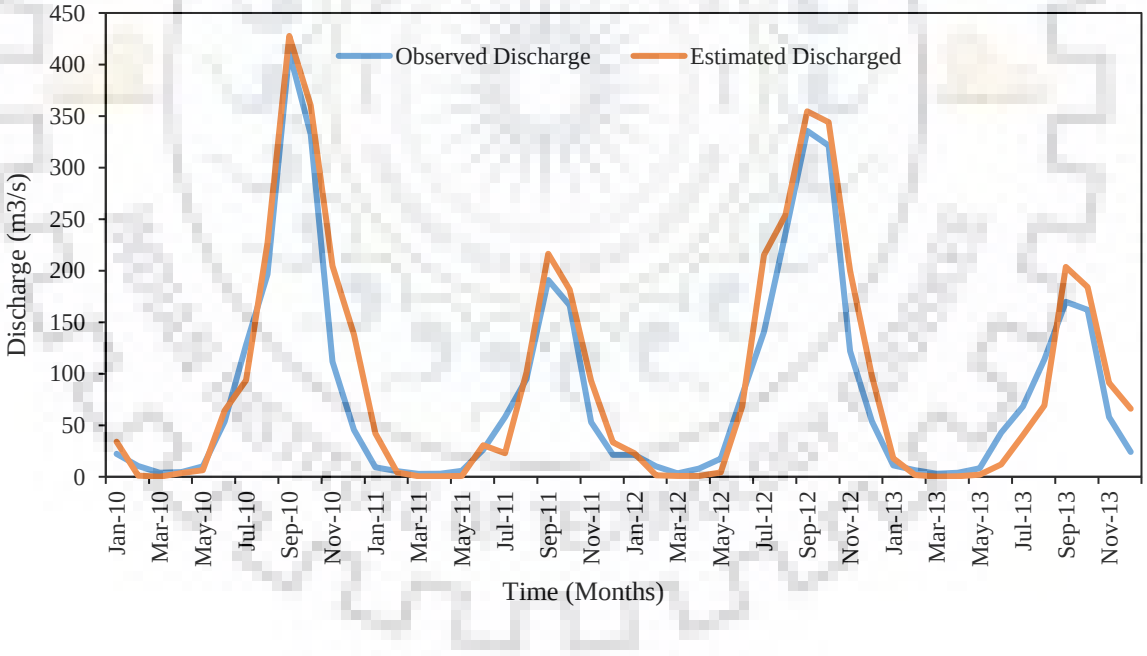

Figure 13: b) Observed and Estimated discharge after validation for the periods of 2010-2013

Besides the comparison of rising and recession curves, it is important to examine the variation of estimated discharge from the observed values. For this purpose, a scatter graph is plotted between the observed and estimated flow values for un-calibrated and calibrated conditions during 2010-2013 as shown in **Fig. 4.14 (a, b)**

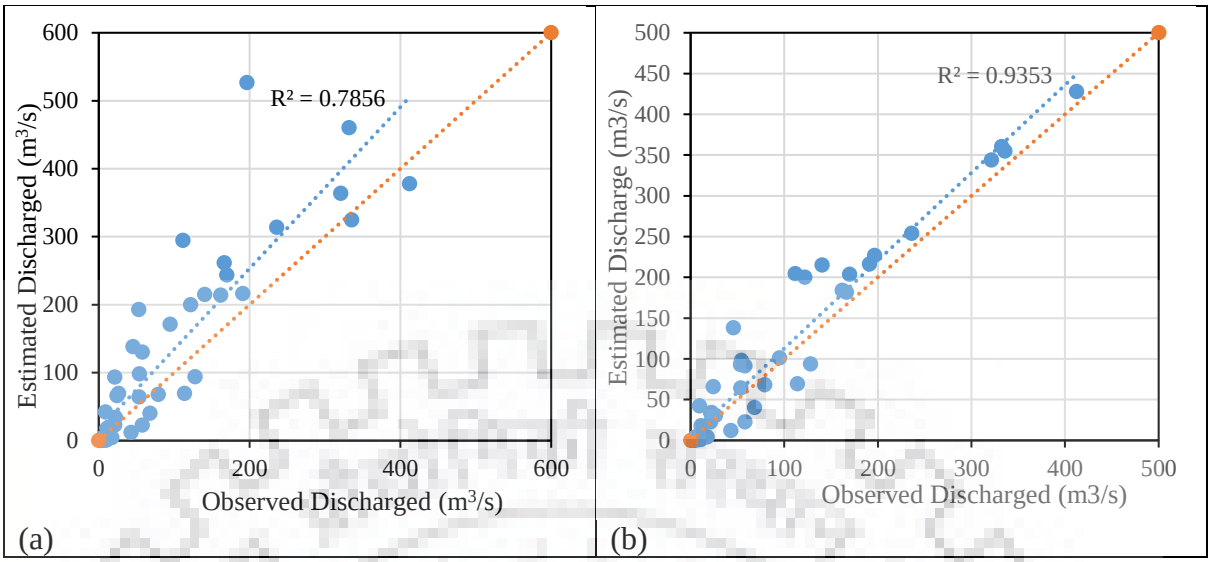

Figure 4. 14: (a, b) scatter plot of observed and estimated discharge before and after Validation outlet of SB-2 during 2010-2013

A 45^{o} line is marked which represents the ideal condition. From Fig. 5.8 it may be observed that though the calibrated model can be accepted and works satisfactorily during the validation period as well. Further, the model efficiency is examined during the validation period. Various performance measures as mentioned earlier are calculated and is reported in Table 5.7. below:

Table 4. 21: Model Performance statistics before and after calibration for the periods of 2010-2013

Parameters	Discharge during calibration Period (2010-2013)		
	Observed	Pre-calibrated	Calibrated
Mean	85.53	102.69	95.20
Standard Deviation	99.82	115.53	115.75
Maximum	455.43	527.50	427.70
Coefficient of determination	-	0.79 (Good)	0.94 Very Good)
Nash-Sutcliffe efficiency	-	0.49 (Unsatisfactory)	0.65 (Good)
Percent Bias	-	36 (Unsatisfactory)	24 (satisfactory)
RSR	-	0.55 (Good)	0.48 (Very Good)

It is evident from Table 5.7 that the R2, N-S efficiency and RSR values are very good during the validation period ((0.96), 0.83 and 0.41). However, PBias is still unsatisfactory due to lack of information about the best management practices (BMPs) being followed by the farmers in the agricultural fields (Basu and Van Meter, 2012; Field et al., 2006). This may be considered as the limitation of the selection of parameter values of the model.

4.6.1 Water Balance of Roke-Seli River Basin

During SWAT Model applications sensitivity analysis was performed, and the model was calibrated and validated for the Rokel-Seli river basin. Results of water balance for the RSRB can be shown in Table 4.23 below:

Table 4. 22: Annual Average water balance for the Rokel-Seli River Basin

Particular	Water Balance Components	Volume in (mm)	Percentage Contribution
A1	**Precipitation**	**2180.7**	
A2	**Actual Evapotranspiration**	**1030.7**	**47.3**
A3	**Surface Runoff**	**461.07**	**21.1**
A4	**Lateral flow**	**49.65**	**2.3**
GW1	Percolation to Shallow Aquifer	639.53	
GW2	Revap from shallow Aquifer	48.43	
GW3	Recharge to deep Aquifer	31.98	
A5	**Return Flow (A5=GW1-GW2-GW3)**	**559.12**	**25.6**
A6	**Other Losses**	**80.16**	**3.7**
	Sub Total	**2180.7**	**100**

The water balance ratios for basin are as follows:

Streamflow/Precipitation	= 0.23
Evaporation/Precipitation	= 0.47
Percolation/Precipitation	= 0.29
Deep recharge/Precipitation	= 0.01
Total	**= 1.00**

Base flow/Total runoff	= 0.53
Surface flow/Total runoff	= 0.43
Losses	= 0.04
Total	**= 1.00**

The hydrology of the Rokel-Seli river basin showing the distribution of all various component of the basin can be further illustrated diagrammatically in **Fig 4.15** as follows:

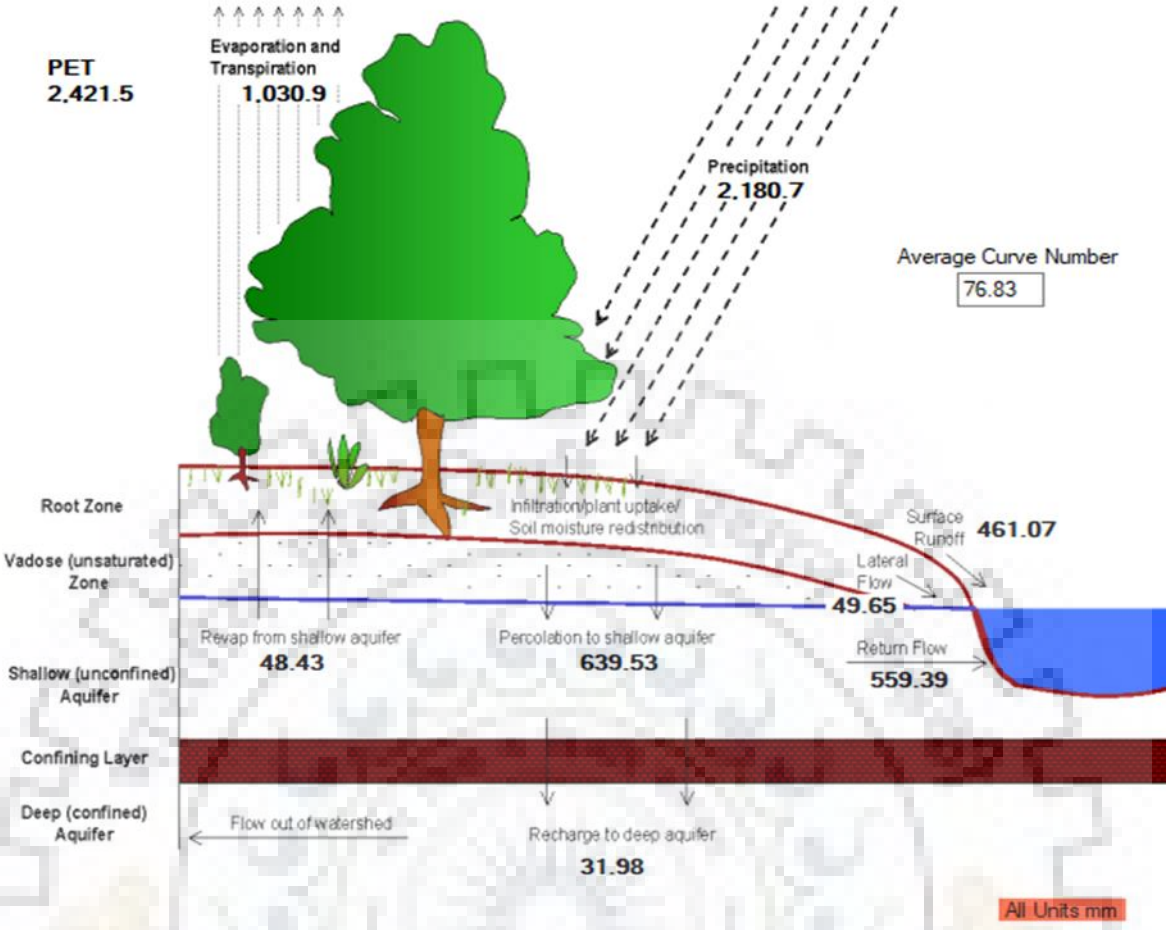

Figure 4. 15: The hydrology of the Rokel-Seli river basin

From the analysis above it can be seen that out of annual average rainfall of 2180.7mm about 49% flows out as surface runoff for the basin. Suitable management practices may be implemented to reduce the amount of runoff and use for in basin needs. Also evapotranspiration account for about 47% of annual precipitation. It is very import to pay attention to evapotranspiration, baseflow and surface flow ratios, hence they are the key components that affect the water balance of any basin.

CHAPTER 5

CONCLUSION AND RECOMMENDATION

OVERVIEW OF CHAPTER

This chapter give a summary of all conclusions arrived at by carrying out this study. It expresses the main output of all the methods and approaches applied. It gives the closing remarks of why the need of the study, what questions about climate variability, rainfall trends, morphometry analysis and water balance over the basin that have been answered concludes of the benefit the study.

CONCLUSIONS

The rainfall over Rokel-Seli river basin varies considerably from the upstream and downstream showing high value of coefficient of variation annually and seasonally. Thus, the high values of CV at these stations shows that less rainfall occurs at these parts of the basin and high rainfall occurring most part at mid of the basin with average rainfall of 2435mm. The non-parametric (MK and MMK) tests were used to detect rainfall trends over the basin during the period of (1961-2005).The accuracy of MMK test in terms of significance level was more precise than MK test at the same level of significance, showing only 3 stations having negatively significant trend and two stations with positively significant trends in the wet and dry seasons. No significant trends was identified annually.

The Sen's slope magnitude varies between −17.354 to 6.951 mm/year annually in the basin (1961–2005), therefore the seasonal slopes were mostly negative for the wet season and positive for the dry season. The Mann–Whitney–Pettitt and SNHT tests were used to identify possible break points in precipitation during the 45year period. However, from the results of the study, it can be concluded that there was no shift change point in the data series. Hence the rainfall data was homogenous for all throughout the time series for the period of 1961 to 2005.

Rainfall projections has been carried out in the basin for the periods of 2020s and 2050s. The average annual rainfall projected in the 2020s (2011-2040) is 2627mm and for 2050s (2041-2017) is 2604mm as compared to the observed value of 2435mm. This means that there would be increase in rainfall of about 7-8% unto 2050s due to climate change. The observed dependable annual rainfall at 95% is 2034mm and the projected dependable rainfall at 95% dependability in 2020s and 2050s is 2320mm and 2462mm respectively. It is very important to

know the dependable rainfall in planning water resources over the basin to identify the minimum water available for various water requirement, also to determine the projected minimum rainfall which could be used for future water resources management. The present study highlights the rainfall variability over the Rokel-Seli River Basin in Sierra Leone.

Base on the morphometric analysis the maximum score is 3.6 (SB-1) and the least score is 2.6 (SB-2 and SB-5) this means that SB-2 and SB-5 should be given more priority in terms of soil conservation measures base on the phenomenon as explained earlier. Hence (SB-1) is considered as best in terms of ranking or requires little or no attention for soil erosion measures. Fig 4.7 shows the map of sub-basins in terms of prioritization for soil conservation measures. I – indicates the most prioritized sub-basin, followed by II and so on.

In conclusion on the water balance of the basin, out of annual average rainfall of 2180.7mm about 23% flows out as surface runoff in the basin. Also evapotranspiration account for about 47% of annual precipitation and 30% as ground water. This study has quantify all the various water components over the basin and hence can be very use to stakeholders for any future water resources management.

The adopted analysis provides key information of basin's water availability and hence this work offers benchmark information that can be used to increase the capacity of long-range water resource planning and management, land use planning, agricultural water development and conservation, and industrial water use over the next several decades at basin level. The results of the study also helps in the assessment of the future impact of climate change over the basin which affects changes in the hydrologic cycle of the basin.

CHAPTER 6

REFRENCES

1) A. K. Prabhakar, K. K. Singh, A. K. Lohani (2015) Spatial and temporal rainfall trends variability analysis at sub-watershed level for Baitarani basin of Odisha State
2) Akinremi O, McGinn S, Cutforth H (1999) Precipitation trends on the Canadian prairies. J Clim 12:2996–3003
3) Alexanderson H (1986). A homogeneity test applied to precipitation data. J. Climatol. **6**: 661–675.
4) Alexandersson H, Moberg A (1997). Homogenization of Swedish temperature data. Part I: a homogeneity test for linear trends. Int. J. Climatol **17**:25–34.
5) Allen, M.R., Ingram, W.J., 2002. Constraints on future changes in climate and the hydrologic cycle. Nature 419, 224–232. http://dx.doi.org/10.1038/nature01092.
6) Amir K. Basheer1, Haishen Lu1, Abubaker Omer1, Abubaker B. Ali3, and Abdeldime M. S. Abdelgader (2016) Impacts of climate change under CMIP5 RCP scenarios on the streamflow in the Dinder River and ecosystem habitats in Dinder National Park, Sudan
7) Anandhi, A., Srinivas, V.V., Nanjundiah, R.S., Nagesh Kumar, D., 2008. Downscaling precipitation to river basin in India for IPCC SRES scenarios using Support Vector Machine. Int. J. Climatol. 28, 401–420. http://dx.doi.org/10.1002/ joc.1529.
8) Bradley, R. S., H. F. Diaz, J. K. Eischeid, P. D. Jones, P. M. Kelly, and C. M. Goodess. Precipitation fluctuations over Northern Hemisphere land areas since the mid-19th century." Science 237, no. 4811 (1987): 171-175.
9) Dinpashoh Y, Mirabbasi R, Jhajharia D, Abianeh H, Mostafaeipour A (2014) Effect of short-term and long term persistence on identification of temporal trends. J Hydrol Eng 19(3):617–625
10) Fawcett R (2004) A long-term trend in Melbourne rainfall? Bull Aust Meteor Oceanographic Soc 17:122-126
11) Frei C, Schar C (1998) Precipitation climatology on the Alps from high resolution rain-gauge observations Int. J Climatol 18:873–900
12) Gajbhiye S, Meshram C, Mirabbasi R, Sharma SK (2015) Trend analysis of rainfall time series for Sindh river basin in India. Doi: 10.1007/s00704-015-1529-4

13) Gajbhiye S, Meshram C, Singh SK, Srivastava PK, Islam T (2016) Precipitation trend analysis of Sindh river basin, India from long term 102 years of record (1901-2002). Atmos Sci Lett 17(1):71–77
14) Goswami BN, Venugopal V, Sengupta D, Madhuso odanam MS, Xavier PK (2006) Increasing trends of extreme rain events over India in a warming environment. Science 314:1442–1445
15) Guhathakurta P, Rajeevan M (2006) Trends in the rainfall pattern over India. NCC Research Report No 2/2006. National Climate Centre. India Meteorological Department, p 23
16) Hamed, K.h., Rao, A.R. A modified Mann Kendall trend test for auto correlated data. Journal of Hydrology, 204: 182–196 (1998).
17) Hennessy KJ, Suppiah R, Page CM (1999) Australian rainfall changes, 1910–1995. Aust Meteor Mag 48:1–13
18) Ho, J.T., Thompson, J.R., Brierley, C., 2016. Projections of hydrology in the Tocantins-Araguaia Basin, Brazil: uncertainty assessment using the CMIP5 ensemble. Hydrol. Sci. J. 61 (3), 551–567.
19) IPCC (2007) Climate change 2007: climate change impacts, adaptation and vulnerability. Working Group II contribution to the Intergovernmental Panel on Climate Change Fourth Assessment Report. Summary for policymakers. p 23
20) McGuffie, K., Henderson-Sellers, A., 1997. A Climate Modeling Primer. John Wiley & sons, West Sussex, England. Mehrotra, R., Sharma, A., 2010. Development and application of a multisite rainfall stochastic downscaling framework for climate change impact assessment.
21) Misra, V., Dirmeyer, P.A., Kirtman, B.P., 2003. Dynamic downscaling of seasonal simulations over South America. J. Clim. 16, 103–117.
22) Mohapatra M, Mohanty UC, Behera S (2003) Spatial variability of daily rainfall over Orissa, India, during the southwest summer monsoon season. Int J Climatol 23:1867–1887
23) Mou Leong Tan, Ab Latif Ibrahim, Zulkifli Yusop, Vivien P. Chua, Ngai Weng Chan (2016) Climate change impacts under CMIP5 RCP scenarios on water resources of the Kelantan River Basin, Malaysia
24) Rodrigo S, Esteban-Parra MJ, Pozo-Vázquez D, Castro-Díez Y (2000) Rainfall variability in southern Spain on decadal to centennial time scales. International Journal of Climatology 20(7):721–732

25) Rodriguez-Puebla C, Encinas AH, Nieto S, Garmendia J (1998) Spatial and temporal patterns of annual precipitation variability over the Iberian Peninsula. Int J Clim 18:299–316
26) Sen, P.K. Estimates of the regression coefficient based on Kendall's tau. Journal of the American Statistical Association, (63): 1379-1389 (1968).
27) Serrano A, Mateos VL, Garcia JA (1999) Trend analysis of monthly precipitation over the Iberian peninsula for the period 1921-1995. Phys Chem Earth (B) 24(1–2):85–90
28) Silberstein, R.P., Aryal, S.K., Durrant, J., Pearcey, M., Braccia, M., Charles, S.P., Boniecka, L., Hodgson, G.A., Bari, M.A., Viney, N.R., McFarlane, D.J., 2012. Climate change and runoff in south-western Australia. J. Hydrol. 475, 441–455.
29) Smith I (2004). An assessment of recent trends in Australian rainfall. Aust Meteor Mag 53:163–173
30) Surendra Kumar Chandniha & Sarita Gajbhiye Meshram, 2016. Trend analysis of precipitation in Jharkhand State, India investigating precipitation variability in Jharkhand State
31) Surendra Kumar Chandniha et' al (2015) Thesis; Watershed Sustainability Index Framework and Its Estimation for a Watershed
32) T.V. Reshmidevi, D. Nagesh Kumar, R. Mehrotra, A. Sharma (2017). Estimation of the climate change impact on a catchment water balance using an ensemble of GCMs
33) Thorsten Pohlert; July 30, 2017; Non-Parametric Trend Tests and Change-Point Detection
34) Van Vuuren, D.P., Edmonds, J., Kainuma, M., Riahi, K., Thomson, A., Hibbard, K., Hurtt, G.C., Kram, T., Krey, V., Lamarque, J.F., Masui, T., Meinshausen, M., Nakicenovic, N., Smith S.J., Rose, S.K., 2011.